

***Identification of PUB22 Targets and Functional
Characterization in PAMP-Triggered Immunity***



**Dissertation zur Erlangung
des naturwissenschaftlichen Doktorgrades
der Julius-Maximilians-Universität Würzburg**

vorgelegt von

Diplom Biologe Martin Stegmann

Geboren am 16.05.1983 in Erlenbach a. Main

Würzburg 2013

Eingereicht am:

Mitglieder der Promotionskommission:

Vorsitzender: Prof. Dr. Wolfgang Rössler

Gutachter: Prof. Dr. med Dr. Martin J. Müller

Gutachter: PD. Dr. Dirk Becker

Tag des Promotionskolloquiums:

Doktorurkunde ausgehändigt am:

Eidesstattliche Erklärung

Hiermit erkläre ich, dass ich die vorliegende Dissertation in allen Teilen selbst angefertigt und keine anderen als die von mir angegebenen Quellen und Hilfsmittel verwendet habe. Ich habe die Dissertation weder in gleicher noch in ähnlicher Form in anderen Prüfungsverfahren vorgelegt. Ich habe bislang noch keine weiteren akademischen Grade erworben oder zu erwerben versucht.

Würzburg, den 16.03.2013

.....

Martin Stegmann

Publikationen

Stegmann, M., Anderson, R. G., Ichimura, K., Pecenkova, T., Reuter, P., Zarsky, V., McDowell, J. M., et al. (2012). The Ubiquitin Ligase PUB22 Targets a Subunit of the Exocyst Complex Required for PAMP-Triggered Responses in Arabidopsis. *The Plant Cell*. doi:10.1105/tpc.112.104463

Index

List of Abbreviations	1
1. Introduction	1
1.1. Plant immunity	1
1.2. Vesicular trafficking in plant immunity	6
1.3. The plant exocyst complex	9
1.4. The ubiquitin modification system	11
1.4.1. Plant U-box proteins (PUBs)	14
1.4.2. Ubiquitination in plant immunity	16
1.4.3. Negative regulation of PTI by PUB22, PUB23 and PUB24	19
1.5. Aim of the present work	22
2. Materials and Methods	23
2.1. Materials	23
2.1.1. Chemicals	23
2.1.2. Media	23
2.1.3. Plants	24
2.1.4. Bacteria	24
2.1.5. <i>Hyaloperonospora arabidopsidis</i>	25
2.2. Methods	25
2.2.1. Cloning	25
2.2.2. Transformations	26
2.2.3. Plasmid preparations	29
2.2.4. Yeast two-hybrid screen	29
2.2.5. Yeast two-hybrid analysis and yeast complementation assays	29
2.2.6. Bimolecular fluorescence complementation	30
2.2.7. Protein isolation from plants	30
2.2.8. Coimmunoprecipitation	31
2.2.9. <i>In vitro</i> assays with recombinant proteins	32
2.2.10. Quantitative Real-Time PCR	34
2.2.11. Genotyping of T-DNA insertion mutants	34
2.2.12. ROS-burst assays	35
2.2.13. MAPK assays	36
2.2.14. Analysis of PAMP-induced gene expression	36
2.2.15. Root growth inhibition assays	36
2.2.16. Pathogen infection assays	37
2.2.17. Statistical data analysis	38

3. Results	39
3.1. Identification of PUB22 candidate targets	39
3.1.1. Yeast two-hybrid screen to identify candidate PUB22 interactors	39
3.1.2. Interaction analysis of PUB22 with additional subunits of the exocyst complex by yeast two-hybrid assay	43
3.1.3. Yeast assay to test the ability of <i>Exo70B2</i> to complement yeast <i>exo70</i> deficiency	44
3.2. Analysis of the impact of PUB22 candidate targets on plant immunity	45
3.2.1. Generation of T-DNA insertion mutants of candidate PUB22 targets	45
3.2.2. ROS-burst assays of candidate PUB22 interactor mutants	46
3.2.3. Pathogen growth assays with candidate PUB22 interactor mutants	47
3.2.4. Gene expression profile upon elicitor treatment of candidate PUB22 interactors	50
3.3. Confirmation of the interaction between PUB22 and Exo70B2	51
3.3.1. Confirmation of the interaction of PUB22 and Exo70B2 by bimolecular fluorescence complementation	51
3.3.2. Confirmation of the PUB22-Exo70B2 interaction by coimmunoprecipitation	54
3.3.3. Analysis of a physical interaction of PUB22 and Exo70B2 by <i>in vitro</i> pull-down	55
3.3.4. Interaction analysis of Exo70B2 with PUB23 and PUB24 using bimolecular fluorescence complementation	56
3.4. Analysis of flg22-dependent PUB22 protein stabilization	58
3.4.1. HA-PUB22 protein accumulation after transient overexpression in <i>Nicotiana benthamiana</i> and <i>Arabidopsis thaliana</i> mesophyll protoplasts	58
3.4.2. Time-course analysis of HA-PUB22 protein accumulation after flg22 elicitation or proteasome inhibition	60
3.5. Analysis of the ubiquitination and degradation of Exo70B2 by PUB22	63
3.5.1. <i>In vitro</i> ubiquitination of Exo70B2 by PUB22	63
3.5.2. Analysis of PUB22-mediated Exo70B2 degradation by bimolecular fluorescence complementation	64
3.5.3. Expression of cMyc-Exo70B2 in wild type and <i>pub22/23/24 Arabidopsis thaliana</i> mesophyll protoplasts	67
3.6. Characterization of the PAMP-triggered responses and disease resistance of <i>exo70B2</i> mutants	69
3.6.1. Isolation of two independent <i>exo70B2</i> T-DNA insertion lines and generation of a <i>pub22/23/24/exo70B2</i> quadruple mutant	69
3.6.2. Analysis of PAMP-triggered responses of <i>exo70B2</i> mutants	71
3.6.3. Disease resistance analysis of <i>exo70B2</i> mutants	78
3.7. Functional redundancy analysis of the <i>Exo70B2</i> homolog <i>Exo70B1</i>	83
3.7.1. Generation of two independent <i>exo70B1</i> T-DNA insertion lines and an <i>exo70B1/exo70B2</i> double mutant	83
3.7.2. Analysis of PAMP-triggered responses of <i>exo70B1</i> mutants	85
3.7.3. Disease resistance analysis of <i>exo70B1</i> mutants	87

4. Discussion	89
4.1. PUB22 targets the vesicular trafficking component Exo70B2 to downregulate PTI signaling	89
4.2. Additional potential target proteins of PUB22 suggest a specialization in the regulation of vesicular trafficking	99
4.3. Additional defense response pathways potentially targeted by PUB22	103
4.4. The function of PUB22 is regulated by posttranslational protein stabilization.....	104
4.5. Working model for the function of PUB22 and Exo70B2 in regulating PTI responses	108
5. Summary	110
6. Zusammenfassung	111
7. Bibliography	112
8. Appendix	130

List of Abbreviations

μM	micromolar	M	molar
μm	micrometer	MBP	maltose-binding protein
AD	activation domain	MDa	Mega Dalton
ADP	Adenosine diphosphate	MES	2-(<i>N</i> -morpholino)ethanesulfonic acid
AEBSF	4-(2-Aminoethyl) benzenesulfonyl fluoride hydrochloride, protease inhibitor	MG132	26S-proteasome inhibitor
AM114	26S-proteasome inhibitor	min	minutes
ARM	armadillo-like repeats	mM	millimolar
ATP	adenosine triphosphate	mRNA	messenger RNA
Avr	avirulence	MS	Murashige and Skoog
BD	binding domain	MVB	multivesicular bodies
<i>Bgh</i>	<i>Blumeria graminis forma specialis hordei</i>	NADPH	nicotinamide adenine dinucleotide phosphate
CBB	coomassie brilliant blue	NB-LRR	nucleotide-binding leucine-rich repeat
cDNA	complementary DNA	nM	nanomolar
CFP	cyan fluorescent protein	nm	nanometer
cfu	colony forming units	nYFP	N-terminal part of YFP
CoIP	coimmunoprecipitation	OD600	optical density at 600nm
Col-0	Wild type <i>Arabidopsis</i> ecotype Columbia-0	PAGE	polyacrylamide gel electrophoresis
ctrl	control	PAMP	pathogen-associated molecular pattern
cYFP	C-terminal part of YFP	PCR	polymerase chain reaction
dai	days after inoculation	Pfu	proofreading DNA Polymerase
DMSO	dimethyl sulfoxide	PR	Pathogenesis related
DNA	deoxyribonucleic acid	PRR	pattern recognition receptor
DTT	dithiothreitol	PSL	photostimulated luminescence
<i>E. coli</i>	<i>Escherichia Coli</i>	<i>Psm</i>	<i>Pseudomonas syringae</i> patovar <i>maculicola</i>
EDTA	ethylenediaminetetraacetic acid,	<i>Pst</i>	<i>Pseudomonas syringae</i> patovar <i>tomato</i>
EE	early endosome	PTI	PAMP-triggered immunity
EF-Tu	translation elongation factor Tu	PUB	plant U-box protein
elf18/elf26	18/26 amino acid peptide derived from EF-Tu	<i>pub22/23/24</i>	<i>pub22/pub23/pub24</i> triple mutant plants
ER	endoplasmic reticulum	PVDF	polyvinylidene fluoride
ETI	effector-triggered immunity	qRT-PCR	quantitative real-time PCR
ETS	effector-triggered susceptibility	R-gene	resistance gene
EV	empty vector	RE	recycling endosome
flg22	22 amino acid peptide derived from flagellin	RFP	red fluorescent protein
g	9,81 m/s ² (gravitation force)	RLK	receptor-like kinase
GFP	green fluorescent protein	RLU	relative light units
GST	glutathione-S-transferase	RNA	ribonucleic acid
h	hours	ROS	reactive oxygen species

HCl	hydrochloric acid	RP	right primer
HECT	homologues to the E6AP carboxyl terminus	s	seconds
HEPES	4-(2-hydroxyethyl)-1-piperazineethanesulfonic acid	S.D.	standard deviation
His	histidine	S.E.M.	standard error of the mean
<i>Hpa</i>	<i>Hyaloperonospora arabidopsidis</i>	SD	single dropout
HR	hypersensitive response	SDS	sodium dodecyl sulfate
hrp	horseradish peroxidase	<i>Taq</i>	<i>Thermus aquaticus</i>
IP	immunoprecipitation	TEMED	tetramethylethylenediamine
IPTG	isopropyl β -D-1-thiogalactopyranoside	TGN	trans-Golgi network
JA	jasmonic acid	Trp	tryptophane
KB	Kings broth	TTSS	type III secretion system
kDa	kilo Dalton	UBC	ubiquitin conjugating (E2-conjugating enzyme)
LB	Luria-Bertami		
LE	late endosome	UMS	ubiquitin modification system
LP	left primer	UPS	ubiquitin proteasome system
LRR	leucine-rich repeat	WT	wild type
Leu	leucine	YFP	yellow fluorescent protein
log ₁₀	decadic logarithm		

1. Introduction

1.1. Plant immunity

Plants are in a constant interaction with microorganisms, which can coexist with plants in a symbiotic relationship or have a pathogenic lifestyle in which they exploit host resources. Numerous plant pathogens colonize plant tissues in a parasitic manner, extracting nutrients and causing disease. However, the world is green and disease is rather the exception, not the rule. The reason is that plants have evolved a sophisticated immune system to detect and fend-off pathogens.

The first layer of immunity consists of preformed mechanisms such as the plant cell wall or its cuticle. When microbes can overcome this barrier, additional resistance mechanisms are induced. The plant immune system has many molecular similarities to the immune system of animals but also important differences. In mammals the key players for immunity are specialized immune cells, such as T lymphocytes and B lymphocytes. Plants do not have adaptive immunity but in contrast to animals every single cell is capable of sensing the presence of a microbe and mounting a defense response (Nürnberger et al., 2004). Detailed understanding of plant immunity is important for the future to reduce crop losses by pests and provide sustainable agriculture to supply an ever growing world population.

Plant induced immunity can be conceptually divided into two branches. The first branch of induced immunity is called pathogen-associated molecular pattern (PAMP)-triggered immunity (PTI) or microbe-associated molecular pattern (MAMP)-triggered immunity (MTI). PAMPs or MAMPs are defined as invariant epitopes within molecules that are fundamental to the pathogens fitness, widely distributed among different microbes, absent in the host and recognized by a wide array of potential hosts (Schwessinger and Zipfel, 2008). PAMPs are in most cases integral components of microbial surface structures. Examples include the bacterial flagellin, the protein building up the filament of eubacterial flagella (Felix et al., 1999), chitin, an important cell-wall component of fungi (Walker-simmons et al., 1983), peptidoclycanes from gram positive bacteria (Gust et al., 2007) and lipopolysaccharides from gram negative bacteria (Dow et al., 2000; Newman et al., 2002). In addition, intracellular proteins can also be

recognized as PAMPs. An example is the bacterial translation elongation factor EF-Tu (Kunze et al., 2004).

The recognition of PAMPs takes place at the cell surface and is carried out by plasma membrane localized pattern recognition receptors (PRRs). A well characterized PRR is the flagellin receptor flagellin sensing 2 (FLS2) in *Arabidopsis thaliana* (Gómez-Gómez and Boller, 2000), a leucine-rich repeat receptor-like kinase (LRR-RLK), which recognizes a highly conserved 22 amino acid peptide, flg22 (Felix et al., 1999). Another example is the *Arabidopsis thaliana* EF-Tu receptor (EFR) (Zipfel et al., 2006), that binds EF-Tu's first 18 to 26 amino acids of its N-terminus (elf18, elf26) (Kunze et al., 2004). Interestingly, EFR is Brassicaceae specific and is not present in solanaceaeous plants such as *Nicotiana benthamiana* (Boller and Felix, 2009). Chitin is perceived in *Arabidopsis* by the receptor chitin elicitor receptor kinase 1 (CERK1), which belongs to a class of receptors with an extracellular carbohydrate-binding module, the LysM domain (Petutschnig et al., 2010; Lizasa et al., 2010). The CERK1 paralogs LYM1 and LYM3 are involved in the recognition of peptidoglycans. They were demonstrated to bind peptidoglycans, which are structurally similar to fungal chitin (Willmann et al., 2011).

After ligand binding FLS2 and EFR almost instantly heterodimerize with the regulatory protein BRI1-associated kinase 1 (BAK1) (Chinchilla et al., 2007) which induces auto and transphosphorylation of FLS2 and BAK1 to trigger downstream signaling events (Schulze et al., 2010; Roux et al., 2011). BAK1 is not involved in the binding of the ligands, however, it is required for the full activation of the receptor complex, as *bak1* mutants are less responsive to flg22 and elf18 (Chinchilla et al., 2007). In contrast to FLS2 and EFR, CERK1 is strictly independent of BAK1 as chitin still elicits PTI responses in *bak1* mutants (Gimenez-Ibanez et al., 2009). An additional kinase associated with the receptor complex is BAK1-interacting kinase 1 (BIK1). BIK1 associates with FLS2 and BAK1 and transphosphorylates both RLKs. BIK1 is also phosphorylated by BAK1 and *bik1* mutants were shown to have reduced PTI responses upon flg22 treatment and increased susceptibility to bacterial pathogens, showing that BIK1 is an important positive regulator of PTI (Lu et al., 2010).

After PAMP-induced receptor complex formation downstream signaling processes are triggered. The cellular responses after flg22 recognition are illustrated in Figure 1-1. Seconds after flg22 recognition ion fluxes across the membrane are prompted, which result in an increase of the intracellular calcium concentration (Jeworutzki et al., 2010). Changes in calcium concentration probably contribute to PAMP-triggered signal transduction by activating downstream calcium-

dependent kinases. Minutes after perception the production of reactive oxygen species (ROS) is triggered (Torres et al., 2002). Interestingly, Ca^{2+} influx and ROS production are independent, suggesting that PAMP-triggered signaling branches very early to activate the respective downstream responses (Jeworutzki et al., 2010). The main enzyme involved in the PAMP-triggered ROS production is the membrane localized NADPH-oxidase respiratory burst oxidase homologue D (RbohD) (Mersmann et al., 2010). ROS are thought to function as signaling compounds. They can trigger stomatal closure to limit the invasion of additional pathogens (Torres, 2010). It was also shown that ROS induces the activity of the oxidative burst-induced kinase 1 (OXI1) and other kinases required for the full activation of defense responses (Rentel et al., 2004; Nakagami et al., 2006). Mitogen-activated protein kinase (MAPK)-cascades are important for the cellular signal transduction to activate downstream PTI responses such as the transcriptional reprogramming of the cell. MPK3 and 6 are positive regulators of PTI, while MPK4 is a negative regulator (Suarez-Rodriguez et al., 2007, Gao et al., 2008).

Later PTI responses (>30min) include the transcriptional activation of defense related genes. Upregulated genes after PAMP perception include At4g20780, which is a predicted calcium binding protein highly upregulated after flg22 treatment (Navarro et al., 2004). Other induced genes include the RbohD and WRKY transcription factors. The WRKY transcription factors are downstream phosphorylation targets of MPKs. An example is WRKY33, which was identified as a substrate of MPK3 and MPK6 in *Arabidopsis* (Mao et al., 2011). WRKY33 was shown to be phosphorylated by MPK3 and 6 at multiple residues in response to *Borerytis cinerea* infection. This promotes the expression of phytoalexin deficient 3 (PAD3) which is required for full induction of camalexin production (Mao et al., 2011). PAD3 is a cytochrome P450 enzyme and carries out the last step of camalexin biosynthesis, which is the major phytoalexin of *Arabidopsis* (Böttcher et al., 2009). Phytoalexins are toxic compounds released into the apoplast and were first associated with defense against insects, however, further studies showed an involvement in plant resistance to fungal and bacterial pathogens as well (Bednarek, 2012). Additional WRKY transcription factors important for immunity include WRKY11, 22 and 29. WRKY22 and WRKY29 are positive and WRKY11 is a negative regulator of innate immunity (Eulgem and Somssich, 2007).

Hours after PAMP perception the biosynthesis of the β 1,3-Glucan polymer callose is detectable. Callose is proposed to reinforce cell walls and therefore hypothesized to limit further colonization of the plant by attacking microbes (Jacobs et al., 2003). However, loss of function

mutants of the PAMP- and wound-induced callose biosynthesis enzyme Glucan synthase-like 5 (GSL5) are paradoxically more resistant to adapted fungal pathogens (Jacobs et al., 2003).

PTI significantly contributes to plant immunity, which was demonstrated by Zipfel and colleagues. They showed that flg22 elicitation not only triggers an instant PTI response but also protects plants from later infections with virulent bacteria (Zipfel et al., 2004).

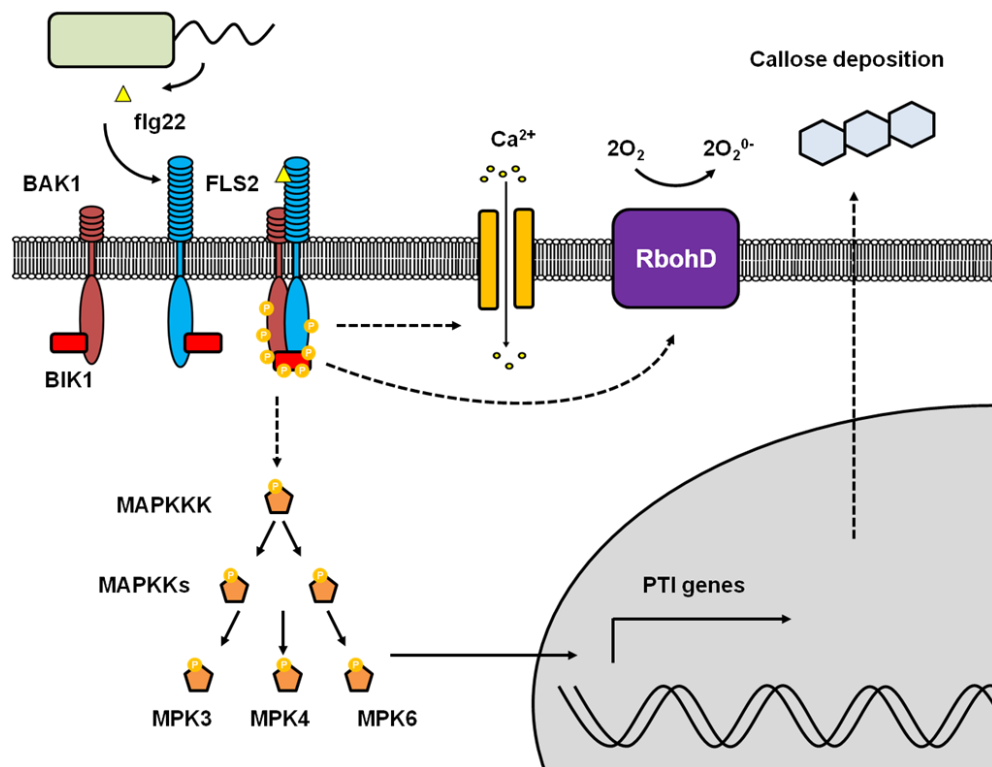


Figure 1-1 Scheme of PAMP-triggered responses: The bacterial flagellin peptide flg22 is recognized by the receptor FLS2. Binding of flg22 to FLS2 induces complex formation with the regulatory protein BAK1, which results in receptor transphosphorylation to trigger signaling. BIK1 interacts with FLS2 and BAK1 and flg22 triggers BIK1 phosphorylation, which in turn transphosphorylates BAK1 and FLS2 to enhance signaling. Calcium ion influx takes place, ROS production by RbohD is activated and a MPK cascade is triggered resulting in the phosphorylation of MPK3, 4 and 6 (early responses). The cell is transcriptionally reprogrammed and callose deposition is induced (late responses). P = Phosphorylation, Ca^{2+} = calcium ions. Dashed lines indicate functional connection.

However, some specialized pathogens can overcome PTI to colonize the host and cause disease. To do so they have evolved effector molecules that can block various PTI pathways. The tomato and *Arabidopsis thaliana* hemibiotrophic bacterial pathogen *Pseudomonas syringae* pv *tomato* (*Pst*) for example uses the type three secretion system (TTSS) to deliver effector proteins into the plant cell (Guo et al., 2009). *Pst* enters plant leaves through stomata, multiplies

in the intercellular space (apoplast), and eventually produces necrotic lesions that are often surrounded by chlorotic halos (Buell et al., 2003). The TTSS is a needle-like structure that connects the plant and the bacterial cytosol. Effectors carry an N-terminal signal required for their translocation (Mudgett et al., 2000). *Pst* secretes about 60 different effectors which are transported into the plant cell (O'Brien et al., 2011). Oomycete pathogens, such as the strictly biotrophic *Arabidopsis thaliana* downy mildew pathogen *Hyaloperonospora arabidopsidis* (*Hpa*) or the causal agent of potato late blight disease, the hemibiotrophic pathogen *Phytophthora infestans*, use a different mechanism to transport effectors into their host. Many oomycete effectors carry a characteristic RxLR amino acid motif (R = arginine, x = any amino acid, L = leucine) and are likely secreted from the extra haustorial matrix and translocated into the plant cell (Torto et al., 2003). However, the exact translocation mechanism remains to be unraveled. There are also apoplastic effectors that affect extracellular targets such as plant secreted proteases and glucanases (Kamoun, 2006).

Fungal pathogens can have very different lifestyles, ranging from biotrophy to necrotrophy. Fungal pathogens also secrete apoplastic effectors or such that are translocated into the plant cell. Effectors have been identified in pathogens with all types of lifestyles (Deller et al., 2011). For translocated effectors no widely conserved translocation motif has been discovered. However, a degenerated Y/FWxC (Y = tyrosin, F = phenylalanine, W = tryptophane, C = cysteine) motif discovered in the biotrophic powdery mildew pathogen *Blumeria graminis* forma specialis *hordei* (*Bgh*) was recently proposed to be conserved among intracellular non-necrotrophic ascomycetes (Godfrey et al., 2010). The exact molecular function of translocated effectors of all different pathogen species can be very different. Important examples are effectors with E3-ubiquitin ligase activity or those interfering with the host ubiquitination system. They will be discussed in more detail in section 1.4.2.2.

To counter effector manipulation, plants have evolved intracellular immune sensors that enable them to mount a second layer of induced defense which is known as effector-triggered immunity (ETI). These sensors are the products of disease resistance (R)-genes. They typically encode nucleotide-binding leucine-rich repeats (NB-LRR) or Toll-interleukin receptor-like (TIR)-NB-LRR proteins (Jones and Dangl, 2006), which sense effector activity and trigger ETI. For instance, the *Arabidopsis thaliana* genome is predicted to encode approximately 125 R-genes. ETI is often accompanied by localized cell death of infected cells which prevents disease spreading. This reaction is part of the so called hypersensitive response (HR) and is used by the plant to fend off biotrophic or hemibiotrophic pathogens such as *Hpa* or *Pst*.

Effectors that are directly or indirectly recognized by R-gene products are historically called *avirulence* (Avr) proteins because they conferred resistance against the pathogen strain carrying it (Jones and Dangl, 2006). A well characterized example is the recognition of the *Pst* effector AvrRpm1 in *Arabidopsis thaliana*. AvrRpm1 induces the phosphorylation of the immune regulatory protein *resistant to Pseudomonas syringae* pv. *maculicola* 1 (RPM1)-interacting protein 4 (RIN4) using the cytoplasmic RIN4-interacting protein kinase (RIPK) (Liu et al., 2011). The phosphorylation of RIN4 is recognized by the NB-LRR resistance protein RPM1 which triggers ETI (Mackey et al., 2002).

In an arms race, pathogens evolve ever more effectors to circumvent PTI and plants on the other hand evolve new resistance proteins to detect effectors and trigger ETI. Evolution drives pathogens to lose ETI-triggering effectors and/or to produce new effectors that either block ETI or evade recognition (Jones and Dangl, 2006).

1.2. Vesicular trafficking in plant immunity

Membrane compartmentalization and vesicular trafficking via the endomembrane system are important processes in all eukaryotic cells. The degree of complexity of the system is even higher in plants in comparison to mammals or yeast (Jurgens, 2004). Plant cells contain several Golgi stacks per cell, distinct storage and lytic vacuoles and different vesicle trafficking routes to those in mammals (Robatzek, 2007; Jurgens, 2004). The importance of vesicular trafficking in the plant response to pathogen attacks has become more and more evident in the last decade. Vesicular trafficking plays important functions at various stages to fend off pathogen invasions. Components of the secretory pathway were described to be involved in the regulation of immune responses (Bednarek et al., 2010). Of note, the endosomal trafficking of receptors has emerged as a key process in the regulation of plant immunity (Beck et al., 2012).

The first evidence that vesicular trafficking plays an important role in plant immunity was given by the involvement of the secretory pathway in these processes. Secretion of defense related secondary metabolites, peptides or proteins was shown to be essential to deploy resistance in many plant pathogen interactions (Bednarek et al., 2010).

Approximately 60 genes in the *Arabidopsis thaliana* genome encode soluble N-ethylmaleimide-sensitive factor adaptor protein receptors (SNAREs). SNAREs can be divided into two categories: vesicle-SNAREs (*v*-SNAREs), which are incorporated into the membranes of transport vesicles during budding, and target or *t*-SNAREs, which are located in the membranes of target compartments. The primary function of SNAREs is to mediate vesicle fusion required for exocytosis. The *t*-SNARE Penetration 1 (PEN1)/SYP121 is an important protein involved in the resistance of *Arabidopsis thaliana* to penetrating fungal powdery mildew pathogens (Collins et al., 2003). PEN1 was isolated in a screen for *Arabidopsis penetration (pen)* mutants that fail to mount a full extracellular defense response against non-adapted powdery mildew pathogens. PEN1 focally accumulates at the sites of attempted penetration and forms a ternary complex with the synaptosome-associated membrane protein of 33 kDa (SNAP33) and the vesicle-associated membrane proteins 721 (VAMP721) and VAMP722 to mediate vesicle fusion (Kwon et al., 2008). Potential cargos of the transported vesicles are precursors of callose or GSL5, the enzyme responsible for the pathogen-induced callose biosynthesis (Jacobs et al., 2003). Callose is important to form papillae-like cell wall fortification structures underneath the attempted penetration site of the pathogen. Two other *pen* mutants are also impaired in secretion upon non-adapted powdery mildew infection. PEN3 is a plasma membrane localized ABC-transporter which also accumulates focally at sites of attempted penetration (Dittgen et al., 2006). PEN2 is a myrosinase which releases glucosinolates from indolglucosinolates (Bednarek et al., 2009). PEN2 and PEN3 act on the same genetic pathway which implies the hypothesis that PEN3 produces antimicrobial glucosinolates that are secreted to the apoplast via the ABC-transporter PEN2 (Bednarek et al., 2010).

During the defense response of the plant against invading pathogens, pathogenesis-related (PR) proteins are secreted. It was shown that the SNARE protein SYP132 is involved in the transport of PR1a into the apoplast of *Nicotiana benthamiana* (Kalde et al., 2007), suggesting that SYP132 is the cognate receptor for exocytosis of vesicles containing PR proteins.

Vesicular trafficking is not only important for the secretion of defense related compounds to the apoplast. Also surface localized PRRs and other plasma membrane proteins associated with immunity, as for example NADPH oxidases, are delivered to their destination membrane via the endomembrane system to fulfill their function. They are synthesized in the endoplasmic reticulum (ER) and are folded and matured in the ER and the Golgi apparatus before being transported via exocytic vesicles to the plasma membrane. In addition, surface proteins are constantly being endocytosed and transported back to the plasma membrane in a recycling

process that also involves distinct transport processes via the endomembrane system (Jurgens, 2004).

Defects in maturation, folding or transport can cause impairments in immune responses. Examples are the *priority in sweet life 1* (*psl1*) and *psl2* mutants, that are impaired in elf18 responses, but not in flg22 responses (Saijo et al., 2009). The *PSL2* gene encodes an UDP-glucose:glycoprotein glucosyltransferase (UGGT) and *PSL1* the ER-resident lectin-like chaperon calreticulin 3 (CRT3). These proteins are required for the correct N-glycosylation and maturation of EFR. In *crt3* and *uggt* mutants the exocytic delivery of EFR is blocked, resulting in its degradation via the ER quality-control (ERQC) with the consequence of reduced elf18 responsiveness. Another group independently showed that additional ER residing proteins are required for elf18 responses. These include the ER resident stromal-derived factor 2 (SDF2) which is involved in ERQC. The *sdf2* loss of function mutants show a reduced accumulation of EFR and are less responsive to elf18. Flg22 responses are also not affected in these mutants, which is probably due to different N-glycosylation events. Loss of function of the N-glycosylation enzyme staurosporin and temperature sensitive 3A (STT3A) are also compromised in elf18 responses but unaffected in flg22-triggered signaling (Nekrasov et al., 2009).

Vesicular trafficking is also associated with the regulation of PAMP-triggered signaling and its attenuation. An example is the flagellin receptor FLS2, which upon activation by flg22 is endocytosed (Robatzek et al., 2006). In *Arabidopsis* lines expressing a functional FLS2-GFP fusion the protein localizes to the plasma membrane in its inactive state. 30 minutes upon flg22 treatment the GFP signal diminishes from the plasma membrane and relocalizes to vesicles (Robatzek et al., 2006). FLS2 enters the endomembrane system and is transported via ARA7-containing early endosomes (EE) and ARA6-containing late endosomes (LE)/multivesicular bodies (MVBs) to the vacuole for degradation. This potentially represents an attenuation mechanism of FLS2 signaling (Beck et al., 2012). Importantly, FLS2 enters two distinct endomembrane trafficking routes depending on its activation status. Non-activated FLS2 is constantly being endocytosed and transported back to the membrane in a Brefeldin A (BFA)-sensitive manner. BFA is a fungal toxin which inhibits the transport of EEs to the trans-Golgi network (TGN) and vice versa by targeting the ADP ribosylation factor-guanine nucleotide exchange factor (ARF-GEF) GNOM (Steinmann, 1999). However, upon flg22 recognition FLS2 enters a distinct endomembrane trafficking route insensitive to BFA but sensitive to other inhibitors, such as Wortmanin, an inhibitor of LE/MVB transport to the vacuole and Concanamycin A, which inhibits the transport from the TGN to LEs (Beck et al., 2012).

The importance of vesicular trafficking for plant immunity is further supported by the fact that it can be targeted by effectors of successful pathogens. An example is the ARF-GEF MIN7, which is targeted by the *Pst* effector HopM1 for proteasomal degradation (Nomura et al., 2006). Interestingly, BFA treatment can restore the virulence function of HopM1 in *Pst* strains expressing a non-functional version of the protein (Nomura et al., 2006). In a later study, MIN7 was isolated in a screen to identify mutants impaired in PIN1 recycling (Tanaka et al., 2009). PIN1 is a member of the PIN-formed family of proteins which exhibit polar localization in plant cells and facilitate the cellular efflux of the plant hormone auxin (Zazimalová et al., 2007). PIN1 recycling is dependent on GNOM (Geldner et al., 2003). These mutants were called *BFA-visualized endocytic trafficking (ben)* mutants and *ben1* was identified by map-based cloning as MIN7. BEN1/MIN7 was shown to localize to the TGN/EE distinct from GNOM-positive endosomes and was identified to be required for mediating early endosomal trafficking (Tanaka et al., 2009).

Other examples for the involvement of secretion in plant immunity arise from studies showing the requirement of the vacuole to establish HR after recognition of *Pst* (Hatsugai et al., 2009). This non canonical secretion involves the fusion of a large vacuolar compartment with the plasma membrane and the release of toxic compounds to the apoplast to kill bacterial invaders. This membrane fusion is suppressed under normal conditions but is triggered after recognition of the *Pst* effectors AvrRpm1 by RPM1 and AvrRpt2 by *resistant to Pseudomonas syringae 2* (RPS2) in a proteasome-dependent manner and involving the proteasome subunit PBA1 (Hatsugai et al., 2009).

1.3. The plant exocyst complex

As mentioned in section 1.2, SNARE-mediated fusion of vesicles is essential for exocytosis. However, upstream components are required to mediate the initial interaction between vesicles and their specific acceptor membrane. This process is called vesicle tethering and involves an octameric protein complex, termed the exocyst. It consists of the subunits Sec3, Sec5, Sec6, Sec8, Sec10, Sec15, Exo84 and Exo70. It was first identified in yeast (TerBush et al., 1996) and

homologs for all subunits of the complex could be identified later in all other eukaryotic systems, including plants (Elias, 2003).

In Yeast, six of the exocyst subunits, Sec5p, Sec6p, Sec8p, Sec10p, Sec15p and Exo84p are associated with the vesicle, while the remaining two components, Exo70p and Sec3p, are associated with the target membrane and are thought to mediate the specific recognition of the complex at the destination site (Boyd et al., 2004). The association of Exo70p and Sec3p with the plasma membrane occurs by an interaction of both proteins with phosphoinositides (Zhang et al., 2008; He et al., 2007). Crystal structure analysis of several exocyst subunits revealed that they all display similar rod-like structural organization, composed of two or more consecutively packed α -helical bundles (Munson and Novick, 2006). This is interesting as they do not share a high degree of sequence homology (He and Guo, 2009). A high degree of structural homology is shared in yeast by the C-terminus of Exo84p and the N-terminus of Exo70p (Dong et al., 2005).

In yeast and mammals, all exocyst subunits are encoded by a single gene. However, in *Arabidopsis* this is only true for Sec6 and Sec8. Other subunits such as Sec3, Sec5 and Sec10 are encoded by two genes, Exo84 by three genes and for Exo70 by 23 different homologous genes in the *Arabidopsis thaliana* genome (Elias, 2003; Cvrčková et al., 2012). In rice the number of Exo70 genes is even higher with 42 homologs. The plant specific expansion of the number of Exo70 genes suggests either that different Exo70 genes are expressed during development and/or in different tissues that perform identical functions or that different Exo70 genes have adopted additional or new functions, most likely participating in plant-specific types of exocytosis (Zhang et al., 2010).

The function of the exocyst complex in yeast has been mainly linked with the tethering of post-Golgi vesicles to the plasma membrane to mediate polarized secretion (Zhang et al., 2010). A first example in plants demonstrates the involvement of the exocyst in the pollen-stigma interaction of *Brassica napus*. Exo70A1, a homolog of the yeast Exo70p, was shown to be required for the acceptance of compatible pollen. It was identified as an interactor of the ARM-containing E3-ubiquitin ligase ARC1, a positive regulator of self-incompatibility (Stone et al., 2003). The pathway seems to be conserved in *Arabidopsis* as *exo70A1* mutants reject pollen in a way comparable to the self-incompatibility reaction (Samuel et al., 2009). Exo70A1 is thought to be required for the polarized secretion of compatibility factors. Exo84b, one of the three homologs of yeast Exo84p in *Arabidopsis*, was shown to be involved in cell plate maturation and

cytokinesis. GFP-tagged Exo84b accumulates at the cell plate during its initiation and maturation phase. The *exo84b* mutants are dwarfed and highly compromised in functional cell division (Fendrych et al., 2010). In the same study GFP-Exo70A1 also localized to the cell plate.

A recent study suggests an involvement of the exocyst complex in plant immunity. Two Exo70 homologs, Exo70B2 and Exo70H1, were shown to be involved in the resistance of *Arabidopsis thaliana* to *Pseudomonas syringae* pathovar *maculicola* (*Psm*). The *exo70B2* and *exo70H1* mutants were demonstrated to be more susceptible to *Psm* infection and, in addition, the cellular responses of the mutants to *Bgh* infection were altered. Both proteins were also shown to interact with the Sec5a and Sec15b exocyst subunits in yeast two-hybrid experiments, suggesting that Exo70B2 and Exo70H1 are functional components of the complex (Pecenková et al., 2011).

1.4. The ubiquitin modification system

The ubiquitin modification system (UMS) is the machinery that mediates the enzymatic attachment or removal of ubiquitin, a 76 amino acid barrel-shaped protein. It was first described about 30 years ago and its discovery was awarded with the Nobel Prize in chemistry in 2004 (http://www.nobelprize.org/nobel_prizes/chemistry/laureates/2004/). Ubiquitin is highly conserved among all eukaryotes and the amino acid sequence of yeast and human ubiquitin shares 96% sequence identity. The name ubiquitin is derived from the adjective “ubiquitous” meaning that “it exists everywhere at the same time and is continuously encountered and widespread”. The covalent addition of ubiquitin molecules is a fundamental process and was first described as a “kiss and death” signal to determine proteins for degradation (Ciechanover et al., 1980; Hershko et al., 1980). However, it is now known that ubiquitination is not only a degradation signal and that it is involved in the regulation of almost all aspects of cellular physiology including the regulation of plant immunity at various steps (Trujillo and Shirasu, 2010; Furlan et al., 2012).

The ubiquitination process is divided into three steps (Vierstra, 2009). In the initiation step, ubiquitin is activated in an ATP-dependent manner and attached to an active cysteine residue of the E1 activating enzyme via a thiol-ester bond. In the second step, the ubiquitin-E1 complex interacts with an E2 conjugating enzyme and the ubiquitin moiety is transferred to the E2 by a switch of thiol-ester bonds, which is independent of ATP. In the final step of the reaction an E3-ubiquitin ligase is recruited to the E2 enzyme. At the same time the E3 ligase binds the target protein and thus determines the specificity of the reaction. Ubiquitin is transferred to the target protein via an isopeptide linkage using the ϵ -amino-group of a lysine residue (Figure 1-3).

E3-ubiquitin ligases have been in the center of attention in the last years as they confer the specificity of the ubiquitination process by determining the target proteins. Depending on their structure and the mechanism of ubiquitin transfer they can be categorized into four classes, the monomeric ligases which include the U-box-, really interesting new gene (RING)- and homologous to the E6AP carboxyl terminus (HECT)-type ligases and the Cullin-RING-ligase (CRL)-type multimeric ligases (Vierstra, 2009). They consist of a Cullin protein, a RING-box (RBX) protein and different adaptors for specific target interactions. S phase kinase-associated protein 1 (SKP1)-Cullin1 (CUL1)-E-box (SCF) ligases consist of a SKP1 subunit and a F-box protein, while BTB ligases have a Bric-a-brac-tramtrack-broad complex subunit (BTB) to interact with a designated target (Trujillo and Shirasu, 2010; Vierstra, 2009). U-box, RING and CRL ligases act as scaffolds to bring the target into close proximity with the E2 enzyme and thus mediate the transfer of ubiquitin to the target. By contrast, HECT ligases catalyze the transfer of ubiquitin by binding ubiquitin in an intermediate step.

In the contrast to the RING domain, which is stabilized by binding of Zn^{2+} ions to a regular spacing of conserved cysteine and histidine residues, the U-box domain is stabilized by intramolecular salt bridges and hydrogen bonds (Aravind and Koonin, 2000). U-box-type E3-ubiquitin ligases consist of an N-terminal U-box domain which mediates the interaction with the E2-ubiquitin complex (Aravind and Koonin, 2000). In plants, U-box proteins frequently contain armadillo-like (ARM) repeat domains at their C-terminus (Nielsen et al., 2012). These domains are responsible for specific protein-protein interactions with a target. Proteins belonging to this class of E3 ligases are called plant U-box proteins (PUBs) and are unique to plants. They will be discussed in more detail in section 1.4.1.

Ubiquitin can be conjugated to a target protein as a monomer or as chains of different lengths linked by any one of its seven lysine residues. The linkage type and grade is responsible for the

fate of ubiquitinated proteins. Proteins that contain ubiquitin binding motifs recognize specific chain-type conformations and thus determine the fate of the target. Lysine48-linked ubiquitin chains display a tightly packed conformation, while lysine63-linked chains have a more relaxed conformation (Ikeda et al., 2010). As an example, the proteasome receptor protein RPN13/ARM1 was shown to stoichiometrically bind to lysine48-linked di-ubiquitin through its C-terminal Pleckstrin-like receptor for ubiubiquitin (PRU) domain (Schreiner et al., 2008; Husnjak et al., 2008). Attachment of lysine48-linked ubiquitin chains is the most prevalent form of ubiquitination and the recognition of this chain-type is involved in the targeting of proteins to the 26S-proteasome for degradation. The 26S-proteasome is a large 2,5 MDa multi-subunit protein complex which is present in the nucleus and the cytoplasm of eukaryotic cells (Vierstra, 2009). In *Arabidopsis thaliana* 6% of all encoded genes are associated with the ubiquitin-proteasome system, which is the cellular machinery for the ubiquitin-dependent degradation of proteins (Finley, 2009; Figure 1-2).

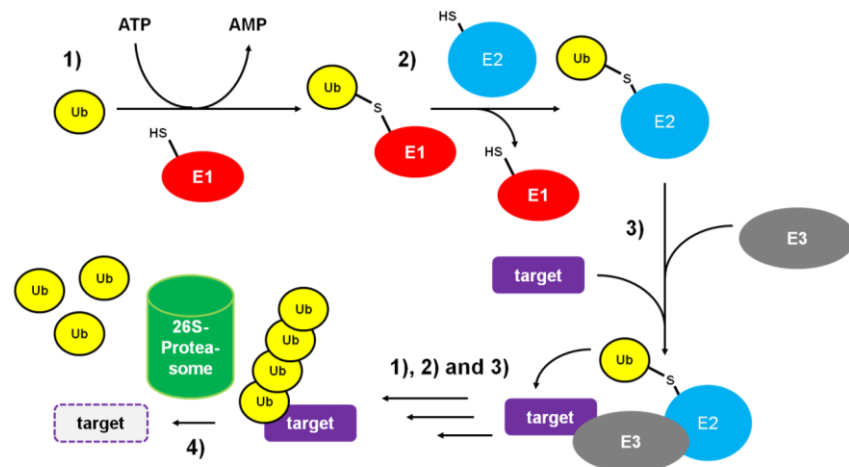


Figure 1-2 Scheme of ubiquitination resulting in proteasomal degradation: (1) Activation of ubiquitin in an ATP-dependent manner by the E1 activating enzyme. (2) Transfer of the ubiquitin moiety to the E2 conjugating enzyme. (3) E3-ubiquitin ligase is recruited and it binds specifically to a target. Ubiquitin is transferred to the target. Several rounds of ubiquitin addition result in a target with lys48-linked polyubiquitin chain. (4) The target is degraded by the 26S-proteasome. Single ubiquitin molecules are released and can be reused.

By contrast, proteins labeled with lysine63-linked polyubiquitin chains have a different fate. This chain-type of ubiquitination was shown to have a crucial role in receptor endocytosis and DNA damage repair processes (Ikeda et al., 2010; Haglund and Dikic, 2012). An example is the epidermal growth factor (EGF) receptor (EGFR). In the presence of high concentrations of its ligand EGF, EGFR is labeled by lysine63-linked polyubiquitin chains, which leads to the lipid-

raft-dependent endocytosis of the receptor (Sigismund et al., 2005). By contrast, low concentrations of EGF induce clathrin-dependent endocytosis. The different internalization routes were shown to affect the fate of EGFR and thus the duration of receptor signaling (Sigismund et al., 2008). EGFR being endocytosed in a clathrin-dependent manner is preferentially recycled, while lipid-raft-dependent endocytosis results in receptor degradation. Another type of ubiquitination is monoubiquitination, which is also associated with the regulation of plasma membrane protein endocytosis. An example is the *Arabidopsis thaliana* iron-regulated transporter 1 (IRT1) which is monoubiquitinated at two cytosolic residues, promoting its endosomal uptake (Barberon et al., 2011).

Ubiquitination is a reversible modification. Enzymes catalyzing the detachment of ubiquitin are called deubiquitinating enzymes (DUBs) which exhibit distinct specificity profiles towards the various ubiquitin chain-types (Clague et al., 2012). Furthermore, DUBs can be associated to the proteasome, allowing some substrates to escape degradation (Finley, 2009).

1.4.1. Plant U-box proteins (PUBs)

Plant U-box proteins (PUBs) are a major class of E3-ubiquitin ligases in plants. The U-box gene family has undergone a large gene expansion suggesting a specialization of these proteins in biological processes specific to plants (Yee and Goring, 2009). Two and 21 U-box genes were identified in the yeast and human genome respectively, compared to 64 and 77 genes in *Arabidopsis thaliana* and rice (Azevedo et al., 2001; Zeng et al., 2008). 64% of all PUBs belong to a class of proteins with additional C-terminal ARM repeats (Mudgil et al., 2004) and the majority of PUBs for which a biological function has been elucidated belong to this subclass (Yee and Goring, 2009). Some U-box-ARM PUBs contain an additional N-terminal domain, termed U-box N-terminal domain (UND) with unknown function.

PUBs can be involved in diverse biological processes, ranging from self-incompatibility to the regulation of symbiosis and plant immunity (Yee and Goring, 2009). One of the first identified PUBs with a distinct biological function was ARC1 which is essential for the rejection of self-pollen in *Brassica napus*. Knockdown lines of ARC1 were shown to be compromised in self-incompatibility (Stone, 1999). ARC1 was shown to be phosphorylated by the S receptor kinase

(SRK), which is required for the interaction with ARC1 (Gu et al., 1998). Later studies suggested the conservation of this pathway in *Arabidopsis thaliana*. The S-domain RLKs *Arabidopsis* receptor kinase 1 (ARK1) and ARK2 were able to phosphorylate the *Arabidopsis* ARC1-homologs PUB9 and PUB13 *in vitro* (Samuel et al., 2008).

Recent studies suggested the involvement of a UND-PUB in the establishment of symbiosis with nitrogen-fixing bacteria in the roots of *Medicago truncatula* (Mbengue et al., 2010). PUB1 was localized by cell fractionation experiments to the plasma membrane and identified as an interactor of lysin motif RLK3 (LYK3), a putative RLK for *Sinorhizoiium meliloti* Nod factors. PUB1 was shown to possess autoubiquitination activity and to be phosphorylated by LYK3. However, PUB1 did not affect levels of LYK3 when both proteins were transiently expressed in *Nicotiana benthamiana* and also *in vitro* ubiquitination of LYK3 by PUB1 was not detected. Nevertheless, overexpression and knockdown experiments suggested that PUB1 is a negative regulator of infection and nodulation by *S. meliloti* (Mbengue et al., 2010), but the mechanism of its function remains unclear.

Recently, different PUBs were identified as important regulators of plant immunity. Trujillo and colleagues (2008) showed that the three *Arabidopsis thaliana* homologs PUB22, PUB23 and PUB24 are negative regulators of PTI. Two additional PUBs, PUB12 and PUB13 are also involved in the downregulation of PTI by mediating FLS2 turnover (Lu et al., 2011). The regulation of PTI by the respective PUBs will be discussed in more detail in sections 1.4.2.1 and 1.4.3.

PUB22 and PUB23 from *Arabidopsis thaliana* were also shown to be involved in drought stress and ABA responses (Cho et al., 2008). Overexpression of PUB22 and PUB23 resulted in enhanced sensitivity to drought stress, while T-DNA knockout mutants were more tolerant. The authors suggest that PUB22 is localized in the cytoplasm and that it interacts with and ubiquitinates RPN12a, a subunit of the proteasome (Cho et al., 2008). A recent publication indicates that PUB22 and PUB23's function in drought stress is independent of ABA (Seo et al., 2012). In the same publication two additional PUBs, PUB18 and PUB19 were identified and shown to also be involved in drought stress response. By contrast, PUB18 and PUB19 function was ABA-dependent. In addition, *pub18/pub19* double mutants were compromised in ABA-dependent stomatal closure (Seo et al., 2012).

1.4.2. Ubiquitination in plant immunity

Ubiquitination is a key process in most defense response pathways. E3-ubiquitin ligases were identified as components of PTI, ETI and defense hormone signaling (Trujillo and Shirasu, 2010). In addition, important pathogen effectors can mimic E3-ubiquitin ligase activity or were shown to manipulate the host ubiquitination machinery, further demonstrating the importance of this post-translational modification for plant immunity.

1.4.2.1. Regulation of plant immune response pathways by ubiquitination

Jasmonic acid (JA) is an important phytohormone majorly required for defense against necrotrophic pathogens and flower development (Glazebrook, 2005; Wasternack et al., 2013). Coronatine-insensitive 1 (COI1) is an F-box protein which functions as the JA receptor and associates with SKP1 and CUL1 to form the SCF^{COI1} E3-ubiquitin ligase complex. COI1 was the first component of the ubiquitination system shown to play a role in plant immunity (Xie, 1998). The *Arabidopsis coi1* mutant was originally identified because of its insensitivity to the bacterial toxin coronatine, which is a JA analog. It was later shown to be required for all JA-dependent responses and *coi1* mutants were shown to be more susceptible to necrotrophic pathogens (Thomma et al., 1998). COI1 binds a JA-isoleucine conjugate (JA-Ile) which induces the interaction between COI1 and its targets, the JA ZIM domain (JAZ) repressor proteins (Chini et al., 2007; Thines et al., 2007). Interaction with COI1 leads to the ubiquitination of JAZ and the consequent degradation by the 26S-proteasome. JAZ degradation results in the transcriptional activation of JA induced genes (Thines et al., 2007). An example for a JA responsive gene is *plant defensin 1.2* (PDF1.2) (Glazebrook, 2005).

Salicylic acid (SA) is a phytohormone important for the immune response against biotrophic pathogens and is antagonistic to the JA-induced pathway. *Pst* infection, for example, triggers the rapid accumulation of SA which is accompanied by the transcriptional activation of *pathogenesis-related* (PR) genes (Glazebrook, 2005). A function of ubiquitination in SA signaling was recently shown by the identification of nonexpressor of PR genes 3 (NPR3) and NPR4 as SA receptors. Both proteins have SA binding capacity and contain BTB domains which act as adaptors for the CUL3-E3-ubiquitin ligase complex BTB^{NPR3/NPR4}. NPR3 and NPR4

mediate the degradation of NPR1, a close homolog which is essential for SA dependent responses and the induction of SA-induced systemic acquired resistance (SAR) (Fu et al., 2012). Although NPR1 was excluded as a SA receptor by Fu and colleagues (2012), this finding was challenged by a study showing that NPR1 has significant SA binding capacity in the presence of copper ions (Wu et al., 2012), suggesting that NPR1 may also act as a receptor for SA.

In the absence of pathogens NPR1 resides in the cytoplasm as an oligomer. Oligomerization is mediated by redox-sensitive intermolecular disulphide bonds (Mou et al., 2003). SA accumulation upon pathogen infection was shown to change the intracellular redox potential. NPR1 monomers are consequently released by reduction of the disulphide bonds. A bipartite nuclear localization sequence targets the released NPR1 monomers to the nucleus where they bind to transcriptional repressors such as TGACG motif-binding factor 2 (TGA2) to negate their function and to induce defense related gene expression (Kinkema et al., 2000; Boyle et al., 2009). Interestingly, NPR1 turnover has been shown to be required for its function in the induction of programmed cell death or SAR (Spoel et al., 2009).

Ubiquitination also plays important functions in the regulation of ETI responses. An example is the F-box protein constitutive expressor of PR genes 1 (CPR1) in the regulation of NB-LRR receptor-mediated defense responses in *Arabidopsis thaliana*. CPR1 interacts with both NB-LRR proteins suppressor of NPR1-1 constitutive 1 (SNC1) and RPS2, controlling their turnover and thus preventing autoimmune responses (Ti et al., 2011). The tobacco and tomato PUB CMPG1 was identified based on its rapid induction upon Avr9 elicitation in tobacco and tomato. Avr9 is a peptide and perceived by the Cf9 receptor-like protein, which induces HR. Tomato CMPG1 knockdown lines were shown to be more susceptible to the biotrophic fungal pathogen *Cladosporium fulvum* (Gonzalez-Lamothe et al., 2006).

An example for ubiquitination involved in PTI responses is the *Xanthomonas oryzae* pv *oryzae* resistance 21 (Xa21), an RLK in rice. Xa21 is the receptor for the type I secreted peptide Ax21 which is highly conserved among *Xanthomonas* species (Lee et al., 2009). Xa21 confers resistance to *Xanthomonas oryzae* pv *oryzae* and interacts with and phosphorylates the RING E3-ubiquitin ligase Xa21-binding protein 3 (XB3). Reduced expression of XB3 results in lower protein levels of Xa21 and decreased resistance to the avirulent *X. oryzae* pv. *oryzae* (Wang et al., 2006).

In the last couple of years it became evident how important the involvement of ubiquitination is for the regulation of PTI signaling. A recent study showed that PUB12 and PUB13 are important regulators of FLS2 signaling. Both E3-ubiquitin ligases associate with BAK1 and are recruited to the receptor complex upon flg22 perception. They are consequently phosphorylated by BAK1 and ubiquitinate FLS2 (Lu et al., 2011). Flg22 induces endocytosis and degradation of the activated FLS2 receptor (Robatzek et al., 2006). In *pub12/pub13* mutants, FLS2 degradation upon flg22 treatment is impaired (Lu et al., 2011). This results in an enhanced sensitivity of *pub12/pub13* to flg22 treatment and an increased resistance to *Pst* and *Psm*, showing that PUB12 and PUB13 contribute to PTI signal attenuation by mediating FLS2 turnover. Three additional important regulators of PTI signaling, PUB22, PUB23 and PUB24, will be discussed in more detail in section 1.4.3.

1.4.2.2. Manipulation by effectors involving the ubiquitin modification system

Manipulation of host defense or metabolism is often associated with the ubiquitination activity of the respective effector proteins. An example is VirF produced and secreted by *Agrobacterium tumefaciens*. VirF was the first identified prokaryotic F-box protein. *Agrobacteria* manipulate host cells by integrating bacterial DNA into the chromosomal DNA, which leads to the development of tumorigenic tissue called crown gall disease (Schrammeijer et al., 2001). Bacterial DNA is bound to the two pathogen proteins VirD2 and VirE2 and to the host protein VIP1. This complex is transported into the plant nucleus, where the effector VirF assists in the uncoating of DNA for integration into the host chromosome. VirF associates with *Arabidopsis* SKPs to form a SCF^{VirF} complex to target VIP1 and VirE2 for proteasomal degradation (Tzfira et al., 2004).

Two well characterized examples of *Pst* effectors that manipulate host defense are AvrPto and AvrPtoB, two sequence distinct effectors promoting virulence on *Arabidopsis thaliana*. AvrPto and AvrPtoB both associate with BAK1 and interfere with its binding to FLS2, thus inhibiting PTI signaling at the very first step, namely PAMP-induced receptor complex formation (Shan et al., 2008). The C-terminus of AvrPtoB has homology to plant U-box/RING domains and is an active E3-ubiquitin ligase (Janjusevic et al., 2006). In its host tomato AvrPtoB ubiquitinates Fen, which is a kinase required for resistance (Rosebrock et al., 2007). In *Arabidopsis thaliana* AvrPtoB ubiquitinates the kinase domains of FLS2 and CERK1 and promotes the degradation of the

receptors. In the case of FLS2, degradation is sensitive to proteasome inhibition (Göhre et al., 2008) and in the case of CERK1 it is sensitive to bafilomycin A (Gimenez-Ibanez et al., 2009), which is an inhibitor of vacuolar degradation. This might suggest different preferences for degradation pathways of receptors targeted by AvrPtoB. However, degradation of FLS2 by the proteasome is unlikely as it is an integral membrane protein.

Another example for an effector with E3-ubiquitin ligase activity was recently identified by Singer and colleagues (2013). They characterized the *Xanthomonas campestris* pv. *vesicatoria* effector XopL and could show that it exhibits E3-ubiquitin ligase activity *in vitro* and *in planta*. Furthermore the effector was shown to induce plant cell death and to inhibit PAMP-induced gene expression. Interestingly, this effector was found to contain a novel C-terminal fold, termed the XL-box, which is not present in any previously characterized E3 ligase (Singer et al., 2013).

Other effectors have been shown to affect the host ubiquitination system by interfering with host enzymes to modify their function. Examples are the effectors Avr3a from the oomycete *Phytophthora infestans* and AvrPiz-t from the fungal pathogen *Magnaporthe oryzae*. Avr3a contributes to the virulence of *Phytophthora infestans* in its biotrophic phase on potato by stabilizing the host E3-ubiquitin ligase CMPG1, a negative regulator of Infestin 1 (INF1)-triggered cell death (Bos et al., 2010). CMPG1 degradation depends on the ubiquitin-proteasome system and Avr3a inhibits the degradation by modifying CMPG1 E3-ubiquitin ligase activity. AvrPiz-t is translocated into cells where it suppresses PTI. It interacts with AvrPiz-t-interacting protein 6 (APIP6), a functional RING E3-ubiquitin ligase. In contrast to Avr3a, AvrPiz-t destabilizes APIP6 which is involved in basal disease resistance. RNAi knockdown lines of APIP6 showed reduced PTI responses and reduced resistance to a virulent *Magnaporthe oryzae* strain (Park et al., 2012).

1.4.3. Negative regulation of PTI by PUB22, PUB23 and PUB24

PUB22, PUB23 and PUB24 are three closely related proteins with a high degree of sequence identity (Mudgil et al., 2004) (Figure 1-3). They consist of an N-terminal U-box domain and four C-terminal ARM-like repeats. The first 75 amino acids of PUB22 build up its U-box domain while the amino acids 76 to 435 represent the four ARM domains of the protein. All three proteins are

close homologs of the *Nicotiana benthamiana* CMPG1, a positive regulator of disease resistance (Gonzalez-Lamothe et al., 2006). PUB22, PUB23 and PUB24 belong to a separate clade from PUB12 and PUB13 and lack a UND domain (Mudgil et al., 2004).

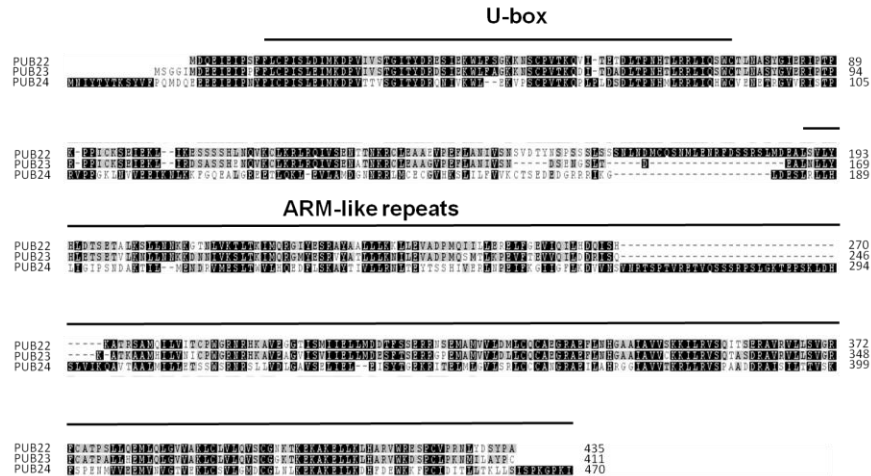


Figure 1-3 Protein sequence alignment of PUB22, PUB23 and PUB24: Sequence alignment was performed using geneious® software. U-box domains and ARM-like repeats are indicated. Colors of highlighted residues indicates grade of conservation: black (conserved in all three proteins), grey (conserved in two proteins).

PUB22, *PUB23* and *PUB24* were shown to be highly transcriptionally induced after treatment of *Arabidopsis* seedlings with flg22 (Navarro et al., 2004; Trujillo et al., 2008). To get more insight into the function of the triplet in plant immunity knockout mutants were characterized for their responses to different PAMPs. They showed increased and prolonged production of ROS after treatment with flg22 (Figure 1-4 A), demonstrating that the PUBs are negative regulators of PTI signaling. The effect was additive as double mutants showed stronger effects than single mutants and the strongest response was measured in the *pub22/23/24* triple mutant. Triple mutants were also more responsive to additional PAMPs, such as chitin and elf18, as well as the danger-associated molecular pattern (DAMP) Pep1. The general nature of the enhanced PTI signaling suggests that the PUBs regulate a cellular process involved in the signaling mediated by different PRRs. Downstream signaling events were also affected and the activity of MPK3 was specifically prolonged in *pub22/23/24* upon flg22 treatment. The transcriptional induction of defense marker genes was also enhanced after flg22 elicitation and the enhanced PAMP responsiveness resulted in an increased disease resistance phenotype of the mutants. The *pub22/23/24* mutants were more resistant to *Pst* (Figure 1-4 B) and *Hpa* infections. *In vitro* ubiquitination experiments revealed that PUB22 (Figure 1-4 C), PUB23 and PUB24 are active

E3-ubiquitin ligases (Trujillo et al., 2008) as shown by their autoubiquitination activity. However, *in vivo* substrates of the ligases were not yet identified and the mechanism by which PUBs regulate PTI responses remains to be unraveled.

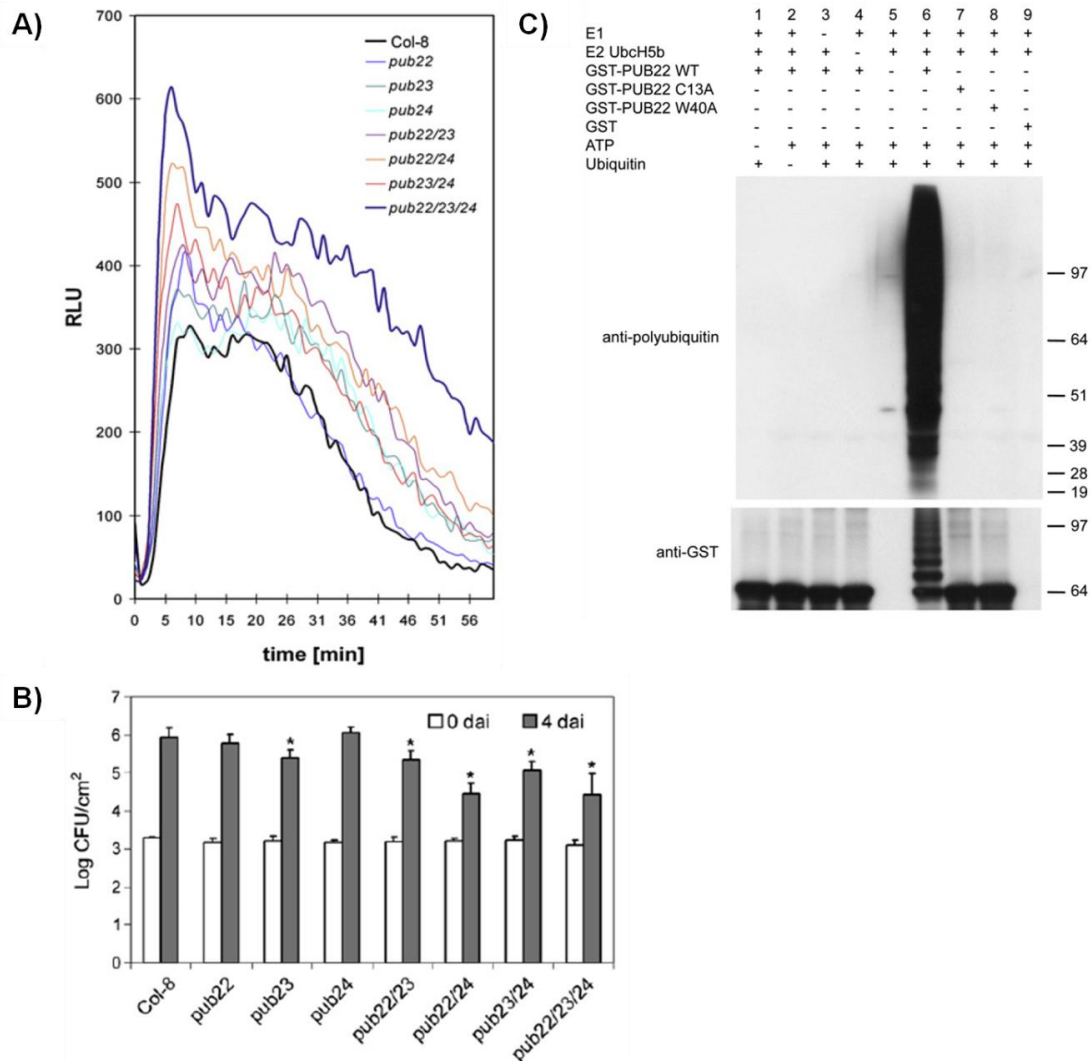


Figure 1-4 PUB22, PUB23 and PUB24 are negative regulators of PTI and possess autoubiquitination activity: (A) *pub22/23/24* triple mutants show an increased and prolonged oxidative burst after treatment of leaf discs with 500nm flg22. (B) *pub22/23/24* triple mutants are more resistant after spray infection of plants with 5×10^8 cfu/ml *Pst* DC3000. (C) PUB22 possesses autoubiquitination activity *in vitro* (Trujillo et al., 2008).

1.5. Aim of the present work

In previous studies by Trujillo and colleagues (2008) the three closely related proteins PUB22, PUB23 and PUB24 were identified as negative regulators of PTI. However, nothing is known about ubiquitination targets of the PUBs or the mechanism of their function. To obtain insight into the cellular processes regulated by the PUBs, a yeast two-hybrid screen was performed to gain information about candidate targets. For the screen PUB22 was used as a bait, because genetic data indicated that it is the most important ligase, together with PUB24, for the observed PTI signaling and disease resistance phenotypes in the *pub22/23/24* mutants (Trujillo et al., 2008). Several candidate PUB22 interactors were isolated from the screen (section 3.1.1).

The aim of the present work was to identify targets of PUB22 with a function in plant immunity. Therefore we aimed to perform reverse genetics to obtain first insights on a potential impact of candidate PUB22 interactors on PTI signaling and plant immunity. Candidates that showed a phenotype and therefore are important for plant immunity were consequently subjected to further detailed characterization, including biochemical and cell biological analysis of the interaction with and ubiquitination by PUB22, potential regulatory mechanisms and a detailed analysis of the candidate's function in PTI signaling and plant immunity. In doing so, we aimed to identify the cellular pathways that are targeted and regulated by PUB22-mediated ubiquitination

2. Materials and Methods

2.1. Materials

2.1.1. Chemicals

All chemicals were used in analytical quality, if not specified differently. Chemicals and antibiotics used in this study were ordered from Merck KGaA (Darmstadt, Germany), SIGMA Aldrich (St. Louis, USA), Carl Roth (Karlsruhe, Germany), Serva (Heidelberg, Germany) and BioRad (Hercules, USA). Plant, yeast and bacterial media ingredients were ordered from Difco (Lawrence, USA), Duchefa (Haarlem, Netherlands) and Carl Roth. Enzymes were distributed by Fermentas (Waltham, USA), Promega (Fitchburg, USA) and Invitrogen (Carlsbad, USA). Soluble and immobilized antibodies were ordered from SIGMA Aldrich, Santa Cruz Biotechnologies (Santa Cruz, USA), Miltenyi Biotec (Bergisch Gladbach, Germany) and Clontech (Saint-Germain-en-Laye, France). Elf18 and flg22 peptides were synthesized by Davids Biotechnologie (Regensburg, Germany). Primers were distributed by MWG (Ebersberg, Germany).

2.1.2. Media

Luria-Bertani medium (LB Medium)

- Yeast extract (5g/l), Tryptone (10g/l), NaCl (5g/l)
- For solid medium 15g/l Agar were added

Kings broth medium (KB Medium):

- Peptone (20g/l), K_2HPO_4 (1,5g/l), $MgSO_4 \cdot 5H_2O$ (1,5g/l), Glycerol (10ml/l)
- For solid medium 15g/l Agar were added

YEB Medium

- Beef extract (5g/l), yeast extract (1g/l), peptone (5g/l), sucrose (5g/l), $MgCl_2$ (0,5g/l)

Murashige and Skoog (MS) Medium:

- MS Salts including vitamins (4,4g/l), MES (0,5g/l), Sucrose (10g/l); pH 5,6 (adjusted with KOH)
- For solid medium 5g/l Phyto Agar was added; For root growth assays Gelrite agar was used

2.1.3. Plants

Arabidopsis thaliana ecotype Columbia (Col-0) and the respective mutant lines were grown under short day condition (20°C, 8 hours light, 16 hours dark) in growth cabinets (Percival) or a growth chamber. For propagation and crossings plants were grown under long day conditions (20°C, 16 hours light, 8 hours dark) in a green house. Sowed seeds were stratified for 2 days at 4°C in the dark. Sterile plants were grown either in liquid MS or on MS-agar plates in a growth cabinet under short day conditions (20°C, 8 hours light, 16 hours dark). T-DNA insertion mutants of candidate PUB22 targets were ordered from NASC (Nottingham, UK). *pub22/23/24* triple mutant lines were generated by Dr Marco Trujillo (Trujillo et al., 2008). The *fls2* mutants were provided by Dr Kohki Yoshimoto (INRA, France). *Nicotiana benthamiana* plants for transient transformation assays were grown under long day conditions (20°C, 16 hours light, 8 hours dark) in a growth chamber or greenhouse.

2.1.4. Bacteria

For cloning work and plasmid preparation the *Escherichia coli* (*E. coli*) strain Top10 (Invitrogen) was used. For expression of recombinant fusion proteins the strain BL21 (DE3) pLyss (Invitrogen) was used. Top10 and BL21 (DE3) pLyss cells were grown on LB-Medium supplemented with the appropriate antibiotics (100µg/ml Ampicillin, 50µg/ml Kanamycin, 100µg/ml Spectinomycin and/or 34µg/ml Chloramphenicol) at 37°C. For *Agrobacterium*-mediated transient transformation of *Nicotiana benthamiana* the strain GV3101 was used. *Agrobacteria* were grown at 28°C in YEB Medium supplemented with the appropriate antibiotics, including Rifampicin (50µg/ml). For bacterial infection experiments *Pseudomonas syringae* pv *tomato* (*Pst*) isolate DC3000 (Whalen et al., 1991) or *Pst* DC3000 $\Delta avrPto/\Delta avrPtoB$ (Lin and

Martin, 2005) were used. *Pst* was grown on KB-Medium plates supplemented with 25µg/ml Kanamycin and 50µg/ml Rifampicin (*Pst* DC3000) or additional 50µg/ml Spectinomycin (*Pst* DC3000 $\Delta avrPto/\Delta avrPtoB$).

2.1.5. *Hyaloperonospora arabidopsidis*

For infection experiments with the oomycete pathogen *Hyaloperonospora arabidopsidis* (*Hpa*) the virulent isolate Emco5 was used (McDowell et al., 2005). Propagation was performed by a weekly repeated infection of two week-old *Arabidopsis thaliana* Col-0 seedlings grown on soil. Experiments with *Hpa* were performed by Ryan Anderson in the laboratory of John McDowell at Virginia Tec, USA.

2.2. Methods

2.2.1. Cloning

PUB22, PUB23, PUB24, Exo70B2 and Exo70A1 coding sequences were PCR amplified from *Arabidopsis thaliana* Col-0 cDNA. Total RNA was extracted using TriFast peqGOLD (Peqlab) following the manufacturer's instructions. 2 µg of DNaseI (Fermentas) treated RNA were reverse transcribed with Maxima Reverse transcriptase following manufacturer's instructions (Fermentas). PCR amplifications were performed using the primers listed in the Appendix, Table 3. 2µl cDNA were mixed with 0,5µl forward primer (100nM), 0,5µl reverse primer (100nM), 2,5µl 10x Pfu buffer (Fermentas), 0,5µl MgSO₄ (25mM), 0,1µl Pfu enzyme (1U) (Fermentas) and 18,9µl water. PCR was performed using 55-60°C annealing temperature and elongation at 72°C for 1 min per kilo-basepair.

The PCR product was analyzed via agarose gel electrophoresis (1% Agarose, 1xTAE buffer (40mM Tris-Acetat; 2mM EDTA pH8,5), purified (GeneJet gel extraction kit, Fermentas) and

cloned into pENTR using the pENTRTM/D-TOPO®-Cloning Kit (Invitrogen). Reactions were performed according to the manufacturer's protocol. PUB22^{ARM} and PUB22^{U-box} constructs were PCR amplified from pENTR-PUB22 and the U-box mutants PUB22^{C13A}, PUB23^{C18A} and PUB24^{C30A} were amplified from in constructs pGEX-4T-1, generated as previously described (Trujillo et al., 2008). All constructs were then cloned into pENTRTM/D-TOPO as described above. Based on the pENTR constructs LR reactions were performed using the LR ClonaseTM II enzyme mix (Invitrogen) to generate the required destination vectors. For bimolecular fluorescence complementation assays PUB22, PUB22^{U-box}, PUB22^{ARM}, PUB22^{C13A}, PUB23^{C18A} and PUB24^{C30A} were cloned into pESPYNE-gw to generate N-terminal cMyc-nYFP fusions (Ehlert et al., 2006). Exo70A1 and Exo70B2 were cloned into pESPYCE-gw to generate n-terminal cYFP fusions. For coimmunoprecipitation assays PUB22^{C13A} was cloned into pEARLEYGATE104 (Earley et al., 2006) to generate N-terminal YFP fusions and Exo70B2 was cloned into pGWB418 (Nakagawa et al., 2007) to generate N-terminal cMyc fusions. For PUB22 stabilization assays PUB22 and PUB22^{C13A} were cloned into pGWB415 (Nakagawa et al., 2007) to generate N-terminal HA fusions.

For *in vitro* pull-down assays and *in vitro* ubiquitination assays Exo70B2 was cloned into pMAL-c2X (New England Biolabs) to generate N-terminal MBP fusions via classical cloning. Exo70B2 CDS was amplified from pENTR-Exo70B2 with primers introducing 5'-SmaI and a 3'-XhoI restriction sites. The PCR product was first cloned into pJET (Fermentas), digested with SmaI and XhoI and introduced in the opened pMAL-c2X vector. Ligation was performed using T4 Ligase (Fermentas). GST-PUB22 and GST-PUB22^{C13A} fusions were generated by cloning into pGEX-4T-1 (Amersham) as previously described (Trujillo et al., 2008). All used constructs are listed in the Appendix, Table 4, including vector name, name and size of encoded fusion protein and selection conditions in bacteria.

2.2.2. Transformations

2.2.2.1. *E.coli*

E.coli strains were transformed using heat shock transformation. Competent cells (50µl) were thawed on ice and the appropriate plasmid was added. Cells were incubated on ice for 20 min

before applying a heat shock (42°C, 45sec). Cells were subsequently incubated for 2 min on ice and 200 µl of LB Medium were added. Cells were incubated with shaking (37°C, 45 min) before they were plated on LB Media supplemented with antibiotics.

2.2.2.2. *Agrobacterium tumefaciens*

Agrobacterium strain GV3101 was transformed using a cold-shock procedure. Competent cells (500µl) were thawed on ice before adding plasmid DNA (1µg). Cells were incubated for 30min on ice. Cold-shock was applied by shock-freezing the cells in liquid nitrogen. After freezing cells were incubated at 37°C for 5 min and then transferred to ice for additional 5 min. 500µl YEB Medium were added and cells were incubated with shaking (28°C, 3 hours) before being plated on LB medium supplemented with antibiotics.

2.2.2.3. Transient transformation of *Nicotiana benthamiana*

50ml YEB Medium supplemented with antibiotics was inoculated with *Agrobacterium* strain GV3101 carrying the plasmid of interest and incubated over night at 28°C with shaking to an OD₆₀₀ of 0,8. Bacteria were centrifuged (2800g, 15min) and washed in resuspension buffer (10mM MES pH 5,6; 10mM MgCl₂). Bacteria were pelleted again (2800g, 15min), resuspended in resuspension buffer and OD₆₀₀ was adjusted to 0,4. Acetosyringone was added (150µM) and the suspension was incubated with slight shaking (RT, 3-4 hours). Bacterial suspension was used to syringe infiltrate 2-3 week-old *Nicotiana benthamiana* leaves. 2 days after transformation leaf samples were harvested for protein extraction.

2.2.2.4. Transient transformation of *Arabidopsis thaliana* protoplasts

Protoplast isolation

Protoplast transformation was performed as previously described (Yoo et al., 2007). 4-5 well-expanded leaves from 5-7 week-old plants were stacked and the top and bottom part of the leaf stalk were removed with a razor blade. The leaves were cut into thin strips (<0,5mm) and dipped into 10ml enzyme solution (0,4M mannitol; 20mM KCl; 20mM MES pH5,7; 1,5% Cellulase R10 (Serva); 0,4% Macerozyme R10 (Serva); 10mM CaCl₂; 0,1% BSA). Dipped leaf strips were vacuum-infiltrated for 30 minutes and incubated in the dark for additional 3 hours. After incubation the enzyme solution containing the leaf strips was carefully shaken to release the protoplasts. An equal volume of W5 buffer (154mM NaCl; 125mM CaCl₂; 5mM KCl; 2mM MES pH5,7) was added to stop the digestion, the protoplasts were centrifuged (1min, 200g) and the supernatant was replaced by 10ml fresh W5. After incubation on ice for 40 min washing was repeated. After additional 40 minutes, supernatant was replaced by 10ml MMG solution (0,4M mannitol; 15mM MgCl₂; 4mM MES pH5,7).

Protoplast transformation

Protoplasts were mixed with plasmid DNA (10µg DNA per 100µl protoplasts) and PEG solution (0,2M mannitol, 0,1M CaCl₂, 40% PEG (Fluka)) was added (1,1 x the volume of protoplasts). After gently resuspending protoplasts were incubated at room temperature for 10 minutes. Transformation was stopped by adding W5 buffer (4,4 x the volume of protoplasts). Cells were centrifuged (1min, 200g), the protoplast pellet was resuspended in W1 buffer (0,5M mannitol; 20mM KCl; 4mM MES pH5,7)(1x the volume of protoplasts) and incubated in the dark over night before being subjected to subsequent analysis

2.2.2.5. Transient transformation of *Arabidopsis thaliana* epidermal leaf cells

Arabidopsis thaliana epidermal leaf cells were transformed using particle bombardment. Tungsten particles (25mg/ml in 50% glycerol) were treated with ultrasound before use to destroy clusters. For each shot 12,5µl tungsten particles were mixed with 0,5µg RFP reporter plasmid and a total of 1µg construct DNA. After mixing 12,5µl Ca(NO₃)₂ (1M) was added drop wise. The

solution was briefly treated with ultrasound (10sec) and incubated at room temperature for 10min. After centrifugation (1min, 12000g) particles were resuspended in 10 μ l water. Transformation was carried out using a custom-made particle gun (cabin 100mbar, Helium 8 bar).

2.2.3. Plasmid preparations

Depending on the amount of DNA required, plasmids were isolated from 5ml LB Medium cultures using Nucleobond® PC 20 Miniprep kit (Macherey Nagel) or from 500ml LB Medium cultures using Nucleobond® PC 500 Maxiprep kit (Macherey Nagel). Isolation was performed according to the manufacturer's protocol.

2.2.4. Yeast two-hybrid screen

Yeast two-hybrid screening was performed by Hybrigenics S.A. (Paris, France). The coding sequence for amino acids 76 to 435 of PUB22 (At3G52450) was cloned into pB27 as a C-terminal fusion to LexA (N-LexA-prolyl 4- hydroxylase-C) and transformed in yeast strain L40. The construct was used as bait to screen a random-primed *Arabidopsis* (WT Col-0) 1 week-old seedling cDNA library constructed into pP6 and transformed in yeast strain Y187. After mating 62,4 million clones (6,2-fold the complexity of the library) were screened. Prey fragments of the positive clones were amplified by polymerase chain reaction and sequenced at 5' and 3' junctions. The resulting sequences were used to identify the corresponding interacting proteins in the GenBank database (NCBI) using a fully automated procedure.

2.2.5. Yeast two-hybrid analysis and yeast complementation assays

Yeast two-hybrid analysis and yeast complementation experiments were performed by Tamara Pecenkova in the laboratory of Viktor Zarsky at the University of Prague (Czech Republic). The yeast two-hybrid assay employed the MATCHMAKER GAL4 two-hybrid system 3 (Clontech),

and all procedures were performed according to the manufacturer's protocols. Full-length PUB22 was cloned into pGAD, all other used constructs have previously been described (Fendrych et al., 2010; Pecenková et al., 2011a). *S. cerevisiae* strain AH109 was transformed with plasmid pairs and grown on -Leu/-Trp selective media. Colonies from double transformants were resuspended in 200µl of sterile water and 10µl plated onto -Leu/-Trp/-His/-Ade medium. Murine p53 and SV40 large T-antigen, provided by the manufacturer kit were used as a positive control, and a combination of empty pGBKT7 vector and pGAD-PUB22 was used as a negative control. For yeast complementation assays *Exo70B2* was subcloned from pENTR using BamHI and XhoI restriction sites into pVT103U, allowing the selection of transformants on SD-Ura medium and placing the cDNA under the constitutive ADH promoter. The obtained construct was used to transform *S. cerevisiae* temperature-sensitive mutant strain *exo70-38* that grows normally at 25°C but fails to grow above 35°C (He et al., 2007). The empty vector was used as a second control for transformation. Transformant colonies, approximately 1mm² in size, were resuspended in 200 µl of sterile water and 10µl were plated as two different dilutions onto -Ura medium. Yeasts were allowed to grow 2-4 days on both 28°C and 37°C.

2.2.6. Bimolecular fluorescence complementation

Constructs were transformed by microbombardment of *Arabidopsis thaliana* Col-0 epidermal cells of 4-5 week-old plants or by transformation of *Arabidopsis thaliana* Col-0 protoplasts. Transformation was carried out as described above (section 2.2.2.4/2.2.2.5). Treatments were applied as indicated 1 day post transformation. Reconstitution of split YFP was assessed by confocal laser scanning microscopy using a LSM710 (Zeiss) with the following settings: YFP excitation: 488nm, Emission band pass 505-550nm, RFP excitation: 543nm, Emission band pass 560-615nm.

2.2.7. Protein isolation from plants

To analyze protein expression in protoplasts cell samples were harvested after the indicated treatments by centrifugation (200g, 1 min), shock frozen in liquid nitrogen and resuspended in protein extraction buffer (50mM Tris-HCl pH 6,8; 4% SDS; 8M urea; 30% glycerol; 0,1M DTT;

0,005% Orange G). Samples were heated (65°C, 10min), centrifuged (10min, max speed) and supernatant was analyzed by SDS-PAGE and Western blot. SDS-PAGE was performed according to Laemmli (Laemmli et al., 1970) using discontinuous gel-electrophoresis with 10% separation gels (10% Acrylamide-bis; 0,375M Tris/HCl pH 8,8; 0,1% SDS; 0,2% TEMED; 0,04% APS), 5% stacking gels (5% Acrylamide-bis; 0,125M Tris/HCl pH 6,8; 0,1% SDS; 0,2% TEMED; 0,04% APS) and 1x running buffer (25mM Tris; 192mM glycine; 0,1% SDS). After electrophoresis protein samples were blotted on PVDF membranes (Whatman™, Maidstone, UK) using wet blotting (25 mM Tris; 192mM glycine; 20% Methanol; 0,01% SDS) for 1 hour (100V).

To check protein expression in *Nicotiana benthamiana* 3-4 leaf discs (0,125 cm²) were harvested, frozen and ground in liquid nitrogen. Proteins were isolated as described for protoplast samples.

cMyc-nYFP and cMyc fusion proteins were detected using anti-cMyc antibodies (SIGMA Aldrich), cYFP and YFP fusion proteins were analyzed by anti-GFP antibodies (Invitrogen) and anti-HA antibodies (SIGMA Aldrich) were used to detect HA fusion proteins. Equal loading was analyzed by staining the blots with Coomassie (10% Acetic acid; 40% ethanol; 0,025% Coomassie G-250) and subsequent destaining (10% Acetic acid; 20% methanol).

2.2.8. Coimmunoprecipitation

pGWB418-Exo70B2 and pEARLEYGATE104-PUB22^{C13A} were transformed in mesophyll protoplasts as described above. For immunoprecipitation 1mL of transfected protoplasts were pelleted (200g, 1min) and resuspended in extraction buffer (20mM HEPES; 50mM KCl; 2,5mM MgCl₂; 10μM ZnCl₂; 2,5mM EDTA; 5mM DTT; 0,1% Triton X100; 10μM AM114; 100μM AEBSF; 1mM NaF; 0,5mM Na₃VO₄; 15mM β-glycerophosphate; 1% Protease Inhibitor Cocktail). The Lysate was cleared by centrifugation (15,000g; 10min) and the supernatant was incubated with anti-cMyc-beads (Clontech) for 3h at 4°C with gentle shaking. Beads were collected and washed 5 times with extraction buffer. Proteins were eluted with 2x LDS buffer (12,5mM Tris HCl pH 6,8; 2,5%SDS; 20% Glycerol; 50mM DTT; 0,005% OrangeG) and analyzed by SDS-PAGE and Western blot using anti-cMyc (SIGMA Aldrich) and anti-GFP (Invitrogen) antibodies.

2.2.9. *In vitro* assays with recombinant proteins

2.2.9.1. Expression and purification of proteins from bacteria

Purification of GST-fusion proteins

pGEX-4T-1-PUB22, pGEX-4T-1-PUB22^{C13A} constructs were transformed in *E.coli* strain BL21 (DE3) pLyss as described above. 5 ml of LB Medium supplemented with 50µg/ml Ampicilin and 34µg/ml Chloramphenicol was inoculated with one bacterial colony containing each construct and incubated with shaking over night at 37°C. 3 ml overnight culture was used to inoculate 200ml fresh LB Medium (Ampicilin 50µg/ml; Chloramphenicol 34µg/ml) and incubation was continued with shaking at 37°C until an OD₆₀₀ of 0,8 was reached. Protein expression was induced by adding 0,1mM Isopropylthiogalactosid (IPTG) for 1-2 hours. Cells were harvested by centrifugation (4500g, 15min) and pellet was frozen in liquid nitrogen. 4ml of chilled (4°C) PBS (140 mM NaCl; 2,7 mM KCl; 10 mM Na₂HPO₄; 1,8 mM KH₂PO₄; pH 7,3; 1mM AEBSF; 1% Protease inhibitor cocktail (Calbiochem); 5mM DTT; 0,15% N-Lauroylsarcosine) was added and cells were resuspended by vortexing. Cells were lysed using sonication on ice (10min, 5s pulse; 3s pause, 60% output). TritonX-100 was added to a final concentration of 1,5% and the suspension was subsequently centrifuged (20000g, 10min). 100µl of Glutathione-resin (Machery Nagel; for GST-PUB22, GST-PUB22^{C13A}) was added to the supernatant and incubated slightly rotating for 30min at 4°C. Beads were pelleted by centrifugation (500g, 3min) and washed three times with 2-4 ml cold PBS buffer. Elution was performed by adding 60µl elution buffer (50 mM Tris-HCl pH 8,0; 15 mM reduced glutathione) and incubating the beads at 30°C for 10 minutes with slight rotation. Elution was repeated 3 times.

Purification of MBP-fusion proteins

pMAL-Exo70B2 construct was transformed in *E.coli* strain BL21 (DE3) pLyss as described above. 5 ml of LB Medium supplemented with 50µg/ml Ampicilin and 34µg/ml Chloramphenicol was inoculated with one bacterial colony containing each construct and incubated with shaking over night at 37°C. 3 ml overnight culture was used to inoculate 200ml fresh LB Medium (Ampicilin 50µg/ml, Chloramphenicol 34µg/ml) and incubation was continued with shaking at 37°C until an OD₆₀₀ of 0,3 was reached. Protein expression was induced by adding 1mM IPTG for 3 hours. AEBSF (100µM) was added and cells were harvested by centrifugation (4500g,

15min, 4°C) and pellet was frozen in liquid nitrogen. 4ml of chilled (4°C) column buffer (20mM Tris HCl pH7,4; 200mM NaCl; 1mM EDTA; 100µM AEBSF; 5mM DTT; 1 spatula tip Lysozyme 1) was added and cells were resuspended by vortexing. Cells were lysed using sonication on ice (10min, 5s pulse, 3s pause, 60% output) and suspension was subsequently centrifuged (12000g, 20min). 100µl of amylose-resin (New England biolabs) was added to the supernatant and incubated with rotation for 30min at 4°C. Beads were pelleted by centrifugation (350g, 3min) and washed three times with 2-4ml cold column buffer. Elution was performed by adding 60µl elution buffer (20mM Tris HCl pH7,4; 200mM NaCl; 1mM EDTA; 100µM AEBSF; 5mM DTT; 10mM maltose) and incubating the beads at 30°C for 10 minutes with gentle agitation. Elution was repeated 3 times.

2.2.9.2. *In vitro pull down assay*

For pull-down assays, recombinant MBP-Exo70B2 or MBP was expressed as described above and immobilized on amylose-resin (New England biolabs). Subsequently, bacterial lysates containing GST-PUB22 was added and co-incubated for 1h at 4°C with slight shaking. Elution was performed by adding elution buffer (20mM Tris HCl pH7,4; 200mM NaCl; 1mM EDTA, 100µM AEBSF; 5mM DTT; 10mM maltose) as described above. Proteins were analyzed by SDS-PAGE and Western blot. GST fusion proteins were detected using anti-GST antibodies (SIGMA Aldrich) and MBP fusion proteins were detected using anti-MBP antibodies (SIGMA Aldrich)

2.2.9.3. *In vitro ubiquitination assay*

Expression of GST-PUB22, GST-PUB22^{C13A} and MBP-Exo70B2 was performed as described above. Additionally, recombinant His-UBA1 and His-UBC8 were expressed and purified using Ni-Ted resin (Macherey-Nagel).

Purified proteins were used for *in vitro* ubiquitination assays. Each reaction of 30µl final volume contained 40mM Tris-HCl pH 7,4; 5mM MgCl₂; 50mM KCl; 2mM ATP; 1mM DTT; 10% glycerol; 200ng E1 His-UBA1; 200ng E2 His-UBC8; 500ng of E3s and 1µg of MBP-Exo70B2. The

reactions were incubated at 30°C for 3h and stopped by adding SDS-PAGE sample buffer and incubating for 5min at 65°C. Samples were separated by SDS-PAGE electrophoresis using 7% SDS-PAGE followed by detection of ubiquitinated substrate by Western-blotting. Polyubiquitinated proteins were detected using anti-ubiquitin antibodies (Santa Cruz biotechnologies), GST and MBP fusion proteins were detected using anti-GST and anti-MBP antibodies (SIGMA Aldrich).

2.2.10. Quantitative Real-Time PCR

Total RNA was extracted using TriFast peqGOLD (Peqlab) following the manufacturer's instructions. Two µg of DNaseI (Fermentas) treated RNA were reverse transcribed with Maxima Reverse transcriptase following manufacturer's instructions (Fermentas).

Real-Time quantitative PCR (qRT-PCR) was performed using the Maxima SYBR Green mix (Fermentas) in a CFX384 qPCR System (BioRad). Gene induction was calculated by using the BioRad software. Reaction volume was 20µl and contained 10µl of the reaction mix, 0,5nmol of each primer and 2µl of cDNA. PCR conditions were as follows: 2min incubation at 50°C and 3min denaturation at 95°C followed by 45 cycles of 95°C for 30s, 60°C for 10s and 72°C for 20s. Subsequently, a dissociation curve was performed. All reactions were carried out in triplicate.

2.2.11. Genotyping of T-DNA insertion mutants

2.2.11.1. DNA extraction from leaf material

For DNA extraction and PCR genotyping of *Arabidopsis thaliana* T-DNA insertion mutants a small leaf fragment was harvested (~5mm²) and ground in 150µl DNA-extraction buffer (1% Sarcosyl; 0,8M NaCl; 0,022M EDTA; 0,22M Tris-HCl pH 8,0; 0,8% CTAB; 0,14M Mannitol; 14µl/10ml β-Meraptoethanol). After grinding another 600µl extraction buffer and 750µl chloroform were added, mixed vigorously and incubated for 1 hour at 65°C. Afterwards samples were centrifuged (7500g, 10min) and 700µl isopropanol was added to the supernatant and

mixed. After centrifugation (7500g, 10min) the pellet was washed with 70% ethanol, dried and dissolved in 20µl water. 2µl of the isolated DNA was used for PCR genotyping.

2.2.11.2. Gene-specific PCR

Polymerase chain reaction (PCR) was used for gene specific genotyping of T-DNA insertion mutants. Primers for genotyping of candidate PUB22 target mutants are depicted in the Appendix, Table 5. PCR reactions were performed with an annealing temperature of 55-60 °C and elongation at 72°C for 1 minute per kilo-base pair. 2 µl of isolated DNA (2.2.11.1) was mixed with 0,5µl of each primer (either LP and RP combination to detect wildtype band or the respective LB/RP combination to detect T-DNA insertion), 2µl of 10x Taq-Polymerase buffer, 0,5µl dNTPs, 0,1 µL Taq-Polymerase (1U/µl) and 14,4 µl water before being subjected to PCR with the above described conditions.

2.2.12. ROS-burst assays

ROS production was measured using a luminol-based assay. Leaf discs (0,125 cm²) of 7 week-old *Arabidopsis thaliana* plants were carefully prepared and incubated over-night in 100 µl water in a 96-well titer plate using one leaf disc per well. The next day water was replaced by 50µl of a mixture containing horseradish peroxidase (hrp) (20µg/ml) and luminol (30µg/ml). 20 minutes after liquid replacement additional 50µl of the hrp/luminol mixture was added containing 1µM flg22 (final concentration 500nM), 1µM elf18 (final concentration 500nM) or 200µg/ml chitin (final concentration 100µg/ml). Immediately after addition of elicitors luminescence was measured using a 1450 Micro Beta Jet Luminescence Counter (Perkin-Elmer) with a signal integration time of 0,5s.

2.2.13. MAPK assays

MAPK activity assays were performed by Kazuya Ichimura from Kagawa University (Japan). MPK3, MPK4, and MPK6 antibodies and immunocomplex kinase assay were performed as previously described (Ichimura et al., 2006). Tissue samples of seedlings were frozen in liquid nitrogen, proteins were extracted and equal amounts of proteins were separated by SDS-PAGE, blotted onto a PVDF membrane and immune detected to determine Kinase amount. For kinase activity, immunoprecipitates were washed and kinase assays were performed in 20µl reactions containing myelin basic protein as a substrate. Phosphorylated myelin basic protein was separated by electrophoresis, blotted and visualized by autoradiography.

2.2.14. Analysis of PAMP-induced gene expression

Seedlings of Col-0 and the respective mutant lines were grown in liquid MS Medium under sterile conditions as described above. 14 day old seedlings were treated with 1µM flg22 for 1 hour and subsequently harvested and frozen in liquid nitrogen. Plant material was ground and RNA isolation, cDNA synthesis and qRT-PCR was performed as described above using the PTI marker gene primers depicted in the Appendix, Table 6.

2.2.15. Root growth inhibition assays

Seeds of the respective mutants were sterilized and grown on MS agar media plates. Seeds were stratified at 4°C for 2 days and grown for 5 days in short day condition vertically (8h light/16h dark). Seedlings were then passed on to square petri dishes with MS agar media supplemented flg22 (1µM) or DMSO (0,01%). Length of the main root was scored 7 days after transfer. Root growth was measured using Image J software.

2.2.16. Pathogen infection assays

2.2.16.1. *Pseudomonas syringae* pv *tomato*

Spray inoculation

For Bacterial growth experiments, six week-old *Arabidopsis thaliana* plants were spray inoculated with *Pseudomonas syringae* DC3000 (*Pst*) or *Pst* Δ *avrPto*/ Δ *avrPtoB*. Bacteria were grown for 3 days on KB medium plates supplemented with the appropriate antibiotics (*Pst*: 25 μ g/ml Kanamycin, 50 μ g/ml Rifampicin; *Pst* Δ *avrPto*/ Δ *avrPtoB*: 25 μ g/ml Kanamycin, 50 μ g/ml Rifampicin, 50 μ g/ml Spectinomycin). Bacteria were resuspended in water and the concentration was adjusted to 5×10^8 cfu/ml ($OD_{600} = 1$). After resuspension Silvet-L77 was added to a final concentration of 0,04%. Plants were copiously sprayed with the suspension and covered hermetically. 4 hours after spraying bacteria that entered the plant apoplast were counted after surface sterilization by washing the leaves in 70% ethanol for 20s and water for 30s. 4 days after inoculation the infection was scored by measuring bacterial growth.

4 plants per line were used for one experiment. At each time point 3 leaves per plant (total of 12 leaves) were harvested and four leaf discs were used for one data point. Leaf discs were ground in 1ml water and 100 μ l were plated on LB Media supplemented with 50 μ g/ml Rifampicin. 4 days after infection dilution series were performed in 96 well plates and 15 μ l of each dilution was plated to assess bacterial numbers. Colony-forming units (cfu) were counted 2 days after incubation of the plates at 28°C.

Flg22-induced protection assay

To analyze the flg22 induced protection effect on a posterior infection with *Pst*, leaves of six-week-old *Arabidopsis thaliana* plants were infiltrated with a solution of 100nM flg22 in water. 1 day after pretreatment plants were challenged by infiltrating the same leaves with 1×10^5 cfu/ml *Pst*. Preparation of bacteria and the assessment of growth was performed as described above.

2.2.16.2. *Hyaloperonospora arabidopsidis*

Hyaloperonospora arabidopsidis (*Hpa*) infections were performed by Ryan Anderson in the laboratory of John McDowell at Virginia Tec (USA). The virulent isolate Emco5 was used, which was propagated on *Ws-1* and *eds1-1 Arabidopsis* plants as described (McDowell, 2011). Sporangial suspensions of 5×10^4 spores/ml were applied with a Preval spray unit and the plants were kept under short day conditions. Plants were switched to 100% relative humidity six days post-inoculation to promote sporulation and scored two weeks after inoculation. Sporangiphore counts were performed with a dissecting microscope. For the visualization of cell death, plants were briefly boiled in a 50% ethanol trypan blue-lactophenol solution and cleared with chloral hydrate overnight.

2.2.17. Statistical data analysis

Significance of results was analyzed using Students T-Test implemented in Microsoft Excel software (Microsoft, Redmont, USA).

3. Results

3.1. Identification of PUB22 candidate targets

The three closely related PUB ligases PUB22, PUB23 and PUB24 act as negative regulators of PAMP-triggered immune responses (Trujillo et al., 2008). PUBs are E3-ubiquitin ligases and are therefore anticipated to mediate the ubiquitination of specific proteins. However, the ubiquitination targets of this PUB triplet and therefore the processes that they regulate remain unknown. The aim of this work was to identify targets of PUB22 which are involved in the regulation of immunity. In assays to test the PAMP responsiveness and the disease resistance of the E3 ligase mutants, *pub22/24* double mutants showed a stronger phenotype in comparison to *pub23/24* or *pub22/23* and the phenotype was comparable to that of the *pub22/23/24* triple mutant. We therefore decided to identify targets of PUB22, because the genetic data indicated that together with PUB24 it is the most important ligase for the regulatory function of the PUB triplet in plant immunity (Trujillo et al., 2008).

3.1.1. Yeast two-hybrid screen to identify candidate PUB22 interactors

To find candidate interactors of PUB22, a yeast two-hybrid screen was performed by Hybrigenics SA. PUB22 is a modular protein that consists of an N-terminal U-box domain, responsible for the interaction with an E2 conjugating enzyme, and a C-terminal ARM domain, which mediates protein-protein interaction and is anticipated to mediate substrate recognition. For the yeast two-hybrid screen only the ARM repeats domain of PUB22 (PUB22^{ARM}, residues 76-435) was used, to prevent the potential ubiquitination and degradation of candidate targets in the yeast cells. Nine candidate targets of PUB22 were isolated from the screen. Table 1 lists the gene name of candidates, their AGI code and the homology-based predicted function of the encoded protein.

29 clones encoding different fragments of general control non-repressible 5 (GCN5) were isolated from the screen, which is predicted to be a soluble-type ABC-transporter. GCN5 displays sequence homology to the yeast GCN20, which is associated to the ribosome and is

involved in the regulation of translation (Marton et al., 1997). However, a function for the *Arabidopsis thaliana* homolog is yet unknown.

Further candidates included two clones containing the N-Terminus of Exo70B2, indicating that the region relevant for the interaction is present in the first 147 amino acids. Exo70B2 is a homolog of the yeast Exo70p subunit of the exocyst, an octameric protein complex involved in the tethering of post-Golgi vesicles to the plasma membrane. Exo70 is thought to associate with the target membrane and acting as a spatial landmark for the specific recognition of the complex before SNARE-mediated vesicle fusion (He and Guo, 2009). The isolated Exo70B2 is one of 23 homologs of the yeast Exo70p subunit in *Arabidopsis thaliana* (Cvrčková et al., 2012).

Table 1 Candidate PUB22 targets isolated in a yeast two-hybrid screen

Gene Name	AGI code	homology	Isolated clones
GCN5	AT5G64840	Soluble ABC transporter	29
Exo70B2	AT1G70000	Exocyst subunit	2
SFH5	AT1G75370	Phosphatidylinositol transfer protein	1
Bam2-like	AT4G28650	Receptor-like kinase, homolog of CLV1	6
HsPro2	AT2G40000	Ortholog of sugar beet Hs1 Pro-1 2	4
Unkown protein	AT1G77580	Myosin heavy chain-related (MHCR)	2
Unkown protein	AT1G62780	Unknown protein with LRR	1
Unkown protein	AT5G08720	Putative polyketide cyclase/dehydrase	4
Ubiquitin-like protein	AT5G42220	Unknown ubiquitin-like protein (UBL)	5

One isolated clone corresponded to a homolog of yeast *sec fourteen p* (Sec14p) *homologs* (SFH), SFH5. SFH5 is one of 31 *Arabidopsis thaliana* homologs of Sec14p, which is the major phosphoinositide transfer protein (PITP) in yeast (Thole and Nielsen, CoPB 2008). Yeast Sec14p and *Arabidopsis* SFH proteins are involved in the regulation of vesicular trafficking and phosphoinositide homeostasis (Mousley et al., 2007). In addition, SFHs are thought to regulate the transfer of phosphoinositides by acting as a “lipid shuttle” to mediate vesicle fusion at target membranes. *Arabidopsis thaliana* SFH1 was shown to be enriched in discrete plasma membrane domains of root hairs and mutants are compromised in root hair expansion (Vincent et al., 2005). SFH3 and SFH12 were shown to be expressed in pollen tubes and suggested to be involved in the regulation of polarized pollen tube growth (Mo et al., 2007). A function for SFH5 has not yet been described.

Six clones matched the C-terminal part of a non-characterized putative RLK, which is a barely any meristem 2-like (Bam2-like) protein and has homology to Clavata 1 (CLV1), a RLK acting together with its homolog CLV2 in the perception of Clavata 3 peptide (CLV3p), which is required for the maintenance of stem cells in apical meristems during plant development (Jun et al. 2008; Wang & Fiers 2010).

Four clones matched HsPro2, which is an *Arabidopsis thaliana* ortholog of the *Heterodera schachtii* (Hs) 1 protein 1-2 (HsPro1-2), a protein conferring resistance to the nematode *Heterodera schachtii* in sugar beet (Cai, 1997). HsPro2 was identified in microarray transcription profiling experiments on the *Arabidopsis thaliana* mutant constitutively induced resistance 1 (*cir1*) to identify novel components of basal resistance against *Pst* (Murray et al., 2007). *HsPro2* is transcriptionally upregulated upon flg22 treatment (Navarro et al., 2004) and *hspro2* knockout mutants were shown to be more susceptible to *Pst* infection (Murray et al., 2007). The molecular function of the protein is yet unknown, but it appears to function downstream of salicylic acid and to be negatively regulated by signaling through jasmonic acid and ethylene (Murray et al., 2007).

One isolated clone encoded a myosin heavy chain-related protein (MHCR). Myosins are molecular motors and essential for a multitude of trafficking processes at various stages (Bond et al., 2011), pointing to the possibility that the candidate MHCR is involved in the regulation of vesicle trafficking.

Other isolated candidate targets included an unknown ubiquitin-like protein (UBL), which was shown to be transcriptionally upregulated in specific developmental processes in the *Arabidopsis thaliana* embryo (Spencer et al., 2007), an unknown protein with a LRR domain, which are associated with protein-protein interactions, and an unknown protein with predicted polyketide cyclase and dehydrase activity, which is therefore anticipated to be involved in secondary metabolism and was found to be expressed in mitochondria in a proteomic approach (Heazlewood et al., 2004).

Detailed tables showing the isolated clones including start and stop nucleotides matching the candidates and the predicted interaction domains can be found in the appendix Table 7.

The interaction data from the screen was confirmed by retransformation of yeast with the plasmids of selected clones. Binding domain (BD) fusion protein of PUB22^{ARM} was transformed into the yeast strain L40 and the fusion proteins of the activation domain (AD) of identified

candidates were transformed into the yeast strain Y187. The corresponding empty vectors were used as a control. After transformation the yeast strains were mated to obtain cells containing both plasmids. Double transformants of mated yeast were selected on SD/-Leu/-Trp Media. To test protein-protein interaction yeast were selected on SD/-Leu/-Trp/-His media. The interaction between BD-PUB22^{ARM} and selected clones could not be confirmed for all clones (Figure 3-1). The interaction in yeast could be confirmed for PUB22 with Exo70B2, SFH5, GCN5 and MHCR. Bam2-like and UBL showed no interaction. HsPro2, the unknown LRR containing protein and the unknown polyketide cyclase/dehydrase protein were not yet tested.

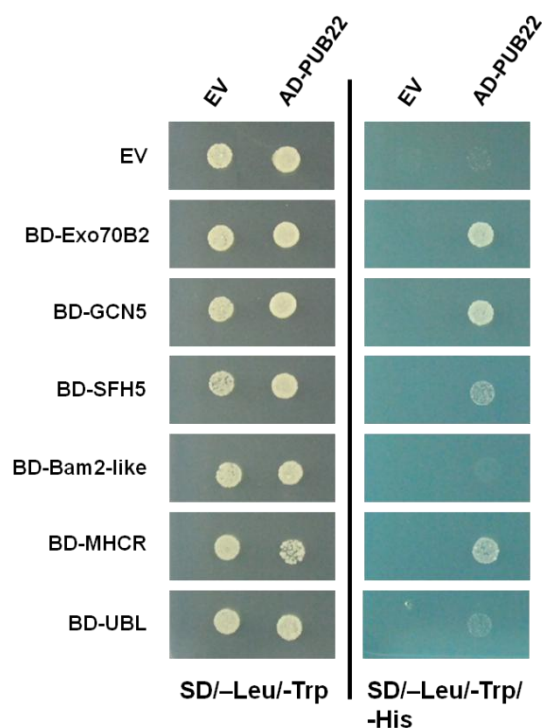


Figure 3-1 Yeast two-hybrid assay to test the interaction of PUB22 with candidate targets: AD-Exo70B2, AD-SFH5, AD-GCN5, AD-Bam2-like, AD-MHCR and AD-UBL were transformed in yeast strain Y187 and BD-PUB22^{ARM} was transformed in yeast strain L40-4. After transformation, yeasts were mated to obtain cells containing both plasmids. Growth of yeast on SD/-Leu/-Trp confirms presence of both vectors, growth on SD/-Leu/-Trp/-His indicates protein-protein interaction.

3.1.2. Interaction analysis of PUB22 with additional subunits of the exocyst complex by yeast two-hybrid assay

The yeast two-hybrid screen suggested an interaction of Exo70B2 with PUB22. Homologs for all subunits of the exocyst are present in *Arabidopsis thaliana* (Cvrckova and Zarsky, 2001). Exo70B2 was shown to interact with Sec5a and Sec15b in yeast two-hybrid experiments, supporting a role as a functional component of the exocyst (Pecenková et al., 2011). As in yeast many of the exocyst subunits have a similar rod shaped structure that consists of α -helical bundles (Wu et al. 2005; Dong et al., 2005), we wanted to test, whether PUB22 also interacts with other complex subunits. This was tested in cooperation with the group of Viktor Zarsky from the University of Prague. For this purpose the N-terminus of the full length PUB22 was fused to the LexA DNA-binding domain and the exocyst complex subunits were fused to the LexA activation domain. The constructs were cotransformed in the yeast strain AH109 and plated on media to select double transformants and on media to assay a protein-protein interaction. The presence of all constructs was confirmed by the growth of all double transformed yeast on SD/-Leu/-Trp medium (Figure 3-2). AD-PUB22 interacted with BD-Exo70B2 as shown by the growth of yeast on interaction selection medium (SD/-Leu/-Trp/-His). By contrast, AD-PUB22 did not interact with any other tested subunit of the complex, except the C-terminal part of Exo84 (Exo84 C). Further supporting the specificity of the interaction, AD-PUB22 also failed to interact with the Exo70B2 homologs Exo70A1 and Exo70H1.

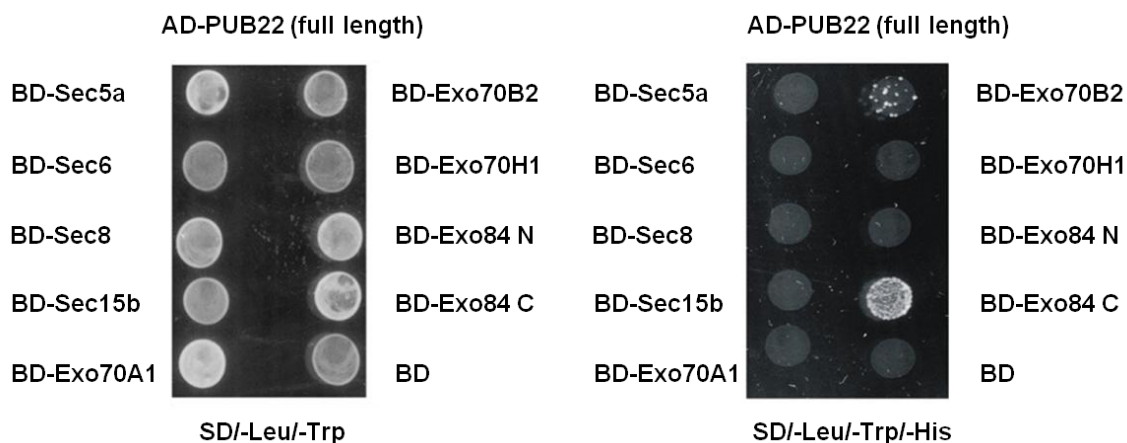


Figure 3-2 Yeast two-hybrid experiment to assay the interaction of PUB22 with other exocyst complex subunits: AD-PUB22 and BD-exocyst complex subunit fusions were transformed into yeast strain AH109. Growth of yeast on SD/-Leu/-Trp shows presence of both plasmids. Growth on SD/-Leu/-Trp/-His indicates protein-protein interaction.

3.1.3. Yeast assay to test the ability of *Exo70B2* to complement yeast *exo70* deficiency

The Exo70 gene family has undergone significant gene expansion in the plant genome with 23 different homologs in *Arabidopsis thaliana*. By contrast, yeast and mammalian genomes encode only one Exo70 gene (Cvrčková et al., 2012). This suggests that plant Exo70 homologs might have adopted new functions. We tested this in collaboration with the group of Viktor Zarsky from the University in Prague in a yeast complementation experiment trying to complement a yeast *exo70-38* mutant strain with *Arabidopsis thaliana Exo70B2*. The *exo70-38* mutant is a temperature-sensitive strain that grows at 28°C but fails to grow at 37°C. The result of the experiment is shown in Figure 3-3, showing that *exo70-38* mutant yeast transformed with *Exo70B2* did not show a difference in growth compared to the vector control transformed cells under restrictive growth conditions at 37°C. This indicates that *Exo70B2* cannot take over the function of yeast Exo70p and therefore suggests that it has adopted new functions.

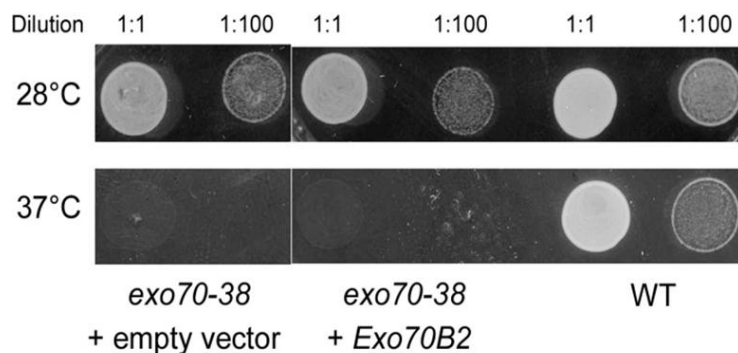


Figure 3-3 Yeast complementation assay: *Arabidopsis thaliana Exo70B2* was transformed into the temperature-sensitive yeast *exo70-38* mutant strain. An empty vector was used as control. Transformed colonies were plated out in two different dilutions (1:1 and 1:100) onto -Ura medium and were grown two to four days on both 28°C and 37°C.

3.2. Analysis of the impact of PUB22 candidate targets on plant immunity

One major aim of the present work is to find targets of PUB22 required for its regulatory function in PAMP-triggered responses and immunity. The *pub22/23/24* triple mutant displays enhanced responses to PAMPs and increased resistance to various pathogens (Trujillo et al., 2008), showing that the PUBs are negative regulators of immunity. Targets of the PUBs are hypothesized to be positive regulators of immunity. The aim was to identify candidate targets with a function in plant defense. Therefore a reverse genetic approach was utilized to analyze the identified candidate PUB22 targets in plant immunity.

3.2.1. Generation of T-DNA insertion mutants of candidate PUB22 targets

T-DNA Insertion mutants were obtained from the NASC Arabidopsis stock center and homozygous lines were generated and identified by PCR-based genotyping. Used primers can be found in the appendix, Table 5. All lines are listed in Table 2, which shows the gene of interest with the corresponding AGI code and the isolated T-DNA Insertion line.

Table 2 T-DNA insertion lines of candidate PUB22 targets

Gene	AGI code	T-DNA Insertion line
<i>GCN5</i>	AT5G64840	SALK_113472C/N664827
<i>Exo70B2</i>	AT1G07000	SALK_091877C
<i>SFH5</i>	AT1G75370	SALK_114805C/N661103
<i>Bam2-like</i>	AT4G28650	SALK_095005/N595005
<i>HsPro2</i>	AT2G40000	SALK_016065.56.00.x
<i>MHCR</i>	AT1G77580	SALK_044287
<i>Unkown protein / LRR</i>	AT1G62780	SALK_047296C
<i>Unkown protein / Cyclase/Dehydrase</i>	AT5G08720	SALK_011411.37.80/N511411
<i>UBL</i>	AT5G42220	SALK_072154/N572154

Homozygous lines could be generated for *exo70B2*, *sfh5*, *bam2-like*, *hspro2*, *ubl* and *mhcr*. For *gcn5* no homozygous lines could be generated. Seeds of propagated heterozygous lines showed a 25% seed mortality (data not shown), indicating that the homozygous *gcn5* mutation is embryo-lethal.

Selected homozygous T-DNA Insertion lines were used to assay their responsiveness to flg22 based on a ROS-burst response and their resistance against *Pst*. Furthermore, we analyzed the transcriptional response upon elicitor treatment using publically available micro array data sets.

3.2.2. ROS-burst assays of candidate PUB22 interactor mutants

The *pub22/23/24* triple mutant plants show enhanced responses to different PAMPs, including flg22 (Trujillo et al., 2008). One of the first measurable responses in plants after PAMP recognition is the transient production of ROS (Nicaise et al., 2009). ROS can be measured after treatment with flg22 in a luminol-based assay using *Arabidopsis thaliana* leaf discs. We used this as a readout to test the PAMP responsiveness of the PUB22 candidate interactor mutants. As the *pub22/23/24* mutant displays elevated ROS production, mutants in PUB targets were hypothesized to show decreased ROS production after flg22 treatment. In Figure 3-4 results are shown for ROS production after flg22 treatment in wild type, *pub22/23/24*, *sfh5*, *exo70B2* and *bam2-like* mutant plants.

While the *pub22/23/24* triple mutant showed enhanced ROS production in comparison to the wild type, both *sfh5* and *exo70B2* mutants showed a decreased burst, not reaching similar maximum levels as wild type plants, seen in the time-course profile (left) and in the quantification of total ROS produced (right). Wild type plants reached a maximum peak value of 105,3 relative light units (RLU) with a total ROS production of 1258,6 RLU +/- 174 S.E.M., while *sfh5* only reached a value of 76,7 RLU with a total of 915,2 RLU +/- 114 S.E.M. and *exo70B2* 75,9 RLU with a total of 983,2 RLU +/- 126 S.E.M. The kinetic however was not altered. Wild type, *sfh5* and *exo70B2* mutants all reached the peak value at 18 min. The *pub22/23/24* mutant did not reach a maximum in the experimental time frame and the last measured value was

292,1 RLU. As expected, the total ROS production was 4510,6 RLU +/- 602 S.E.M. and therefore much higher in comparison to the wild type. The *bam2-like* mutants showed only a slightly reduced total ROS production in comparison to the wild type (1094,2 RLU +/- 180 S.E.M.), but interestingly they reached a slightly higher peak value (110,1 RLU) at an earlier time point (12 min) (Figure 3-4). Due to time reasons other candidate PUB22 target mutants have not yet been assayed for their flg22-induced ROS-burst response. In summary, ROS production assays of candidate PUB22 target mutants revealed reduced ROS production for *exo70B2* and *sfh5* mutant plants.

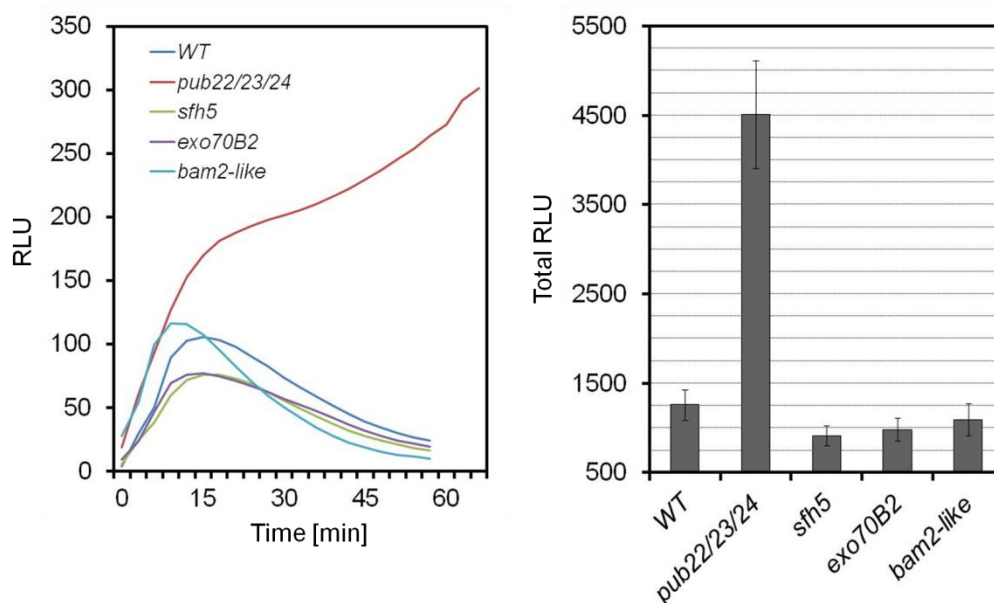


Figure 3-4 ROS-burst time-course and total ROS production after treatment with flg22: ROS production was measured in leaf discs of six to seven week-old plants of the indicated mutant lines in a luminol-based assay after treatment with 500nM flg22. Each time point (left) represents the average of 24 independent samples. Total ROS production (right) is calculated by integration of the area under the curves (left). Error bars represent +/- S.E.M. of three independent experiments. RLU = relative light units.

3.2.3. Pathogen growth assays with candidate PUB22 interactor mutants

The enhanced responsiveness of *pub22/23/24* mutants is accompanied by enhanced disease resistance (Trujillo et al., 2008). To analyze a potential impact of the candidate targets on plant immunity, pathogen growth assays with *Pst* were performed. To mimic a natural *Pst* infection,

plants were spray inoculated, allowing the detection of phenotypes related to PTI, as previously shown for *fls2* mutant plants (Zipfel et al., 2004). Two different *Pst* were used, the full virulent strain DC3000 and a less virulent mutant lacking the two important effectors AvrPto and AvrPtoB (*Pst* Δ *avrPto*/ Δ *avrPtoB*; Lin and Martin, 2005).

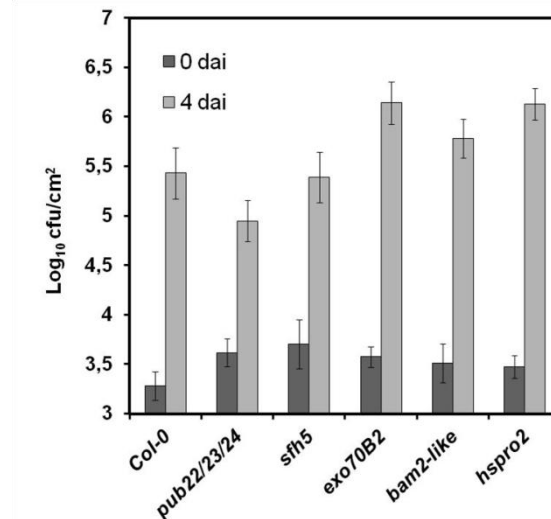


Figure 3-5 Pathogen growth assay of candidate PUB22 target mutants with *Pst* DC3000: Inoculation was carried out spraying a solution of 5×10^8 cfu/ml bacteria on six week-old plants of the indicated lines. Bacterial growth was measured three hours (0 dai) and four days after inoculation (4 dai). Three samples each with four leaf discs from twelve leaves derived from three independent plants, were harvested to assess bacterial growth. Shown is the average value \pm S.E.M. of three independent experiments. CfU = colony forming units.

The results of Spray infection experiments of candidate PUB22 target mutants with the fully virulent strain *Pst* DC3000 are shown in Figure 3-5. The *pub22/23/24* triple mutant plants were more resistant in comparison to the wild type 4 days after infection, consistent with previous results (Trujillo et al, 2008). The cfu/cm² of *Pst* was 4,95 log₁₀ \pm 0,2 S.E.M. in *pub22/23/24* in comparison to 5,43 log₁₀ \pm 0,15 S.E.M. in wild type plants. The *sfh5* (5,39 log₁₀ cfu/cm² \pm 0,3 S.E.M) and *bam2-like* mutants (5,78 log₁₀ cfu/cm² \pm 0,2 S.E.M) showed no evident difference in bacterial growth in comparison to the wild type, while *exo70B2* (6,14 log₁₀ cfu/cm² \pm 0,2 S.E.M.) and *hspro2* plants (6,13 log₁₀ cfu/cm² \pm 0,15 S.E.M.) showed clearly enhanced levels of bacteria, indicating that both mutants are compromised in their defense response to *Pst*.

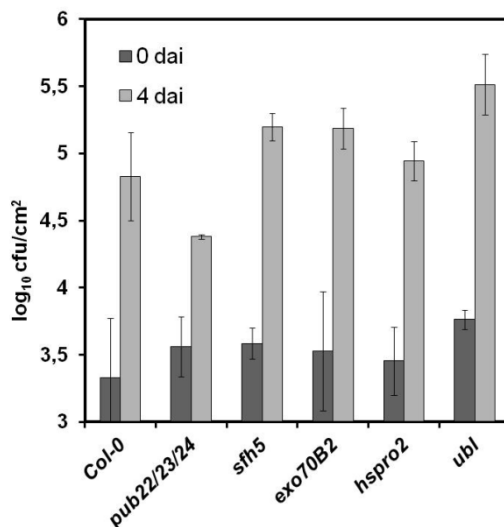


Figure 3-6 Pathogen growth assay of candidate PUB22 target mutants with *Pst DC3000 ΔavrPto/ΔavrPtoB*: Inoculation was carried out spraying a solution of 5×10^8 cfu/ml bacteria on six week-old plants of the indicated lines. Bacterial growth was measured three hours (0 dai) and four days after inoculation (4 dai). Three samples each with four leaf discs from twelve leaves derived from three independent plants were harvested to assess bacterial growth. Shown is a representative experiment +/- S.D. of three independent samples. Similar results were obtained in two independent experiments.

Due to the virulence of *Pst DC3000* it is possible that small changes in susceptibility related to PAMP-triggered immunity cannot be detected in an infection with the virulent strain. Therefore additional spray infection experiments were carried out using the mildly virulent mutant *Pst DC3000 ΔavrPto/ΔavrPtoB*. A representative result is shown in Figure 3-6.

The *sfh5* ($5,19 \log_{10} \text{ cfu/cm}^2 \pm 0,15 \text{ S.D.}$), *exo70B2* ($5,2 \log_{10} \text{ cfu/cm}^2 \pm 0,1 \text{ S.D.}$) and *hspro2* ($4,95 \log_{10} \text{ cfu/cm}^2 \pm 0,15 \text{ S.D.}$) mutant lines showed slightly enhanced bacterial growth in comparison to the wild type ($4,83 \log_{10} \text{ cfu/cm}^2 \pm 0,3 \text{ S.D.}$). The *ubl* ($5,51 \log_{10} \text{ cfu/cm}^2 \pm 0,2 \text{ S.D.}$) mutants showed stronger enhanced bacterial growth, but the result was not reproducible. The *pub22/23/24* triple mutant ($4,38 \log_{10} \text{ cfu/cm}^2 \pm 0,1 \text{ S.D.}$) showed reduced bacterial growth in comparison to the wild type, as expected. The experiment was repeated once with *exo70B2* and *hspro2* mutant plants showing similar tendencies.

Due to time reasons, the *mhcr*, *cyclase/dehydrase* and *unknown Irr* mutants have not yet been assayed for *Pst* resistance phenotypes. Taken together with the infection experiment data using the fully virulent strain *Pst DC3000*, both *exo70B2* and *hspro2* mutant lines consistently showed elevated bacterial growth in comparison to the wild type, indicating that both mutants are compromised in immunity.

3.2.4. Gene expression profile upon elicitor treatment of candidate PUB22 interactors

In addition to the analysis of immunity-related phenotypes of candidate PUB22 interactors, we performed data analysis of gene expression profiles of the candidates upon flg22 and elf18 treatments. The data was analyzed from publically available microarray data (Navarro et al., 2004; Zipfel et al., 2006) using Genevestigator software (Hruz et al., 2008) (Figure 3-7). *Exo70B2* is highly transcriptionally induced upon treatment with elf18 in leaves and flg22 in seedlings with a 13 and 11 fold change respectively. *HsPro2* was weaker induced upon flg22 treatment (5 fold) but highly upregulated upon elf18 treatment (21 fold). Other candidate genes did not show significant changes upon elicitor treatments.

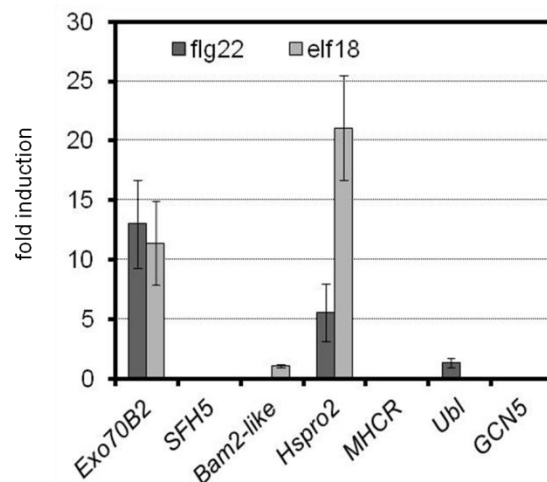


Figure 3-7 Gene expression data of candidate PUB22 interactors: Flg22 (1 μ M) treatment was applied to seedlings for 1 hour and elf18 (1 μ M) treatment to adult leaves (1 hour) of *Arabidopsis thaliana* wild type plants. Data was analyzed from publically available microarray data (Navarro et al., 2004; Zipfel et al., 2006) using Genevestigator software (Hruz et al., 2008).

In summary, results obtained for ROS-burst and infection assays of candidate PUB22 target mutants and the gene expression profile upon flg22 and elf18 treatment revealed that *Exo70B2* is the most interesting candidate for further analysis.

3.3. Confirmation of the interaction between PUB22 and Exo70B2

The *exo70B2* mutant plants showed the clearest phenotype after infection (section 3.2.3) and flg22-induced ROS production experiments (section 3.2.2) and *Exo70B2* was highly transcriptionally upregulated upon PAMP treatment (section 3.2.4). Therefore *Exo70B2* was the most interesting candidate for further analysis. *Exo70B2* was isolated as a candidate interactor of *PUB22* in a yeast two-hybrid screen which are known to produce a fair amount of false positives. Therefore, it was necessary to confirm the interaction between both proteins *in vivo* and *in vitro*.

3.3.1. Confirmation of the interaction of *PUB22* and *Exo70B2* by bimolecular fluorescence complementation

Bimolecular fluorescence complementation (BiFC), also known as Split-YFP, is a method to visualize protein-protein interaction in living cells. It is based on separated N-terminal and C-terminal YFP fragments fused to proteins of interest. YFP reconstitutes when both proteins come into close proximity, suggesting a protein-protein interaction (Hu et al., 2002). To assay the interaction of *PUB22* and *Exo70B2* using BiFC, the ARM domain ($PUB22^{ARM}$) and the U-box domain of *PUB22* ($PUB22^{U-box}$) were fused to the N-terminal part of YFP (nYFP) with an additional N-terminal cMyc-tag. *Exo70B2* was fused to the C-terminal part of YFP (cYFP). With cMyc-nYFP- $PUB22^{ARM}$ a similar truncated construct was used as in the yeast two-hybrid screen, again to prevent potential ubiquitination and degradation of the candidate interaction partner. The cMyc-nYFP- $PUB22^{U-box}$ represents the first 75 amino acids of *PUB22* (Figure 1-3) and was used as a negative control. Constructs were transiently expressed in *Arabidopsis thaliana* epidermis cells after particle bombardment or in *Arabidopsis thaliana* mesophyll protoplasts by PEG-mediated transformation. YFP reconstitution was measured using confocal laser-scanning microscopy.

After transformation of *Arabidopsis thaliana* epidermal leaf cells, coexpression of cMyc-nYFP- $PUB22^{ARM}$ with cYFP-*Exo70B2* led to a clear reconstitution of YFP, localized in punctate structures throughout the cell and surrounding the nucleus (Figure 3-8 A). Free RFP was co-transformed to label the cytoplasm and the nucleus. The U-box domain construct cMyc-nYFP-

PUB22^{U-box} did not reconstitute YFP when cotransfected with cYFP-Exo70B2 (Figure 3-8 B) suggesting that the ARM domain PUB22^{ARM} is required and sufficient for an interaction with Exo70B2 *in vivo*.

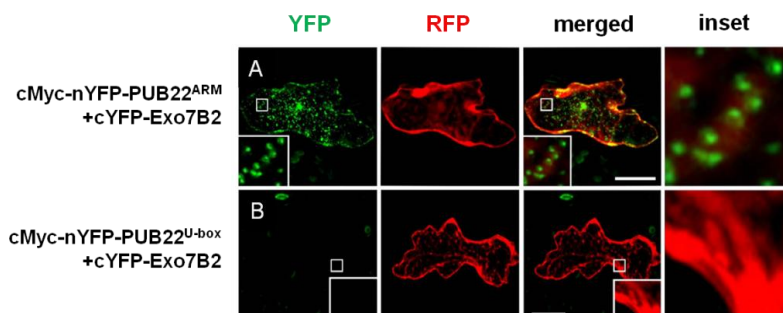


Figure 3-8 Bimolecular fluorescence complementation of cMyc-nYFP-PUB22^{ARM} with cYFP-Exo70B2 in *Arabidopsis thaliana* epidermal leaf cells: (A) nYFP-PUB22^{ARM} or (B) nYFP-PUB22^{U-box} was co-transformed with cYFP-Exo70B2 and free RFP in *Arabidopsis thaliana* epidermal leaf cells via particle bombardment. YFP reconstitution was measured using confocal laser scanning microscopy. White square labels inset area, scale bar = 50 μ m. Similar results were obtained in at least three independent experiments.

A caveat of the transient expression in epidermal leaf cells via particle bombardment is that protein expression analysis by western blot cannot be performed to confirm protein expression.

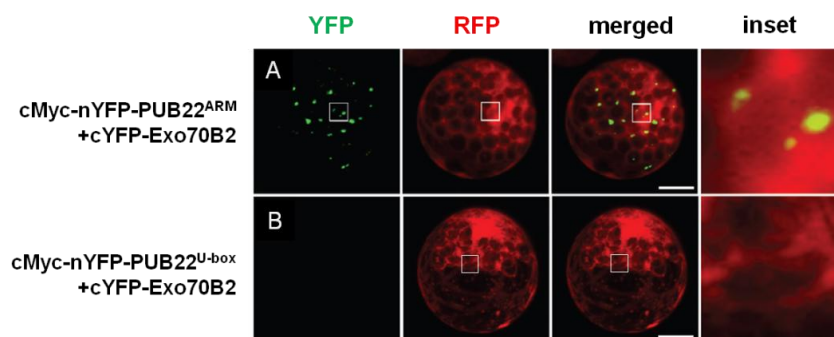


Figure 3-9 Bimolecular fluorescence complementation of cMyc-nYFP-PUB22^{ARM} or cMyc-nYFP-PUB22^{U-box} with cYFP-Exo70B2 in *Arabidopsis thaliana* mesophyll protoplasts: (A) cMyc-nYFP-PUB22^{ARM} or (B) cMyc-nYFP-PUB22^{U-box} were cotransformed with cYFP-Exo70B2 and free RFP in *Arabidopsis thaliana* mesophyll protoplasts via PEG-mediated transfection. YFP reconstitution was analyzed using confocal laser-scanning microscopy. White square labels inset area, scale bar = 50 μ m. Similar results were obtained in at least three independent experiments.

Therefore it cannot be excluded that the lack of fluorescence in cells coexpressing cMyc-nYFP-PUB22^{U-box} and cYFP-Exo70B2 (Figure 3-8 B) was caused by a lack of protein expression of

one or both of the used constructs. To exclude this possibility, the experiment was repeated by transiently expressing these constructs in *Arabidopsis thaliana* mesophyll protoplasts using PEG-mediated transformation. Results shown in Figure 3-9 confirmed YFP reconstitution after coexpression of cMyc-nYFP-PUB22^{ARM} and cYFP-Exo70B2. By contrast, no fluorescence could be observed after coexpression of cMyc-nYFP-PUB22^{U-box} and cYFP-Exo70B2. Also, the localization of the interaction was similar; localized in punctate structures throughout the cell.

As Exo70B2 has 22 homologues in *Arabidopsis* (Cvrčková et al., 2012), we assayed the specificity of the PUB22-Exo70B2 interaction by testing the Exo70B2 homolog Exo70A1. Coexpression of cMyc-nYFP-PUB22^{ARM} and cYFP-Exo70A1 did not result in YFP-reconstitution (Figure 3-10), suggesting that the interaction of PUB22 with Exo70B2 is specific.

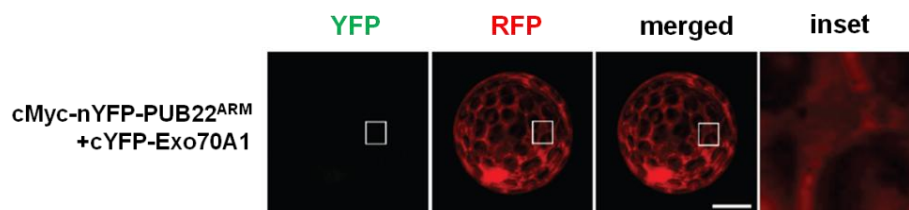


Figure 3-10 Bimolecular fluorescence complementation of cMyc-nYFP-PUB22^{ARM} and cYFP-Exo70A1 in *Arabidopsis thaliana* mesophyll protoplasts: cMyc-nYFP-PUB22^{ARM} was cotransformed with cYFP-Exo70A1 and free RFP in *Arabidopsis thaliana* mesophyll protoplasts via PEG-mediated transfection. YFP reconstitution was analyzed using confocal laser scanning microscopy. White square labels inset area, scale bar = 50 μ m. Similar results were obtained in at least three independent experiments.

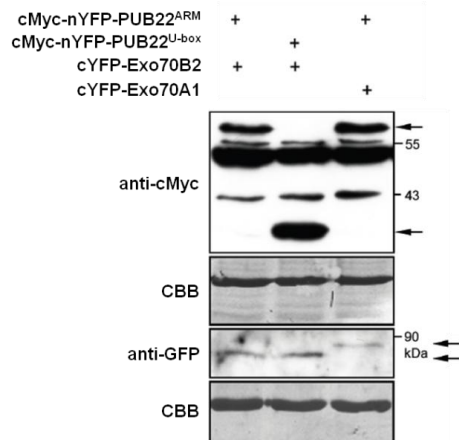


Figure 3-11 Western blot analysis to confirm protein expression in BiFC experiments: Proteins were isolated from BiFC samples separated by SDS-PAGE gels. Immunoblot analysis of cMyc-nYFP fusion proteins was carried out using anti-cMyc antibodies. cYFP fusion proteins were detected using anti-GFP antibodies. Arrows indicate size of fusion proteins. Coomassie brilliant blue stain = CBB. Similar results were obtained in three independent experiments.

As mentioned above, an advantage of BiFC in mesophyll protoplasts is the possibility to confirm protein expression by western blot. The Expression of all fusion proteins from Figure 3-9 and Figure 3-10 were confirmed by SDS-PAGE separation and western-blotting of the according samples after protein isolation, as shown in Figure 3-11.

3.3.2. Confirmation of the PUB22-Exo70B2 interaction by coimmunoprecipitation

The data from the BiFC experiments suggest that PUB22^{ARM} and Exo70B2 can interact *in vivo* in a specific manner, supporting the data from the yeast two-hybrid screen (3.1.1). But BiFC can also be subject to artifacts. The fluorescent protein fragments are able to form fluorescent complexes with low efficiency even in the absence of a specific interaction (Hu et al., 2002). Although we included several controls in our BiFC experiments to exclude unspecific interactions, we wanted to further confirm the PUB22-Exo70B2 interaction with other methods. Additionally, interaction of the PUB22 full-length with Exo70B2 *in vivo* had yet to be demonstrated. So far only the truncated PUB22 containing the protein-protein interaction domain, namely PUB22^{ARM}, was demonstrated to interact with Exo70B2 in BiFC assays (section 3.3.1).

To further support the PUB22-Exo70B2 interaction and to analyze the interaction with full-length PUB22, we employed a coimmunoprecipitation assay in *Arabidopsis thaliana* mesophyll protoplasts. For this purpose we generated YFP-PUB22^{C13A} and cMyc-Exo70B2 fusion proteins. The employed full-length construct carried a mutation in the U-box, namely a cysteine to alanine exchange at the 13th amino acid (C13A). The mutant lacks the ability to interact with the E2 conjugating enzyme, abolishing its ubiquitination activity (Trujillo et al., 2008). After transformation of both constructs in protoplasts, protein samples were harvested and subjected to immunoprecipitation using anti-cMyc beads. Western blots were performed using anti-cMyc antibodies to detect immunoprecipitated cMyc-Exo70B2 and anti-GFP antibodies to detect potential co-purified YFP-PUB22^{C13A}.

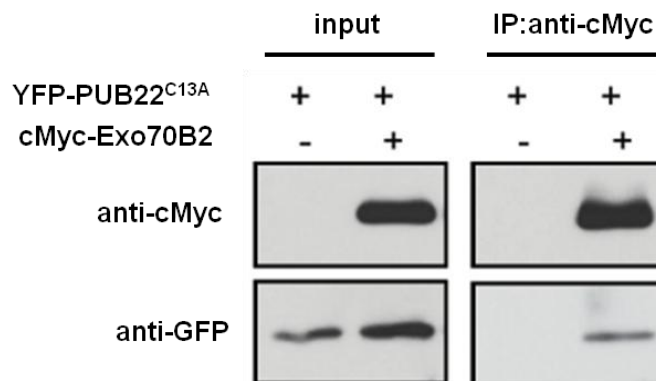


Figure 3-12 Coimmunoprecipitation assay with cMyc-Exo70B2 and YFP-PUB22^{C13A} in *Arabidopsis thaliana* mesophyll protoplasts: YFP-PUB22^{C13A} and cMyc-Exo70B2 were transiently expressed in *Arabidopsis thaliana* mesophyll protoplasts. After immunoprecipitation with anti-cMyc beads, proteins were loaded on SDS-PAGE and subjected to Western-blot analysis. Blots were incubated with anti-cMyc antibodies to detect cMyc-Exo70B2 and with anti-GFP antibodies to detect co-purified YFP-PUB22^{C13A}. Similar results were obtained in three independent experiments.

As can be seen in Figure 3-12, cMyc-Exo70B2 efficiently coimmunoprecipitated YFP-PUB22^{C13A}. In the absence of cMyc-Exo70B2, YFP-PUB22^{C13A} cannot be detected, showing that the protein does not bind unspecifically to the beads. This data confirms the *in vivo* interaction of PUB22 and Exo70B2, additionally showing that the full-length proteins do interact.

3.3.3. Analysis of a physical interaction of PUB22 and Exo70B2 by *in vitro* pull-down

To assay a direct interaction of PUB22 and Exo70B2, an *in vitro* pull-down assay with recombinant GST-PUB22 and MBP-Exo70B2 was performed. MBP-Exo70B2 was expressed in bacteria and the bacterial lysate was incubated for 1 hour in the presence of amylose resin. Subsequently bacteria that expressed GST-PUB22 were lysed and added. After elution with a buffer containing free amylose the samples were analyzed via SDS-PAGE and Western blot. The result of that experiment is shown in Figure 3-13. In the presence of MBP-Exo70B2, GST-PUB22 is clearly co-purified. In the presence of MBP, GST-PUB22 cannot be detected, showing that the protein does not bind to the amylose resin. These data show that both proteins interact

in vitro, indicating that the interaction observed in BiFC and CoIP assays is due to a direct physical interaction of Exo70B2 and PUB22 *in vivo*.

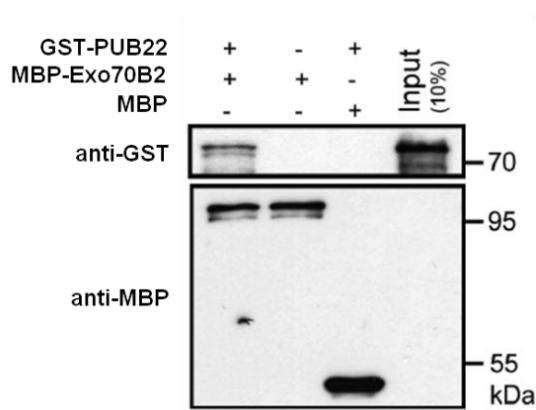


Figure 3-13 *In vitro* pull-down assay with GST-PUB22 and MBP-Exo70B2: GST-PUB22 and MBP-Exo70B2 were expressed and isolated from *E.coli*. Pull-down was performed using amylose-resin beads. Anti-GST and anti-MBP antibodies were used to detect fusion proteins. Similar results were obtained in three independent experiments.

3.3.4. Interaction analysis of Exo70B2 with PUB23 and PUB24 using bimolecular fluorescence complementation

PUB22 acts in concert with PUB23 and PUB24 to downregulate PAMP-triggered immune responses (Trujillo et al., 2008). PUB23 and PUB24 are the two closest homologs of PUB22, sharing respectively 76% and 35% of sequence identity. As the PUB22-Exo70B2 interaction could be confirmed, we wanted to assay the ability of PUB23 and PUB24 to interact with Exo70B2. This was tested using BiFC. PUB23^{C18A} and PUB24^{C30A}, which are inactive mutant variants, were fused N-terminally to cMyc-nYFP. Coexpression of both cMyc-nYFP-PUB23^{C18A} (Figure 3-14A) and cMyc-nYFP-PUB24^{C30A} (Figure 3-14 B) resulted in the reconstitution of YFP in presence of cYFP-Exo70B2, suggesting that both proteins interact. Expression of the fusion proteins was confirmed by Western blot analysis (Figure 3-14 C).

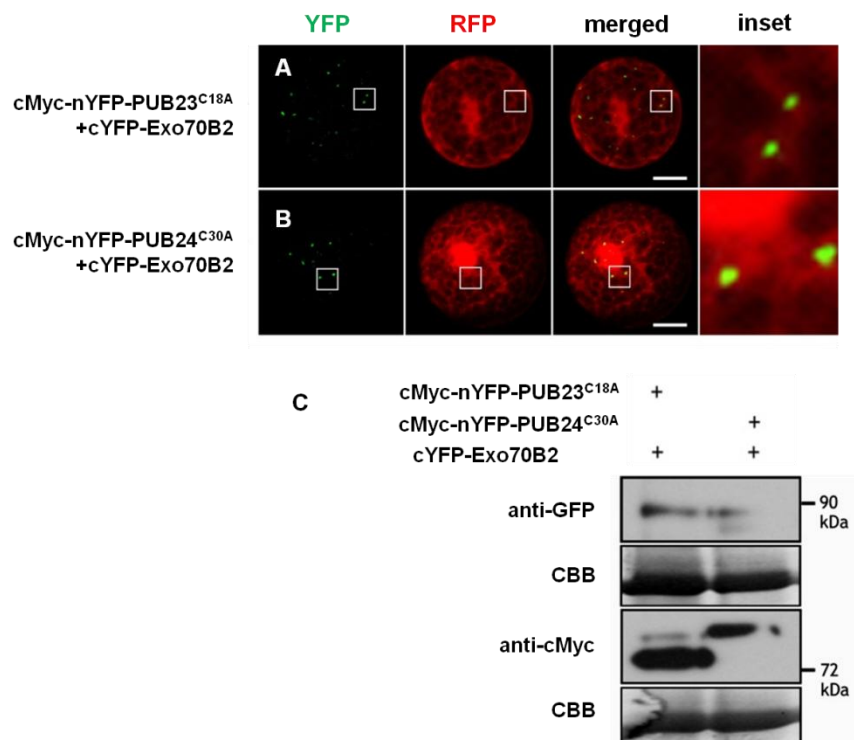


Figure 3-14 Bimolecular fluorescence complementation of cMyc-nYFP-PUB23^{C18A} or cMyc-nYFP-PUB24^{C30A} in *Arabidopsis thaliana* mesophyll protoplasts: (A) cMyc-nYFP-PUB23^{C18A} or (B) cMyc-nYFP-PUB24^{C30A} were cotransformed with cYFP-Exo70B2 and free RFP in *Arabidopsis thaliana* mesophyll protoplasts. YFP reconstitution was measured using confocal laser scanning microscopy. White square labels inset area, scale bar = 50 μ m. (C) Expression of fusion proteins was analyzed by Western blot using anti-GFP antibodies to detect cYFP-Exo70B2 and anti-cMyc antibodies to detect cMyc-nYFP-PUB23^{C18A} and cMyc-nYFP-PUB24^{C30A}. Coomassie brilliant blue stain = CBB. Similar results were obtained in three independent experiments.

3.4. Analysis of flg22-dependent PUB22 protein stabilization

The data showing the interaction of PUB22 and Exo70B2 suggests that both proteins interact constitutively. In BiFC assays (3.3.1) and in CoIP assays PUB22 can interact with Exo70B2 without the requirement of an external stimulus, such as PAMPs. We therefore analyzed, whether the interaction is regulated by a different mechanism. From previous work it was known that PUB22 is able to autoubiquitinate *in vitro* (Trujillo et al., 2008). This could represent a regulatory mechanism *in vivo*, controlling the levels of PUB22 and thus the interaction with Exo70B2. To address this question we transiently expressed wild type PUB22 fusion proteins to investigate their accumulation in *Nicotiana benthamiana* and *Arabidopsis thaliana* mesophyll protoplasts. Because PUBs are E3 ligases and they are involved in the regulation of plant immunity we included treatments with flg22 and a 26S-proteasome inhibitor to determine potential changes on the protein levels.

3.4.1. HA-PUB22 protein accumulation after transient overexpression in *Nicotiana benthamiana* and *Arabidopsis thaliana* mesophyll protoplasts

PUB22 is an active E3-ubiquitin ligase and was shown to possess autoubiquitination activity *in vitro*. Autoubiquitination is often associated with high turnover of a ligase and thus leading to protein instability. An example is the tomato CMPG1, which is a homolog of PUB22. CMPG1 was shown to be unstable because of its autocatalytic ubiquitination (Bos et al., 2010). In all the interaction experiments previously described either a truncated version of PUB22, PUB22^{ARM}, or a U-box mutant variant, PUB22^{C13A}, were used. Both proteins are inactive in their autoubiquitination activity and are therefore expected to be stable, as shown for CMPG1 (Bos et al., 2010). Indeed both proteins accumulate in *Arabidopsis thaliana* mesophyll protoplasts, without the requirement of any specific treatment (Figure 3-11 and Figure 3-12). However, in none of the described experiments a wild type, active PUB22 fusion protein was used. To analyze the protein levels of wild type PUB22 we generated N-terminal HA-fusion proteins. Protein accumulation after transient overexpression was analyzed in *Nicotiana benthamiana* after *Agrobacterium* mediated transformation or in *Arabidopsis thaliana* mesophyll protoplasts.

Samples were treated either with flg22 or with a 26S-proteasome inhibitor to analyze changes of HA-PUB22 protein levels.

For expression of the protein in *Nicotiana benthamiana* leaves from three week-old plants were syringe-infiltrated with *Agrobacteria* carrying the appropriate constructs. Two days after inoculation leaves were treated with 1 μ M flg22 for 1 hour or 50 μ M of the 26S-proteasome inhibitor AM114 for 4 hours. Protein samples were subsequently harvested and analyzed via SDS-PAGE and Western blot (Figure 3-15). In samples expressing HA-PUB22 without treatment, the protein was not detectable. After treatment with flg22 or AM114 the abundance of the protein was strongly increased, as seen by the appearance of a clear band. These data suggests that HA-PUB22 requires the treatment of flg22 to accumulate and that its instability is mediated by the 26S-proteasome, as seen by protein levels in samples treated with the inhibitor AM114.

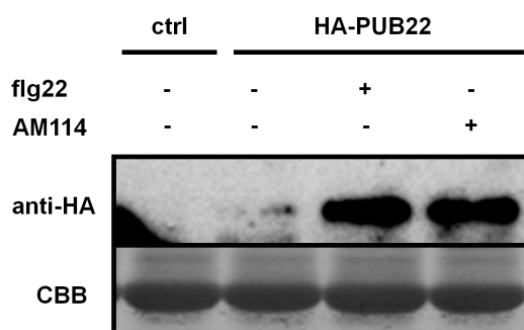


Figure 3-15 Accumulation of HA-PUB22 in *Nicotiana benthamiana*: HA-PUB22 was expressed in three week-old *Nicotiana benthamiana* leaves after *Agrobacterium*-mediated transformation. Treatments with 1 μ M flg22 or 50 μ M of the 26S-proteasome inhibitor AM114 were performed two days after infiltration. Proteins were harvested one hour after treatment and analyzed via SDS-PAGE and Western blot with anti-HA antibodies. Control (ctrl) protein samples are from untransformed protoplasts. Coomassie brilliant blue stain = CBB. Similar results were obtained in three independent experiments.

Because *Nicotiana benthamiana* is a heterologous system, we wanted to confirm the HA-PUB22 stabilization in *Arabidopsis thaliana*. Therefore, the experiment was repeated by transient expression of the fusion protein in *Arabidopsis thaliana* mesophyll protoplasts using PEG-mediated transfection. Results are shown in Figure 3-16. In accordance with the observation made in *Nicotiana benthamiana*, HA-PUB22 did only accumulate weakly in untreated samples. By contrast, protein levels strongly increased 1 hour after elicitation with 1 μ M flg22 or 4 hours after treatment with AM114, confirming the stabilization data from *Nicotiana benthamiana*. An additive effect after double treatment with both the elicitor and the inhibitor on the protein levels was observed compared to the single treatments. In the same experiment the

U-box inactive mutant HA-PUB22^{C13A} was also tested. In comparison to the wild type, HA-PUB22^{C13A} accumulation was much stronger. Additionally, the levels are not affected by any of the tested treatments. The accumulation of HA-PUB22^{C13A} is consistent with previous results, showing the stable accumulation of YFP-PUB22^{C13A} in the ColP assays (section 3.3.2).

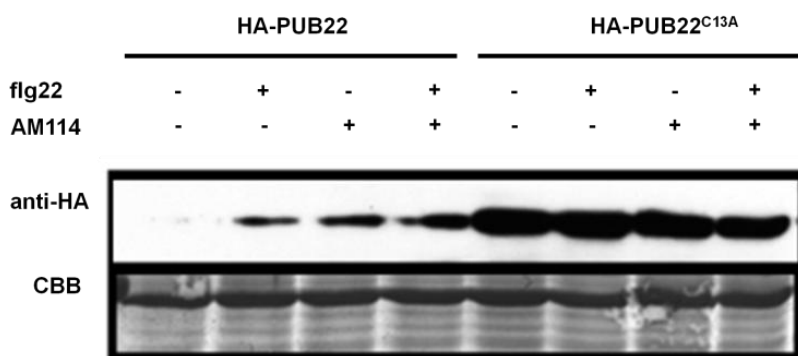


Figure 3-16 Accumulation of HA-PUB22 in *Arabidopsis thaliana* mesophyll protoplasts: HA-PUB22 or HA-PUB22^{C13A} were expressed in *Arabidopsis thaliana* mesophyll protoplasts after PEG-mediated transformation. Treatments with 1 μ M flg22 or 20 μ M of the 26S-proteasome inhibitor AM114 were performed one day after transformation. Proteins were harvested one hour after treatment and analyzed via SDS-PAGE and Western blot with anti-HA antibodies. Coomassie brilliant blue stain = CBB. Similar results were obtained in three independent experiments.

3.4.2. Time-course analysis of HA-PUB22 protein accumulation after flg22 elicitation or proteasome inhibition

The protein accumulation data of HA-PUB22 in *Nicotiana benthamiana* and *Arabidopsis thaliana* after transient overexpression suggested that wild type PUB22 has a high turnover *in vivo* and requires an external cue, such as flg22, to be stabilized. The next question we wanted to address was how fast PUB22 stabilization takes place. Therefore we performed time-course experiments after flg22 and AM114 treatments to detect changes in protein accumulation. This was achieved by transient overexpression of the constructs in *Nicotiana benthamiana* and in *Arabidopsis thaliana* mesophyll protoplasts.

After expression in *Nicotiana benthamiana* flg22 treatment induced the accumulation of HA-PUB22 as soon as 15 minutes after elicitation (Figure 3-17). At later time points (30 minutes and 60 minutes) the protein levels further increased. At the 0 time point and in the water control

lower protein amounts were detected. Of note, for HA-PUB22 a clear double band was consistently observed throughout these experiments. The expected size for the HA-PUB22 fusion protein is 54 kDa, but an additional band migrating at a higher molecular weight was clearly detectable. The intensity of this band was increased after flg22 treatment. After longer exposure of the blot in Figure 3-15 a double band for HA-PUB22 was observed as well (data not shown).

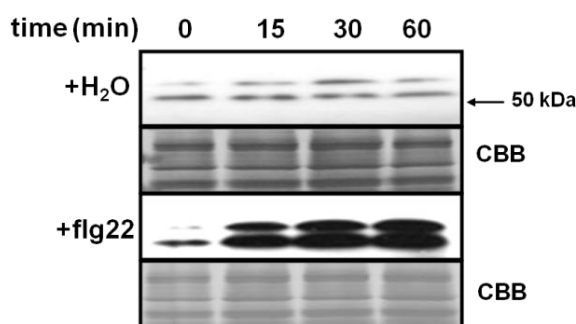


Figure 3-17 Stabilization time-course of HA-PUB22 after different treatments: HA-PUB22 was expressed in three week-old *Nicotiana benthamiana* leaves after *Agrobacterium*-mediated transient transformation. Treatment with 1 μ M flg22 or water (control) was performed two days after infiltration. Samples were taken at the indicated time points after elicitation and analyzed via SDS-PAGE and Western blot using anti-HA antibodies. Coomassie brilliant blue stain = CBB. Similar results were obtained in two independent experiments.

Similar experiments were performed using transient overexpression in *Arabidopsis thaliana* mesophyll protoplasts. In accordance to the observations made in *Nicotiana benthamiana*, 30 minutes after flg22 treatment the protein levels of HA-PUB22 markedly increased. To further assess the protein stabilization time-course, additional time points were included (5 minutes and 180 minutes). As early as 5 minutes after treatment of the cells with 1 μ M flg22, a clear increase in HA-PUB22 protein levels became evident (Figure 3-18). The amount of protein reached a maximum between 30 to 60 minutes. The transient nature of the stabilization was reflected by a reduction of protein levels 180 minutes after treatment in which the signal strength was comparable to basal levels. We also assessed the stabilization time-course in protoplasts after 26S-proteasome inhibition. Application of 20 μ M AM114 also rapidly stabilized HA-PUB22, although in contrast to flg22 treatment, the levels did not decrease at later time points. A control treatment with water did not induce HA-PUB22 accumulation. On the contrary, protein levels appeared to constantly decrease. Unlike the expression of HA-PUB22 in *Nicotiana benthamiana*, no double band migrating at a higher molecular weight could be detected in

protoplasts, not even after very long exposure of the blots (data not shown). In summary, these data indicate that PUB22 is rapidly stabilized in response to flg22 treatment.

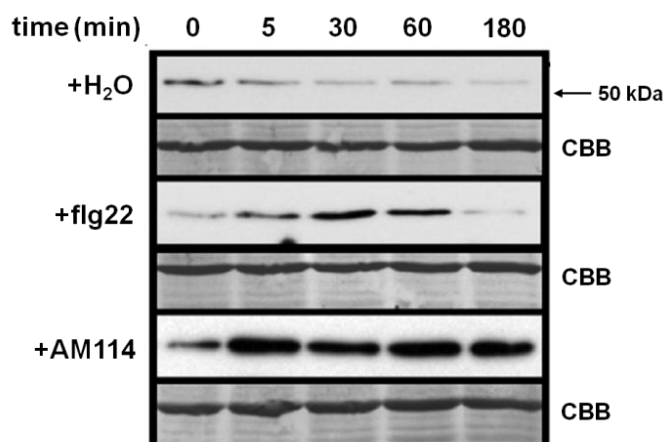


Figure 3-18 Stabilization time-course of HA-PUB22 after different treatments: HA-PUB22 was expressed in *Arabidopsis thaliana* mesophyll protoplasts and treated with 1 μ M flg22, 20 μ M AM114 or water (control) one day after transformation. Samples were taken at the indicated time points and analyzed via SDS-PAGE and Western blot with anti-HA antibodies. Coomassie brilliant blue stain = CBB. Similar results were obtained in three independent experiments.

3.5. Analysis of the ubiquitination and degradation of Exo70B2 by PUB22

The interaction of PUB22 and Exo70B2 was confirmed by using different methods (section 3.3). PUB22 is an active E3-ubiquitin ligase, as previously shown (Trujillo et al., 2008). We wanted therefore to address the question whether PUB22 is also able to ubiquitinate Exo70B2. The most prominent fate of ubiquitinated proteins is their degradation via the 26S-proteasome (Vierstra, 2009). We therefore also investigated a potential involvement of PUB22 in the degradation of Exo70B2.

3.5.1. *In vitro* ubiquitination of Exo70B2 by PUB22

To test whether Exo70B2 can be used by PUB22 as a substrate for ubiquitination, we performed an *in vitro* ubiquitination assay with bacterially-expressed purified proteins. We expressed recombinant MBP-Exo70B2 and GST-PUB22 in *E. coli* BL21(DE3)pLyss cells, purified the proteins and mixed them with all components required for the ubiquitination reaction, ATP, ubiquitin, an E1 activating and an E2 conjugating enzyme. The used E1 was His-tagged UBA1 (AT2G30110) and the E2 was His-tagged UBC8 (AT5G41700) from *Arabidopsis thaliana*.

In the presence of all the necessary components, MBP-Exo70B2 was efficiently ubiquitinated by PUB22 (Figure 3-19, lane 5), as seen by the high molecular smear observed after incubation of the blot with anti-MBP or anti-ubiquitin antibodies. Absence of any of the components abrogated ubiquitination activity (Figure 3-19, lane 1-4). Additionally, the U-box mutant PUB22^{C13A} did not ubiquitinate Exo70B2 (Figure 3-19, lane 6).

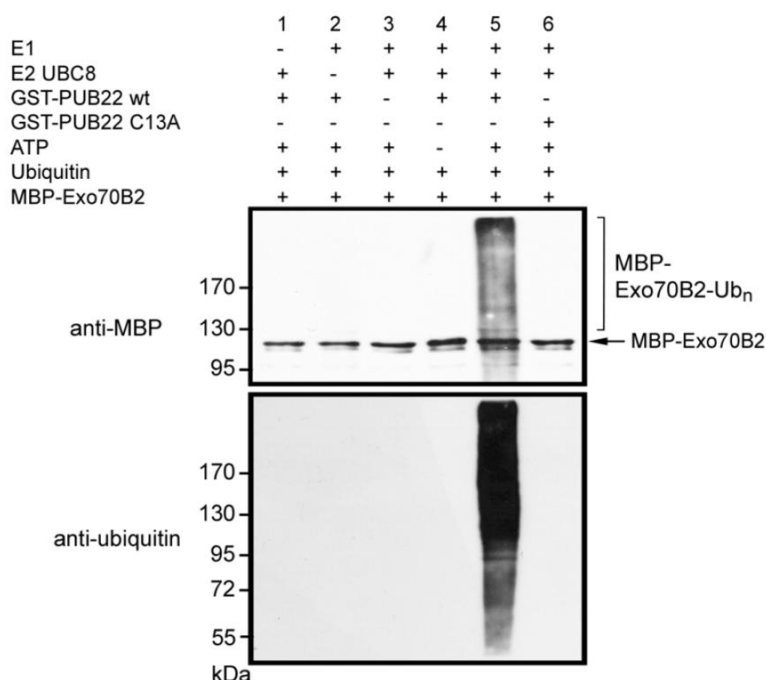


Figure 3-19 *In vitro* ubiquitination assay of Exo70B2 by PUB22: GST-PUB22, the mutant variant GST-PUB22^{C13A} and MBP-Exo70B2 were tested using the *A. thaliana* His-UBA1 and His-UBC8. Lanes one to four and six are negative controls. Proteins were separated by SDS-PAGE and detected by Western blotting using the indicated antibodies.

3.5.2. Analysis of PUB22-mediated Exo70B2 degradation by bimolecular fluorescence complementation

Exo70B2 interacted with PUB22 *in vivo* and was efficiently used as a substrate for ubiquitination *in vitro*. The modification of substrates with Lys48-linked polyubiquitin chains is one of the prevalent forms of ubiquitination and it results in the degradation of labeled proteins by the 26S-proteasome. For this reason we analyzed the effect of PUB22 and Exo70B2 coexpression on Exo70B2 protein levels in *Arabidopsis thaliana* mesophyll protoplasts. To address this we employed a BiFC approach using the wild type full-length PUB22 protein and the U-box inactive mutant PUB22^{C13A}. N-terminal cMyc-nYFP-fusions of both wild type and mutant proteins were generated for subsequent coexpression with cYFP-Exo70B2 and free RFP. Co-expression of RFP allowed determining the transformation efficiency. Furthermore, it

allowed the quantification of BiFC efficiency by calculating the ratio of cells displaying YFP fluorescence to those displaying RFP fluorescence (YFP/RFP). Transfected cells were treated with flg22 or the 26S-proteasome inhibitor AM114 to analyze any differences in the number of cells displaying YFP fluorescence.

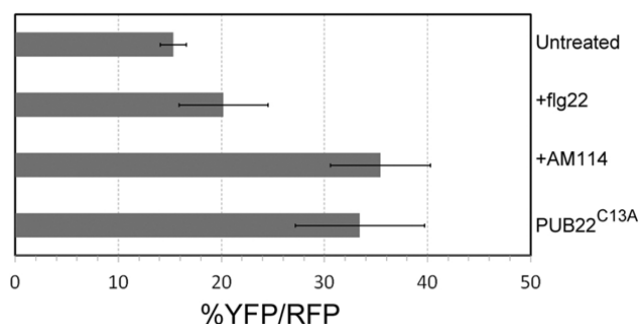


Figure 3-20 Amount of YFP reconstitution per total transformed cells (RFP) in BiFC experiments: cMyc-nYFP-PUB22 or cMyc-nYFP-PUB22^{C13A} were co-expressed with cYFP-Exo70B2 and free RFP in *Arabidopsis thaliana* mesophyll protoplasts. The number of YFP-positive cells per total RFP expressing cells was assessed using confocal laser-scanning microscopy. Cells were treated with 1 μ M flg22 for one hour or 20 μ M AM114 for four hours as indicated. Error bars represent +/- S.D. of three independent experiments, each with n> 80.

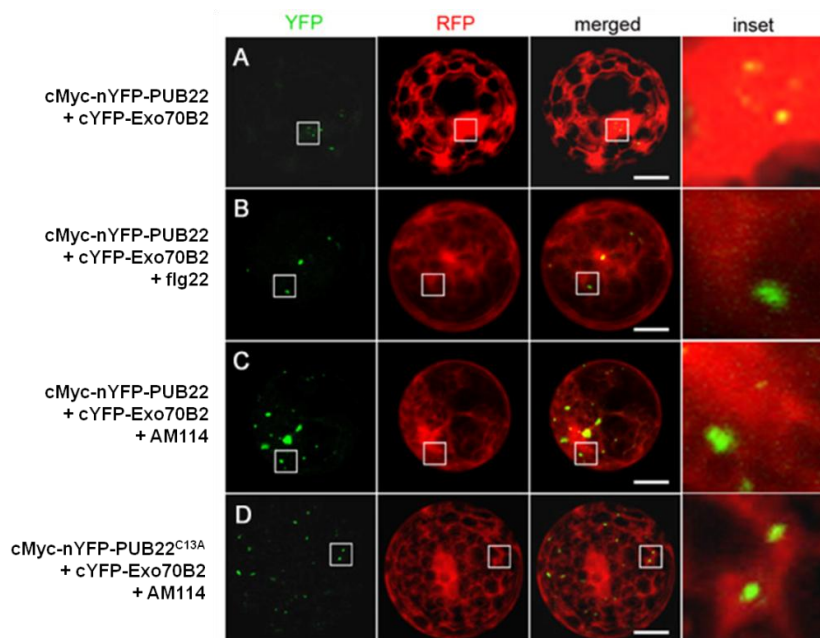


Figure 3-21 Microscopy pictures of BiFC experiment in Figure 3-20: Coexpression of cMyc-nYFP-PUB22 with cYFP-Exo70B2 and free RFP after (A) control treatment (water), (B) treatment with flg22 (1 μ M) or (C) AM114 (20 μ M). (D) Coexpression of cMyc-nYFP- PUB22^{C13A} with cYFP-Exo70B2 and free RFP. Proteins were transiently expressed in *Arabidopsis thaliana* protoplasts. Co-expressed free RFP labels cytoplasm and nucleus. Pictures are representative of three independent experiments with similar results. Scale bar = 50 μ m.

First, we analyzed the ratio of YFP-reconstitution per RFP-positive protoplasts co-expressing cMyc-nYFP-PUB22 and cYFP-Exo70B2 (Figure 3-20). There was only a small amount of RFP positive cells displaying YFP fluorescence (15%). Also the number of punctae within the positive cells was low (Figure 3-21 A) in comparison to BiFC data showing the interaction of PUB22^{ARM} with Exo70B2 (section 3.3.1). After treatment with flg22 the amount of YFP reconstitution slightly increased to 20%. However, this change was not significant and also the amount of punctae was not markedly increased (Figure 3-21 B). On the other hand, treatments with AM114 led to a clear increase of cells displaying YFP reconstitution (33%). Also the amount of YFP fluorescence within the positive cells strongly increased (Figure 3-21 C), as judged by the number and size of punctae. When cMyc-nYFP-PUB22^{C13A} was used instead of cMyc-nYFP-PUB22, the YFP reconstitution was also clearly enhanced in transformed cells (35%), as reflected by the increased number of punctae within positive cells (Figure 3-21 D). The size of punctae however did not increase.

To analyze the levels of the different fusion proteins from the BiFC experiments we performed Western blot analysis. Protein samples were analyzed via SDS-PAGE and Western blot (Figure 3-22).

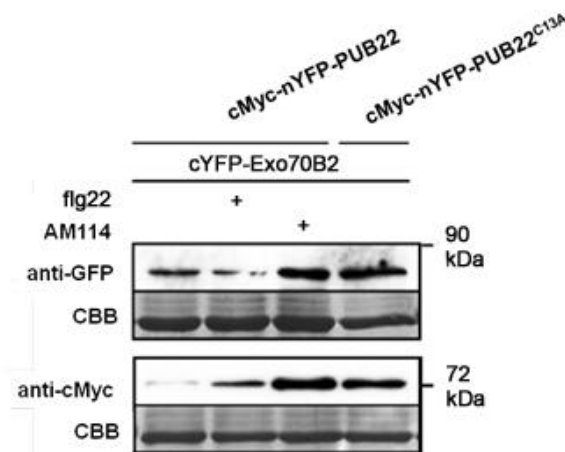


Figure 3-22 Western blot analysis of BiFC samples from Figure 3-20 and Figure 3-21: Samples were analyzed via SDS-PAGE and Western blot. Detection of fusion proteins was carried out with the indicated antibodies. Coomassie brilliant blue stain = CBB. Similar results were obtained in three independent experiments.

After treatment with flg22, cMyc-nYFP-PUB22 levels strongly increased (Figure 3-22, anti-cMyc panel), consistent with previous results. Levels of cYFP-Exo70B2 on the other hand mildly decreased after flg22 elicitation, as shown by the band intensities in the anti-GFP panel in

Figure 3-22. After application of the 26S-proteasome inhibitor AM114 or in the coexpression with the U-box inactive mutant cMyc-nYFP-PUB22^{C13A}, both proteins accumulated much stronger. These results are consistent with the percentage of YFP reconstitution per RFP fluorescence, shown in Figure 3-20, indicating that PUB22 mediates the degradation of Exo70B2 in response to flg22 perception *in vivo*.

3.5.3. Expression of cMyc-Exo70B2 in wild type and *pub22/23/24 Arabidopsis thaliana* mesophyll protoplasts

The presented data demonstrated the physical interaction of PUB22 with Exo70B2 (section 3.3), the *in vitro* ubiquitination of Exo70B2 by PUB22 (section 3.5.1) and the PUB22 dependent degradation of Exo70B2 *in vivo* (section 3.5.2). In addition the two close homologs of PUB22, PUB23 and PUB24, were able to interact with Exo70B2 (section 3.3.4).

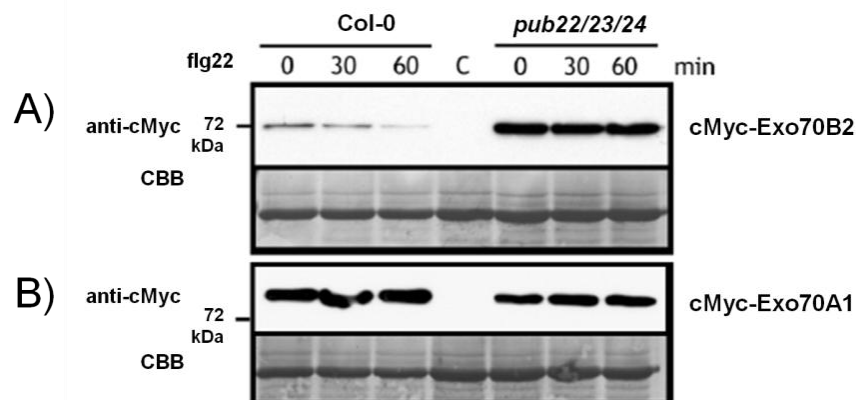


Figure 3-23 Expression of recombinant cMyc-Exo70B2 and cMyc-Exo70A1 in wild type and *pub22/23/24* protoplasts: *Arabidopsis* protoplasts derived from wild type or *pub22/23/24* plants were transformed with (A) cMyc-Exo70B2 or (B) cMyc-Exo70A1. Cells were treated with 1 μ M flg22 and harvested at the indicated time points after elicitation. Proteins were analyzed via SDS-PAGE and Western blot using anti-cMyc antibodies. Coomassie brilliant blue stain = CBB. Similar results were obtained in three independent experiments.

To further confirm the degradation of Exo70B2 by PUB22, and potentially also by PUB23 and PUB24, we performed an experiment in protoplasts in which cMyc-Exo70B2 was expressed in two different genetic backgrounds, namely in wild type and in *pub22/23/24* triple mutant

protoplasts. Protein levels of cMyc-Exo70B2 were compared in both genetic backgrounds and changes induced by treatment with 1 μ M flg22. Samples were harvested and analyzed via SDS-PAGE and Western blot using anti-cMyc antibodies.

The levels of cMyc-Exo70B2 proteins continuously decreased after treatment of cells with 1 μ M flg22 in wild type derived protoplasts 30 minutes and 60 minutes after treatment (Figure 3-23 A), indicating that Exo70B2 is degraded in response to flg22. In protoplasts from *pub22/23/24* plants the levels did not decrease after flg22 treatment. Importantly, the basal protein level of cMyc-Exo70B2 was much higher in the *pub22/23/24* background. To rule out a general effect, we included in the same experimental setup the homolog of Exo70B2, Exo70A1. No decrease of cMyc-Exo70A1 protein levels after treatment of wild type cells with flg22 could be observed. In addition, basal levels of the protein in *pub22/23/24* were comparable to wild type (Figure 3-23 B). This data provides additional evidence for the PUB22-mediated degradation of Exo70B2 in response to flg22 treatment.

3.6. Characterization of the PAMP-triggered responses and disease resistance of *exo70B2* mutants

First experiments with *exo70B2* mutants showed reduced ROS production after flg22 treatment and enhanced susceptibility to *Pst* infection. Therefore, *exo70B2* mutant plants displayed the opposite phenotype of the *pub22/23/24* mutant (Trujillo et al., 2008). These data indicate a function of Exo70B2 in the positive regulation of PAMP-triggered immune responses. Data confirming the interaction between PUB22 and Exo70B2, as well as with PUB23 and PUB24 (section 3.3) additionally support the notion that Exo70B2 is a PUB target involved in the PUB-mediated regulation of immune responses. However, only one mutant allele of *exo70B2* was analyzed so far and the possibility that the observed phenotypes are caused by second site mutations cannot be excluded. Therefore, an additional mutant allele of *exo70B2* was generated and subjected to further detailed phenotypical analysis. Moreover, an epistatic effect of *exo70B2* on the *pub22/23/24* mutation was analyzed by generating a *pub22/23/24/exo70B2* quadruple mutant.

3.6.1. Isolation of two independent *exo70B2* T-DNA insertion lines and generation of a *pub22/23/24/exo70B2* quadruple mutant

The T-DNA insertion line initially analyzed was SALK-091877C, previously described as *exo70B2-1* (Pecenková et al., 2011). We isolated a second T-DNA insertion mutant, the GABI-Kat line GK-726G07, which we named *exo70B2-3*. A scheme of both alleles shows the T-DNA insertion sites in exons (Figure 3-24 A). The homozygous plants were isolated by gene specific PCR genotyping of seeds propagated from heterozygous parents. RNA of both lines was isolated and used as a template for reverse transcription PCR. Transcript level of *Exo70B2* was checked by primers binding to the positions indicated by arrows (Figure 3-24 A). Both *exo70B2-1* and *exo70B2-3* did not show any *Exo70B2* mRNA expression, showing that both lines are knockouts (Figure 3-24 B).

The *exo70B2-1* and *exo70B2-3* mutant plants were analyzed for potential developmental defects. Both lines showed plant growth, morphology, flowering time and seed yield similar to wild type Col-0 plants. Only a slight difference in shoot branching and size could be observed for both *exo70B2-1* and *exo70B2-3*. The *pub22/23/24* triple mutant did not show detectable developmental phenotypes, as previously reported (Trujillo et al., 2008). The morphologies of Wild type Col-0, *pub22/23/24*, *exo70B2-1* and *exo70B2-3* are shown in Figure 3-25.

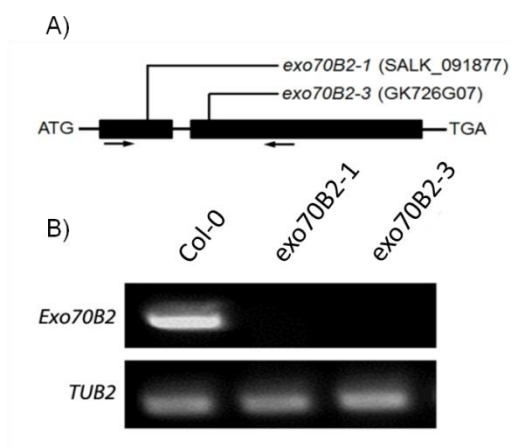


Figure 3-24 Characterization of *exo70B2* T-DNA Insertion lines: (A) Gene structure of *Exo70B2*. Black boxes represent exons, line represents intron. Positions of T-DNA insertions are marked. (B) Transcript accumulation of *Exo70B2* in *exo70B2-1* and *exo70B2-3*. Primer binding sites are marked by arrows in (A).



Figure 3-25 Comparison of plant morphology of wild type Col-0, *pub22/23/24*, *exo70B2-1* and *exo70B2-3*: photographs of flowering plants of the indicated mutants. Plants were grown for six weeks under long day conditions (16h light/8h dark).

To analyze potential epistatic effects of the *exo70B2* mutation on the *pub22/23/24* triple mutant, a quadruple mutant was generated by crossing *exo70B2-1* with *pub22/23/24*. The resulting heterozygous plants were further propagated and homozygous quadruple mutant lines were isolated by PCR genotyping using primers specific for all four genes. Sequences of the used primers are listed in the appendix, Table 5. The *pub22/23/24/exo70B2-1* mutant did not display any transcript accumulation of *PUB22*, *PUB23*, *PUB24* and *Exo70B2* and also did not show any significant developmental phenotypes (data not shown).

3.6.2. Analysis of PAMP-triggered responses of *exo70B2* mutants

The *pub22/23/24* triple mutants display an enhanced ROS-burst which is not specific for elicitation with flg22 and is detectable after treatment with different PAMPs or DAMPs. In addition, mutants are more resistant to different pathogens (Trujillo et al., 2008). As mentioned before, *exo70B2-1* displayed a compromised ROS-burst after flg22 elicitation and an increased susceptibility to *Pst DC3000*. The reduced PAMP responsiveness phenotype was confirmed using the second independent allele, *exo70B2-3*. This was achieved by using different PAMPs and DAMPs such as elf18, chitin and Pep1, and additional readout methods including flg22-induced MPK activation, PTI gene expression analysis and flg22-induced root growth inhibition.

3.6.2.1. Analysis of the ROS-burst triggered by various elicitors

After treatment with 500nM flg22 both *exo70B2-1* and *exo70B2-3* showed a reduced ROS production in comparison to wild type (Figure 3-26 A). The *exo70B2-1* mutant peaked with 59 RLU and *exo70B2-3* with 65 RLU, while wild type plants reached a maximum of 117 RLU. The pattern of the ROS-burst was unchanged; both alleles peaked at similar time points to wild type at 6 min. The total ROS production was significantly compromised in both *exo70B2* alleles compared to the wild type. The *exo70B2-1* mutants had a total ROS production of 343 RLU +/- 146 S.D. ($p < 0,01$) and *exo70B2-3* 298,2 RLU +/- 154 S.D. ($p < 0,01$), while wild type had a total

of 592 RLU +/- 151 S.D.. The *pub22/23/24* mutant responded much stronger, as expected, with 1783 total RLU +/- 409 S.D. ($p < 0,001$).

In another experiment, leaf discs were treated with 500 nM elf18 (Figure 3-26 B). Both *exo70B2-1* (6,2 RLU) and *exo70B2-3* (5,1 RLU) displayed lower peak values compared to the wild type (17,4 RLU). The pattern was not changed and all mutants reached their maximum at 10 min. The *pub22/23/24* triple mutant peaked higher (81,5 RLU) and the signal persisted much longer, as expected. The total ROS production was significantly reduced in both *exo70B2-1* (48,9 RLU +/- 25,7 S.D.; $p < 0,001$) and *exo70B2-3* (49,5 RLU +/- 26,7 S.D.; $p < 0,001$) after elicitation with elf18 in comparison to the wild type (149,1 RLU +/- 37,6 S.D.) and significantly enhanced in *pub22/23/24* (1689 RLU +/- 563 S.D.; $p < 0,001$).

After treatment with 100 µg/ml chitin *exo70B2-1* showed only a slight reduction (30,7 RLU) in the ROS maximum in comparison to the wild type (33,1 RLU) (Figure 3-26 C). By contrast, *exo70B2-3* showed a clear reduction (19,0 RLU). The kinetic was not affected and all three lines reached peak values at 21 min. The total ROS production in *exo70B2-1* (225 RLU +/- 158 S.D.) showed a slight, but not significant decrease in comparison to the wild type (258 RLU +/- 162,5 S.D.). The *exo70B2-3* mutant showed a significant reduction (98,1 RLU +/- 49,5 S.D.; $p < 0,05$). The *pub22/23/24* mutants peaked higher (41,6 RLU) and the signal did not reach basal levels in the experimental time frame. Also, the total ROS production was significantly enhanced (833,9 RLU +/- 563 S.D.; $p < 0,05$). However, because the ROS production triggered by chitin is weak, the results need to be interpreted with precaution.

Elicitation with Pep1 resulted in a similar phenotype (Figure 3-26 D). The pattern of the ROS-burst was not affected and the maximal value was reached at 18min. Both *exo70B2-1* (5,9 RLU) and *exo70B2-3* (3,3 RLU) had a reduced maximum in comparison to the wild type (7,2 RLU) and also the total ROS production was significantly compromised in both mutants (*exo70B2-1*: 86 RLU +/- 29,2, S.D.; $p < 0,05$; *exo70B2-3*: 55 RLU +/- 18,9 S.D.; $p < 0,001$; wild type: 124 RLU +/- 32 S.D.). The *pub22/23/24* mutants reached a much higher peak value (42.2 RLU) and also, the total ROS production was strongly elevated (611 RLU +/- 321 S.D.; $p < 0,01$). In summary, treatment with all tested elicitors triggered reduced responses in comparison to the wild type in *exo70B2* mutant lines.

To test whether *Exo70B2* is on the same genetic pathways as *PUB22*, *PUB23* and *PUB24* we assayed the *pub22/23/24/exo70B2-1* quadruple mutant for its ROS-burst after treatment with flg22. The result is shown in Figure 3-26 E.

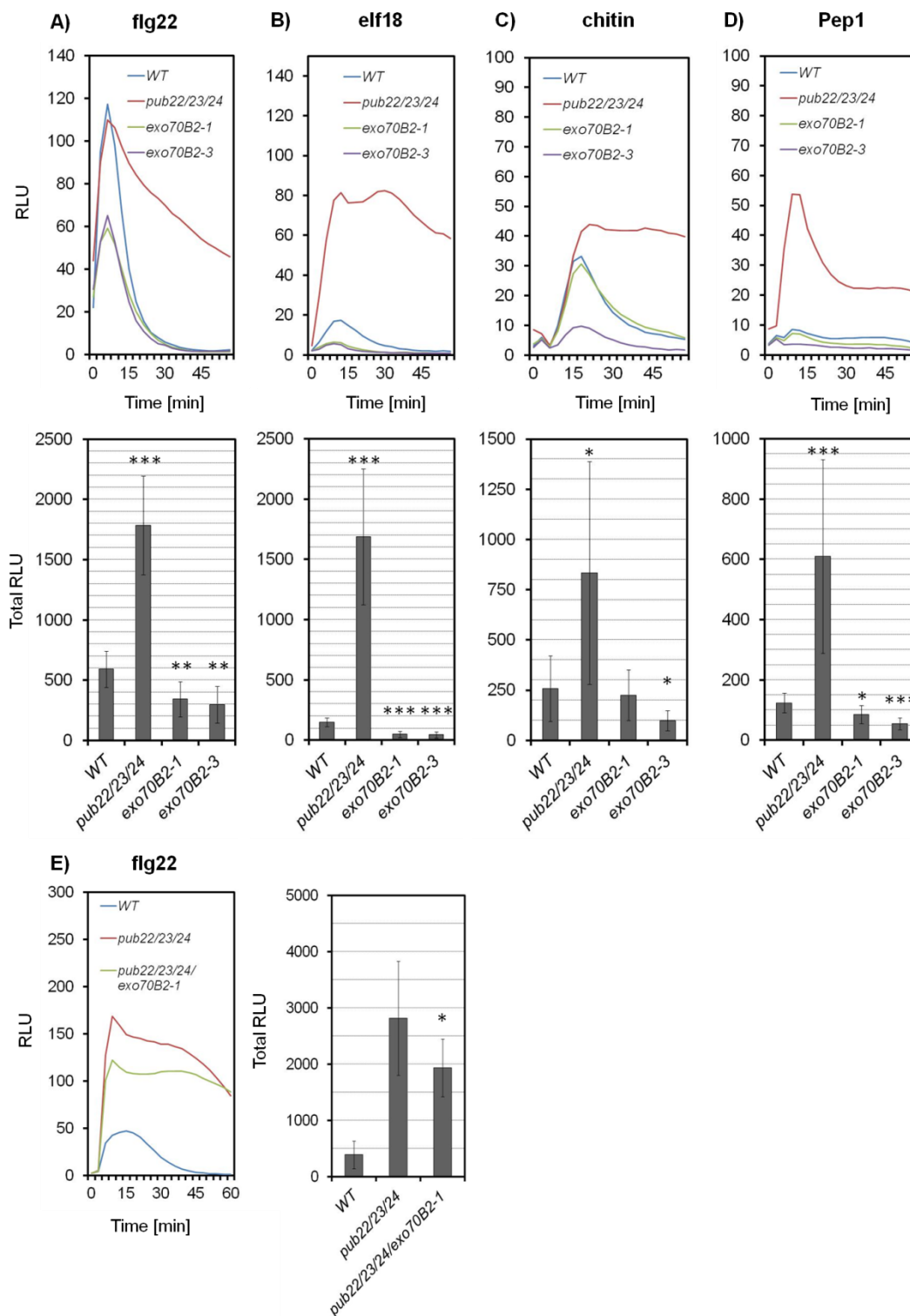


Figure 3-26 ROS-burst kinetic and total ROS production after treatment with different elicitors: ROS production was measured in leaf discs of six to seven week-old plants of the indicated mutant lines in a luminol-based assay after treatment with (A) 500nM flg22, (B) 500nm elf18, (C) 100µg/ml chitin, (D) 500nm Pep1 and (E) 500nm flg22. Each time point represents the average of eight independent samples. Total ROS production is calculated by the integration of the area under the kinetic curves. Error bars represent +/- S.D. of eight independent samples. Statistical significance is indicated by asterisks (Student's *t* test, **p* < 0,05, ***p* < 0,01, ****p* < 0,001). RLU = relative light units. Similar results were obtained in three independent experiments.

The peak value of *pub22/23/24/exo70B2-1* (122 RLU) was lower than *pub22/23/24* (168 RLU), but still higher than the wild type (47 RLU). Both *pub22/23/24* and *pub22/23/24/exo70B2-1* (9 min) also peaked earlier than wild type (15 min). *pub22/23/24* (2814 RLU +/- 1014 S.D.) and *pub22/23/24/exo70B2-1* (1934 RLU +/- 510 S.D) had an enhanced total ROS production in comparison to the wild type with *pub22/23/24/exo70B2-1* being significantly reduced compared to *pub22/23/24* ($p < 0,05$).

This data shows that in terms of ROS-burst after flg22 elicitation, *exo70B2* has an epistatic effect on the *pub22/23/24* triple mutation and therefore, the enhanced responsiveness of *pub22/23/24* to flg22 is compromised in *pub22/23/24/exo70B2-1*. In summary, this data indicates that *Exo70B2* is required to mount a full ROS-burst response, which is not limited to the perception of distinct PAMPs but extends to different PAMPs and DAMPs as well.

3.6.2.2. MPK activity assay

After PAMP perception a signaling cascade is triggered, involving the three kinases MPK3, MPK4 and MPK6. While MPK3 and MPK6 are positive regulators, MPK4 was proposed to be involved in the downregulation of immunity (Suarez-Rodriguez et al., 2007, Gao et al., 2008). We tested the activity of MPK3, MPK4 and MPK6 in response to flg22 treatment in an immunocomplex kinase assay (Ichimura et al., 2006). Analysis was performed by Kazuya Ichimura from the Kagawa University in Japan.

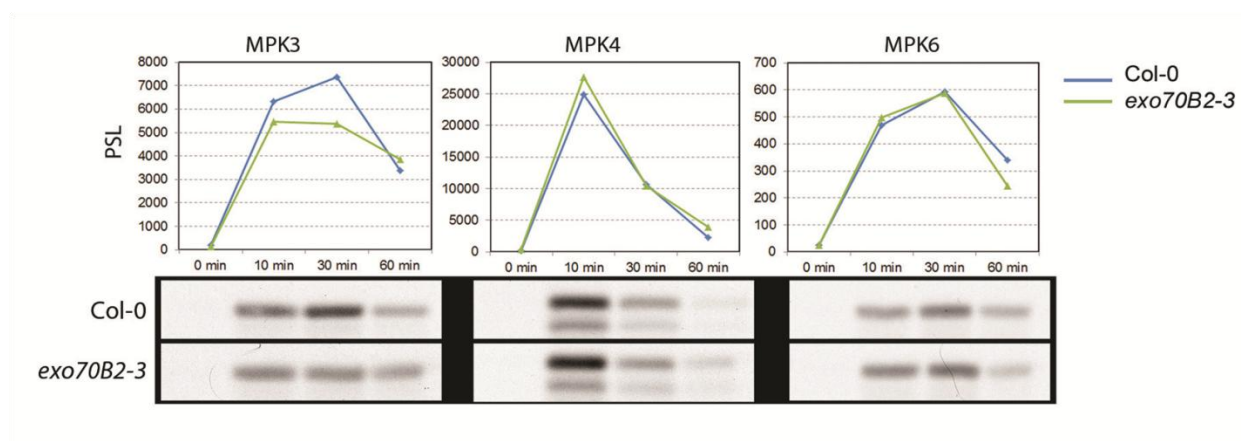


Figure 3-27 MPK activity assay of *exo70B2-3* in comparison to Col-0: Two weeks-old seedlings were elicited with 1 μ M flg22 and an immunocomplex kinase activity assay was performed for MPK3, MPK4, and MPK6. Results are shown as Photostimulated luminescence (PSL) in arbitrary units. Similar results were obtained in two independent experiments.

The *exo70B2-3* mutants showed a reduced activity for MPK3 (5500 μ Photostimulated luminescence (PSL)) in comparison to the wild type (7000 PSL). MPK4 and MPK6 are not affected. The *exo70B2-3* mutants showed the opposite phenotype of the *pub22/23/24* mutant, which has been shown to have a specifically increased activity of MPK3 (Trujillo et al., 2008). This data indicates that Exo70B2 is required for the full activation of MPK3 after PAMP perception.

3.6.2.3. Expression analysis of defense related genes

A more downstream response induced by the perception of PAMPs is the transcriptional activation of defense related genes, which takes place between 30-60 minutes after recognition. Flg22 elicitation induces the expression of genes in *Arabidopsis* seedlings, including marker genes such as *At4g20780*, *RbohD* and the *WRKY* transcription factors 11, 22 and 29 (Navarro et al., 2004).

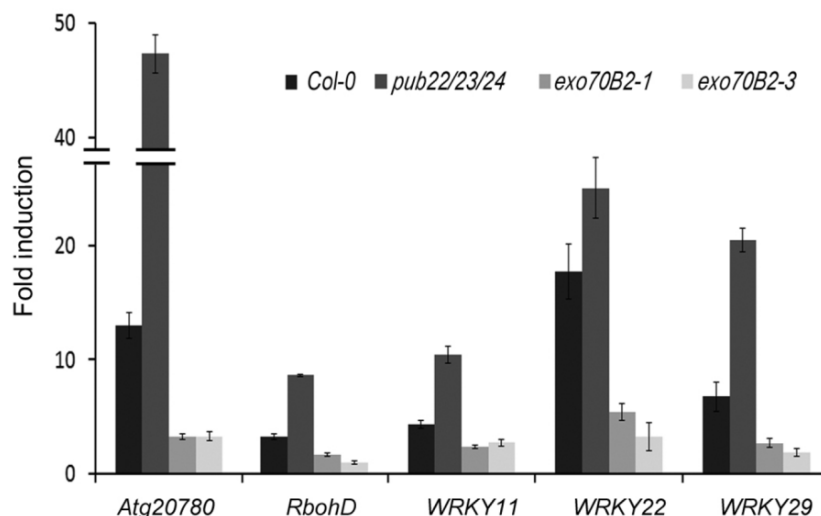


Figure 3-28 Expression analysis of defense related genes after flg22 treatment: Seedlings were treated with 1 μ M flg22 or water (control) for one hour. Samples were taken and total RNA was extracted for cDNA synthesis and subsequent quantitative real time PCR. *ACT2* was used as a reference gene. Data shown as mean \pm S.D. (n=3). Similar results were obtained in three independent experiments.

We tested the transcript accumulation of the 5 genes via quantitative real time PCR using cDNA of seedlings treated for 1hour with flg22. Results show the fold induction of gene expression in reference to Actin 2 (*ACT2*, AT3G18780) (Figure 3-28). All 5 tested genes displayed a reduction

of the transcriptional activation in *exo70B2-1* and *exo70B2-3*, while the expression was enhanced in *pub22/23/24*, as expected.

We also analyzed the transcriptional activation of *PR1*, a marker gene of the salicylic acid pathway, after inoculation with *Pst DC3000* (Figure 3-29). One day after syringe inoculation of leaves with a solution of 10^7 cfu/ml, the *PR1* expression was compromised in both *exo70B2-1* and *exo70B2-3* in comparison to the wild type. In *pub22/23/24* the expression of *PR1* was enhanced.

PTI marker gene expression after flg22 treatment (Figure 3-28) and also the expression of *PR1* after *Pst* infection (Figure 3-29) was reduced in both mutant alleles in comparison to the wild type, indicating that *Exo70B2* is required to mount a full transcriptional response upon flg22 perception and *Pst* invasion.

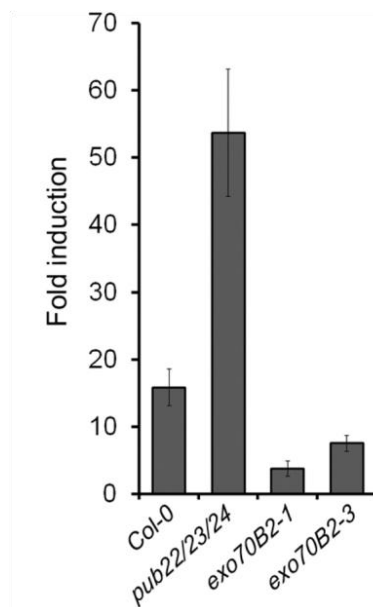


Figure 3-29 *PR1* expression in leaves after *Pst* infection: Plants were syringe-infiltrated with a bacterial solution containing 1×10^7 cfu/ml or water (control) and harvested for RNA extraction, cDNA synthesis and quantitative real time PCR 24 hours after inoculation. *ACT2* was used as a reference gene. Data is shown as mean \pm S.D. (n=3). Similar results were obtained in three independent experiments.

3.6.2.4. Root growth inhibition assay

When seedlings are grown in media containing flg22, their growth is inhibited due to the constant activation of PTI. We analyzed the growth inhibition of the main root in seedlings as an additional readout to quantitatively assay the PAMP responsiveness of *exo70B2* and *pub22/23/24* mutants.

Seedlings were grown horizontally for 7 days under short day conditions and transferred on MS media supplemented with 1 μ M flg22. Wild type Col-0 plants displayed a 32,7% \pm 4,8 S.E.M. decrease in root growth compared to untreated controls (Figure 3-30), consistent with previous reports (Bethke et al., 2009). In *pub22/23/24* the root growth inhibition was significantly stronger with 49,3% \pm 5,1 S.E.M ($p < 0,01$), which is in line with previous data showing enhanced PAMP responsiveness of the triple mutants (Trujillo et al., 2008). By contrast, root growth inhibition in *exo70B2* mutants was strongly and significantly reduced compared to the wild type, with 15,2% \pm 7,1 S.E.M. ($p < 0,01$) in *exo70B2-1* and 13,5% \pm 6,8 S.E.M. ($p < 0,01$) in *exo70B2-3*. The epistatic effect of *exo70B2* on *pub22/23/24* was analyzed by testing the *pub22/23/24/exo70B2-1* mutant. The enhanced root growth inhibition of *pub22/23/24* (49,3%) was slightly compromised in *pub22/23/24/exo70B2-1* (44,4% \pm 9,4 S.E.M.), in accordance to the results obtained in ROS-burst experiments (Figure 3-26). In summary, this data indicates that *exo70B2* mutants are impaired in PTI signaling triggered by flg22. Furthermore, it supports a function of *Exo70B2* in the same genetic pathway as *PUB22*, *PUB23* and *PUB24*.

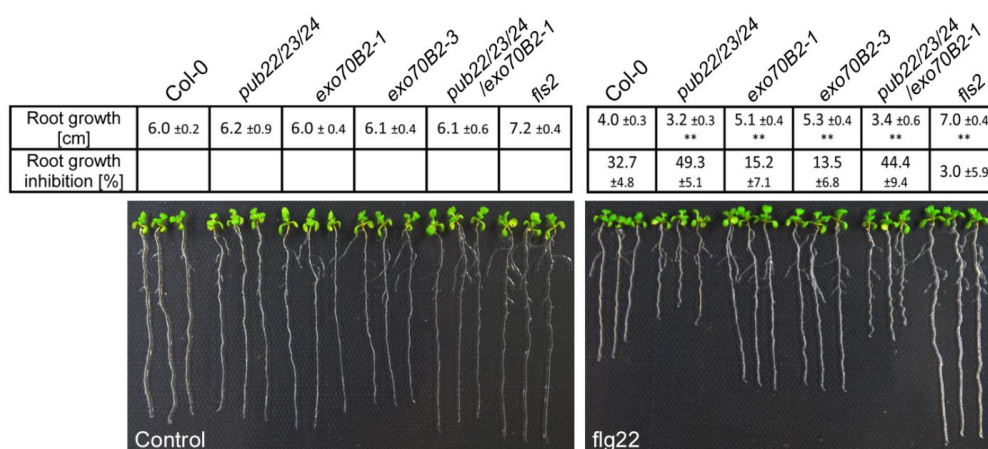


Figure 3-30 Flg22-induced root growth inhibition: Root growth inhibition was assayed on media containing 1 μ M flg22 containing. Seedlings were grown for seven days before they were transferred to flg22 containing media. Length of the main root was measured seven days after transplanting. Data is shown as the mean of three independent experiments \pm S.E.M. ($n \geq 60$). Statistical significance compared to Col-0 plants is indicated by asterisks (Student's *t* test, ** $p < 0,01$, *** $p < 0.001$). Similar results were obtained in three independent experiments.

3.6.3. Disease resistance analysis of *exo70B2* mutants

In all assays performed to analyze the effects of PAMP treatment, *exo70B2* mutants were less responsive in comparison to wild type and always showed the opposite phenotype than the *pub22/23/24* triple mutant. The production of ROS was compromised in *exo70B2* mutants after treatment of leaf discs with flg22, elf18, chitin and Pep1 (3.6.2.1). The activation of MPK3 was less pronounced (3.6.2.2), the transcriptional induction of defense marker genes was reduced (3.6.2.3) and the root growth inhibition was strongly impaired in *exo70B2* mutants (3.6.2.4).

In the *pub22/23/24* triple mutants the enhanced PAMP responsiveness results in an enhanced disease resistance to *Pseudomonas syringae* DC3000 and *Hyaloperonospora arabidopsidis* (Trujillo et al., 2008). To test whether the reduced responsiveness of the *exo70B2* mutants resulted in enhanced disease susceptibility we performed different pathogen infection experiments.

3.6.3.1. Pathogen growth assays with *Pseudomonas syringae* DC3000

The preliminary experiments (section 3.2.3) showed an enhanced susceptibility of *exo70B2-1* mutants to *Pst* after spray infection experiments (Figure 3-5). This enhanced susceptibility was confirmed by using the second T-DNA insertion allele, *exo70B2-3*.

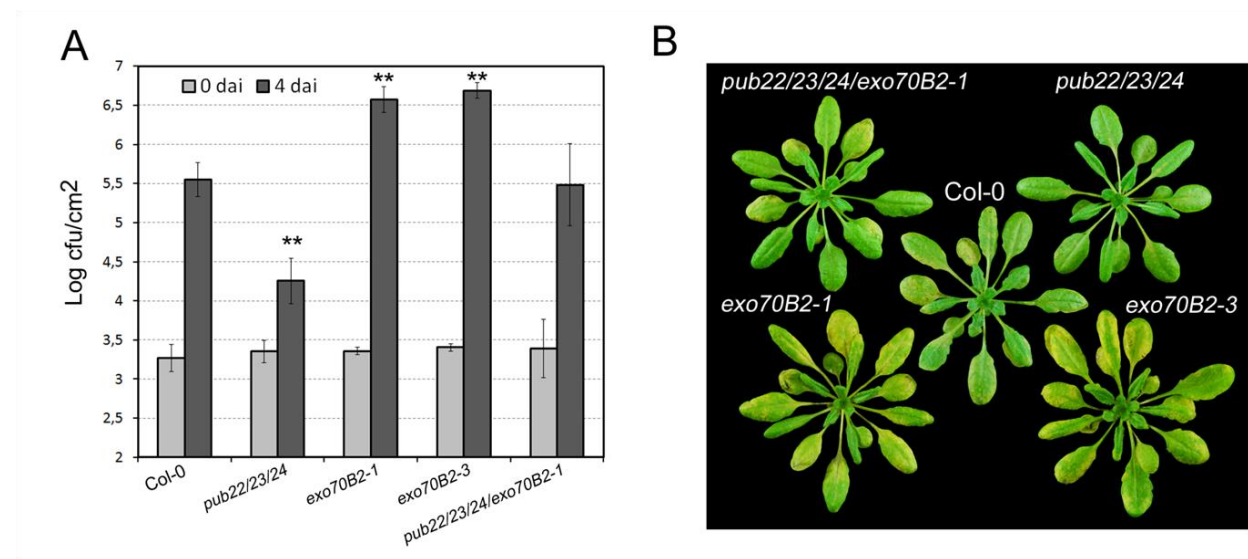


Figure 3-31 Pathogen growth assay with *Pst* DC3000: Six week-old plants of the indicated mutant lines were spray-inoculated with a bacterial suspension of 5×10^8 cfu/ml. (A) Infection and bacterial growth was assessed at zero and four days after inoculation (dai). Data shown as mean \pm S.D. (n=5). Statistical significance is indicated by asterisks (Student's *t* test, ***p* < 0,01). (B) Representative pictures of plants from (A). Similar results were obtained in three independent experiments.

Four days after spray infection of plants with a bacterial solution of 5×10^8 cfu/ml, both *exo70B2-1* and *exo70B2-3* showed a significantly enhanced bacterial growth of $6,6 \log_{10}$ cfu/cm² \pm 0,2 S.D. ($p < 0,01$) and $6,7 \log_{10}$ cfu/cm² \pm 0,1 S.D. ($p < 0,01$) respectively. This represents an increase of the bacterial growth of $1,1 \log_{10}$ and $1,2 \log_{10}$ respectively in comparison to the wild type Col-0, which displayed a value of $5,5 \log_{10}$ cfu/cm² \pm 0,2 S.D.. As expected, the *pub22/23/24* mutant was significantly more resistant with $4,3 \log_{10}$ cfu/cm² \pm 0,3 S.D. ($p < 0,01$; Figure 3-31 A). The statistically significant differences in bacterial growth were also reflected by the increased development of disease symptoms. Both *exo70B2-1* and *exo70B2-3* showed enhanced leaf yellowing in comparison to the wild type, while *pub22/23/24* mutants showed almost no symptoms (Figure 3-31 B). The *pub22/23/24/exo70B2-1* quadruple mutants showed bacterial growth similar to the wild type ($5,6 \log_{10}$ cfu/cm² \pm 0,5 S.D.; Figure 3-31 A) and also the development of disease symptoms was comparable (Figure 3-31 B). The enhanced disease resistance of *pub22/23/24* was suppressed in *pub22/23/24/exo70B2-1*, underpinning the epistatic effect of *exo70B2* on *pub22/23/24* phenotypes. This data indicates that *Exo70B2* is required for plant immunity against *Pst* infections.

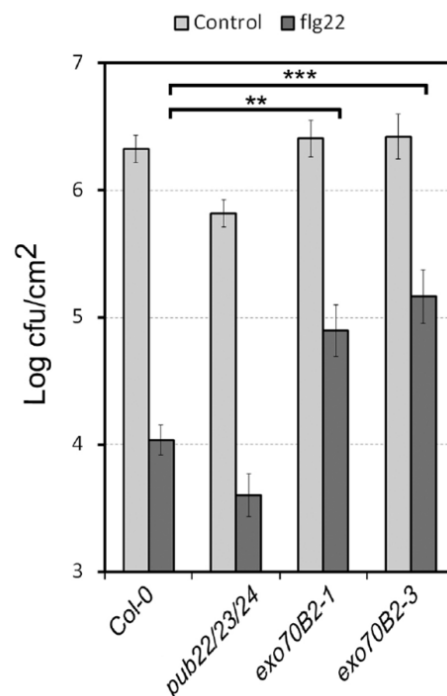


Figure 3-32 Protection effect of flg22 treatment prior to *Pst* infection: Six week-old plants of the indicated mutants were pretreated with 100nm flg22 or water (control) for 24 hours before syringe inoculation with *Pst* (5×10^5 cfu/ml). Two days after infection bacterial growth was assessed. Data is shown as the mean of three independent experiments \pm S.E.M. ($n = 18$). Statistical significance is indicated by asterisks (Student's *t* test, ** $p < 0,01$, *** $p < 0,001$).

Activation of immunity by PAMPs prior to an infection was shown to have a protective effect by priming immune responses for posterior infections (Zipfel et al., 2004). This is manifested by reduced growth of virulent *Pst* in plants that have been pretreated with flg22. We performed this experiment with *exo70B2*, *pub22/23/24* and wild type to compare the efficiency of PAMP-triggered priming in the different lines. Plants were treated with 100nM flg22 or with water as a control one day before syringe infiltration with a bacterial suspension of 5×10^5 cfu/ml. Three days after infection bacterial growth was assessed. Results are shown in Figure 3-32.

Wild type plants showed a bacterial growth of $6,3 \log_{10}$ cfu/cm² +/- 0,11 S.E.M. without flg22 pretreatment. Priming with flg22 resulted in a reduction of bacterial growth by $2,3 \log_{10}$ cfu/cm² to $4,0 \log_{10}$ cfu/cm² +/- 0,12 S.E.M.. Water treated *exo70B2-1* ($6,4 \log_{10}$ cfu/cm² +/- 0,15 S.E.M.) and *exo70B2-3* ($6,4 \log_{10}$ cfu/cm² +/- 0,18 S.E.M.) mutants showed bacterial levels comparable to the control treated wild type. By contrast, pretreatment with flg22 resulted in both *exo70B2-1* ($4,9 \log_{10}$ cfu/cm² +/- 0,2 S.E.M.) and *exo70B2-3* ($5,2 \log_{10}$ cfu/cm² +/- 0,21 S.E.M.) in a significantly impaired reduction of growth, which amounted to a difference of $1,5 \log_{10}$ cfu/cm² ($p < 0,01$) and $1,3 \log_{10}$ cfu/cm² ($p < 0,001$) respectively in comparison to the wild type ($\Delta \log_{10}$ cfu/cm² = 2,3). The *pub22/23/24* mutants showed a slight reduction in bacterial levels without pretreatment ($5,8 \log_{10}$ cfu/cm² +/- 0,11 S.E.M.) and flg22 treatment resulted in a further reduction of growth by $2,2 \log_{10}$ cfu/cm² to $3,6 \log_{10}$ cfu/cm² +/- 0,17 S.E.M.. These data show that the flg22-induced protection effect is compromised in both *exo70B2* mutant alleles, indicating that *Exo70B2* is required for the full induction of the PAMP-triggered protection effect.

3.6.3.2. Infection experiments with *Hyaloperonospora arabidopsidis*

In cooperation with the group of John McDowell from Virginia Tec, USA, we tested the resistance of *exo70B2* mutants to another *Arabidopsis thaliana* pathogen, namely the strictly biotrophic oomycete *Hyaloperonospora arabidopsidis* (*Hpa*). The virulent isolate Emco5 (McDowell et al., 2005) was used to inoculate two week-old seedlings. Seven days after infection the ability of the pathogen to colonize the plants was assessed by counting the number of sporangiophores. To test a potential influence on cell death, samples were stained with trypan blue and subsequently quantified for scoring. Results are shown in Figure 3-33.

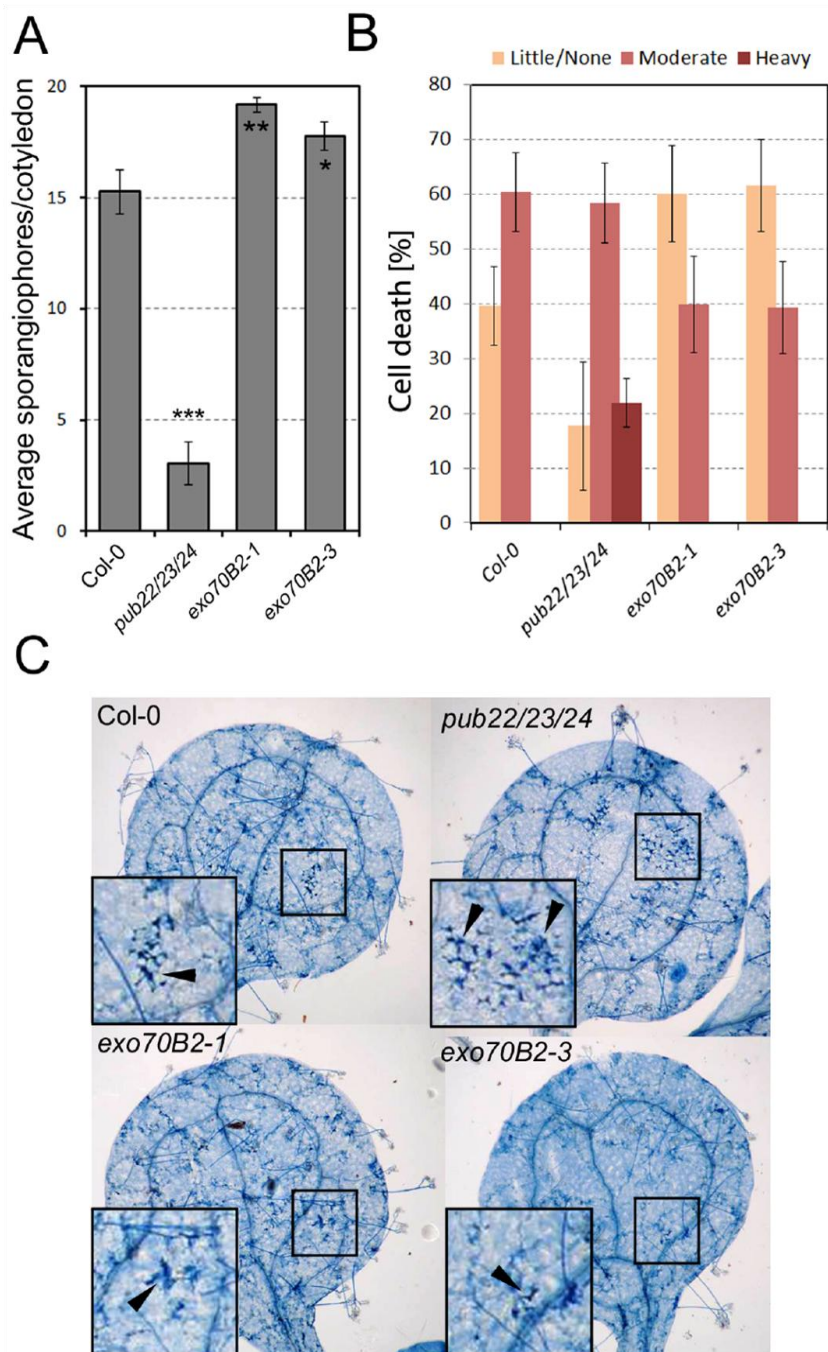


Figure 3-33 *Hyaloperonospora arabidopsidis* infection assay in seedlings: (A) Two week-old seedlings were inoculated with a solution of 5×10^4 spores/ml. Growth was assessed by the number of sporangiophores seven days after inoculation on at least 50 cotyledons \pm S.E.M. Experiment was repeated five times with similar results. Statistical significance is indicated by asterisks (Student's t-test; * $p < 0,05$, ** $p < 0,01$, *** $p < 0,001$). (B) Cotyledons from (A) were stained with trypan blue and cell death was scored as heavy, moderate or little/none. Shown are the percentages for averages of each category of cell death from three independent experiments \pm S.E.M. ($n \geq 60$). (C) Representative pictures of trypan blue stained cotyledons displaying cell death (arrowheads) in the indicated mutant lines. Similar results were obtained in five independent experiments.

Both *exo70B2-1* and *exo70B2-3* were more susceptible compared to the wild type as shown by the significantly increased number of sporangiophores per cotyledon (Figure 3-33 A). The average number was assessed to be 19,5 +/- 0,4 S.E.M. ($p < 0,01$) for *exo70B2-1* and 17,5 +/- 0,6 S.E.M. ($p < 0,05$) for *exo70B2-3*, while wild type showed 15 +/- 1,0 S.E.M. sporangiophores per cotyledon. The *pub22/23/24* mutant was significantly more resistant, showing 3,5 +/- 1,0 S.E.M. ($p < 0,001$) sporangiophores per cotyledon.

The enhanced susceptibility of *exo70B2-1* and *exo70B2-3* was accompanied by reduced cell death. Cell death was scored by trypan blue staining of infected cotyledons. Depending on the number of trypan blue stained cells, cell death was categorized as little/none, moderate or heavy. Scoring of the trypan blue staining revealed that wild type plants showed 40% (Figure 3-33 B) cell death categorized as little/none and 60% as moderate, while both *exo70B2-1* and *exo70B2-3* showed the opposite distribution with 60% little/none compared to 40% moderate cell death reactions. The response was strongly increased in *pub22/23/24* with 20% little/none, 60% moderate and 20% heavy cell death. Representative pictures of the cell death responses are shown in Figure 3-33 C. Areas of cell death are marked with an arrow.

Pathogen infection experiments with *Pseudomonas syringae* DC3000 and with *Hyaloperonospora arabidopsidis* isolate Emco5 showed that *exo70B2* mutants are more susceptible and are compromised in their defense response. Together, data shown supports a function of *Exo70B2* in the negative regulation of PAMP-triggered responses mediated by PUB22 and potentially PUB23 and PUB24.

3.7. Functional redundancy analysis of the *Exo70B2* homolog *Exo70B1*

As supported by the presented data, *Exo70B2* is required for the full activation of PAMP-triggered responses. Nevertheless, observed phenotypes for *exo70B2-1* and *exo70B2-3* were discrete. For example in ROS-burst analysis the phenotypes were not evident as in the case of other mutants affected in PTI signaling, such as the *psl* mutants (Saijo et al., 2009). A possible explanation is the functional redundancy of *Exo70B2* homologs. We hypothesized that close homologs of *Exo70B2* could have overlapping functions in regulating PTI responses. To address this question we generated two independent T-DNA insertion mutants of *exo70B1* and also generated an *exo70B1/exo70B2* double mutant and analyzed PAMP responses using flg22-triggered ROS production and flg22-induced root growth inhibition. Additionally, we also assayed the disease resistance of *exo70B1* mutants by infection with *Pst* DC3000.

3.7.1. Generation of two independent *exo70B1* T-DNA insertion lines and an *exo70B1/exo70B2* double mutant

Exo70B1 (AT5G58430) is the closest homolog of *Exo70B2*, sharing 53% amino acid sequence identity. We isolated two independent T-DNA insertion mutants and named them *exo70B1-1* (GK-114C03.04) and *exo70B1-2* (GK-156G02.07). Homozygous plants were generated by propagation of heterozygous parents and identified by gene specific PCR genotyping. T-DNA insertion sites are shown and the primer binding sites are indicated with arrows in Figure 3-34 A. Both lines are knockouts as no transcript could be detected by gene specific PCR using cDNA (Figure 3-34 B).

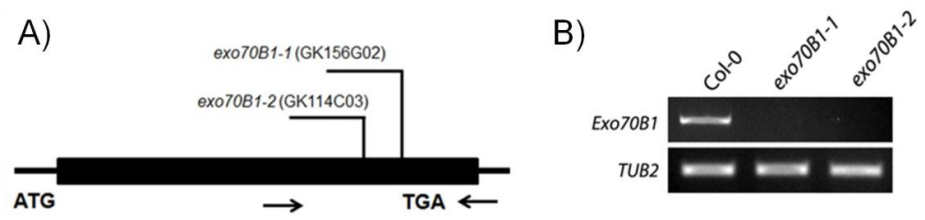


Figure 3-34 Characterization of *exo70B1* T-DNA insertion lines: (A) Gene structure of *Exo70B1*. Black box represents the exon. Positions of T-DNA insertions are marked. (B) Transcript accumulation of *Exo70B1* mRNA in *exo70B1-1* and *exo70B1-2*. Positions of primers are marked by arrows in (A).

The *exo70B1-1* mutants were crossed with *exo70B2-1* mutants to generate double mutants. Homozygous double mutants were isolated by gene specific PCR after propagation of heterozygous plants. Importantly, *exo70B1-1* and *exo70B1-2* showed developmental phenotypes with a stunted growth, spontaneous leaf lesions and involute leaves when grown under short day conditions, as can be seen for *exo70B1-1* in Figure 3-35. This phenotype was partially suppressed in *exo70B1/exo70B2* double mutants.

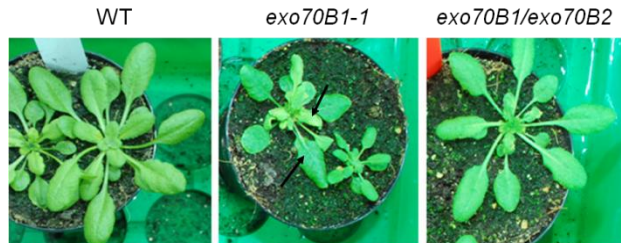


Figure 3-35 Developmental phenotypes of *exo70B1* and *exo70B1/exo70B2* mutants: Shown are representative pictures of five week-old plants grown under short day conditions. Arrowheads indicate lesions and involute leaves of *exo70B1-1*.

3.7.2. Analysis of PAMP-triggered responses of *exo70B1* mutants

3.7.2.1. Analysis of the ROS-burst triggered by *flg22*

We analyzed the ROS production triggered by *flg22* in leaf discs of *exo70B1-1*, *exo70B1-2* and *exo70B1/exo70B2* mutants after treatment with 500nM *flg22*. We included *exo70B2-1* and *exo70B2-3* in the same experiment to compare the ROS production to that of *exo70B1/exo70B2* to analyze a potential additive effect.

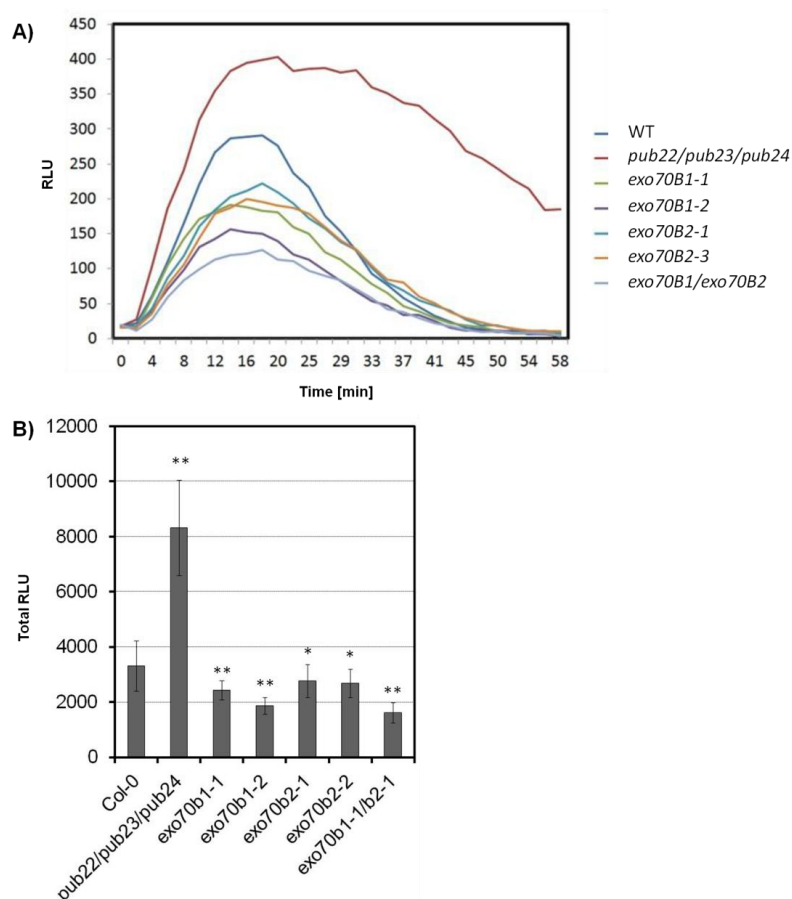


Figure 3-36 ROS-burst kinetic and total ROS production after treatment with *flg22*: (A) ROS production was measured in leaf discs of six to seven week-old plants of the indicated mutants in a luminol-based assay after treatment with 500nM *flg22*. Each time point represents the average of eight independent samples. RLU = relative light units. (B) Total ROS production is calculated by the integration of the area under the curves in (A). Error bars represent +/- S.D. of eight independent samples. Statistical significance is indicated by asterisks (Student's *t* test, **p* < 0,05, ***p* < 0,01). Similar results were obtained in three independent experiments.

The ROS-burst pattern was similar in all tested lines and the maximum was reached after 16 minutes. The *exo70B1-1*, *exo70B1-2*, *exo70B2-1*, *exo70B2-3* and *exo70B1/exo70B2* mutants displayed lower peak values in comparison to the wild type, while *pub22/23/24* mutants reached a higher maximum. The total ROS production was significantly compromised in all assayed *exo70B1*, *exo70B2* and *exo70B1/exo70B2* mutants compared to the wild type (*exo70B1-1*: 2429 RLU +/- 342 S.D., $p < 0,01$; *exo70B1-2*: 1863 +/- 298 S.D., $p < 0,01$; *exo70B2-1*: 2762 +/- 595 S.D., $p < 0,05$; *exo70B2-3*: 2674 +/- 512 S.D., $p < 0,05$; *exo70B1/exo70B2*: 1612 +/- 373 S.D., $p < 0,01$). *pub22/23/24* showed a significantly elevated ROS production (8318 +/- 1726 S.D., $p < 0,01$). The ROS production of *exo70B1/exo70B2* was not significantly different to the respective single mutants. In summary, *exo70B1* mutants showed a similar phenotype in terms of ROS production upon flg22 treatment, indicating that *Exo70B1* is an additional component required to mount a full ROS-burst upon PAMP perception.

3.7.2.2. Root growth inhibition assays with *exo70B1* and *exo70B1/exo70B2* mutants

Both alleles of *exo70B1* and the double mutant *exo70B1-1/exo70B2-1* were assayed for root growth inhibition on flg22-containing medium (Figure 3-37). Plants did not exhibit any detectable developmental phenotypes. The *exo70B1-1* (19,2% +/- 4,8 S.E.M.; $p < 0,01$) and *exo70B1-2* mutants (23,7% +/- 0,4 S.E.M.; $p < 0,01$) showed a reduced root growth inhibition in comparison to the wild type (32,7% +/- 4,8 S.E.M.), showing the opposite phenotype of *pub22/23/24*, which showed significantly enhanced root growth inhibition (49,3% +/- 5,1 S.E.M.; $p < 0,01$). The root growth inhibition of *exo70B1* alleles was comparable to that of *exo70B2* mutants (Figure 3-30). However, no additive effect of root growth inhibition could be observed in *exo70B1-1/exo70B2-1* double mutants. This data indicates that *Exo70B1* is involved in late PTI signaling and that it does not functionally overlap with *Exo70B2*.

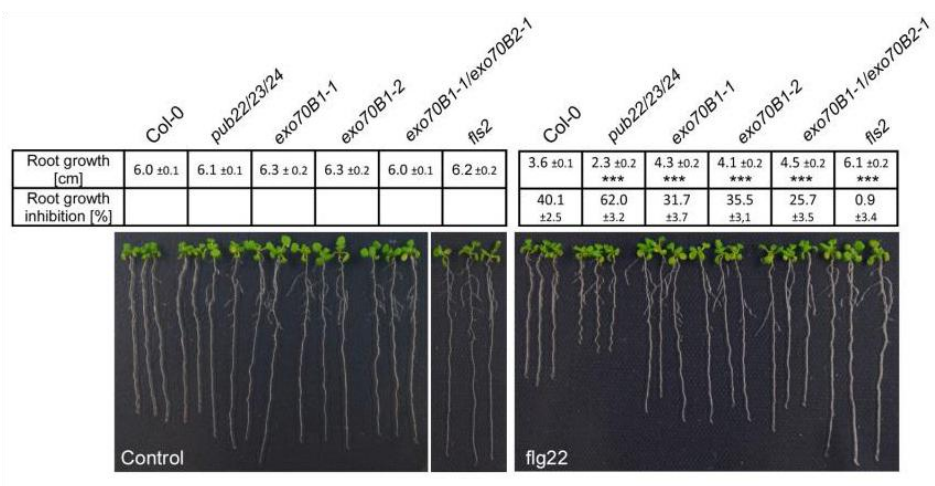


Figure 3-37 Flg22-induced root growth inhibition: Root growth inhibition was assayed on media containing 1 μ M flg22. Seedlings were grown for seven days before they were transferred to flg22 containing medium. Length of the main root was measured seven days after transplanting. Data is shown as the mean of three independent experiments \pm S.E.M. ($n \geq 60$). Statistical significance compared to Col-0 plants is indicated by asterisks (Student's t test, ** $p < 0.01$). Experiment was repeated three times with similar results.

3.7.3. Disease resistance analysis of *exo70B1* mutants

We also analyzed the disease resistance phenotype of *exo70B1* mutant alleles. Both alleles were spray inoculated with a solution of 5×10^5 cfu/mL *Pst DC3000* and four days after infection the bacterial growth was assessed. Both alleles showed an enhanced growth in comparison to the wild type. The bacterial counts were $6,2 \log_{10}$ cfu/cm² \pm 0,1 S.E.M. for *exo70B1-1* and $6,3 \log_{10}$ cfu/cm² \pm 0,1 S.E.M. for *exo70B1-2* in comparison to $5,7 \log_{10}$ cfu/cm² \pm 0,2 S.E.M in wild type Col-0 plants. Both *exo70B1* alleles were significantly more susceptible ($p < 0,05$). In summary, *exo70B1* mutants showed a similar resistance phenotype to *Pst DC3000* as *exo70B2* mutants, indicating that Exo70B1 is a positive regulator of plant immunity. However, results have to be interpreted with caution, because *exo70B1* mutants showed developmental phenotypes and spontaneous cell death lesions when grown under short day conditions (section 3.7.1). Cell death possibly influenced the plant immunity phenotype.

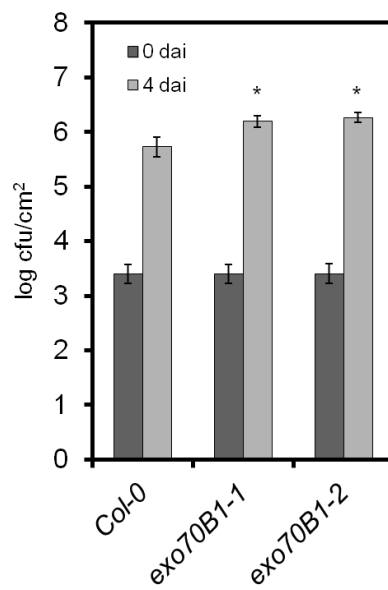


Figure 3-38 Pathogen growth assay of *exo70B1* mutant lines with *Pst* DC3000: The indicated mutants were spray-inoculated with a bacterial suspension of 5×10^8 cfu/ml. Bacterial growth was assessed at zero and four days after inoculation (dai). Data shown as mean \pm S.D. (n=5). Statistical significance is indicated by asterisks (Students T-test, *p < 0,05). Experiment was repeated three times with similar results.

4. Discussion

The three closely related Plant U-box type E3-ubiquitin ligases PUB22, PUB23 and PUB24 potentially participate in the downregulation of PAMP-triggered immune signaling. The *pub22/23/24* triple mutant plants display enhanced responses to PAMPs and are more resistant to different pathogens. The triplet are active E3-ubiquitin ligases, as shown by their *in vitro* autoubiquitination activity (Trujillo et al., 2008). However, the cellular targets involved in the PUB22, PUB23 and PUB24-mediated regulation of plant immunity and the underlying mechanisms were unknown. This work aimed at shedding light on the function of the PUB triplet in the regulation of PAMP-triggered immunity by identifying and analyzing immunity-related target proteins of PUB22. In order to achieve this, a yeast two-hybrid screen was performed with PUB22. *PUB22*, together with *PUB24* play more important functions in PTI because the respective double and single mutants displayed the strongest PTI phenotype as judged by the tested PAMP response and resistance assays (Trujillo et al., 2008).

The yeast two-hybrid screen revealed nine candidate interacting proteins of PUB22, namely Exo70B2 (AT1G70000), SFH5 (AT1G75370), HsPro2 (AT2G40000), MHCR (AT1G77580), Bam2-like (AT4G28650), UBL (AT5G42220) and two proteins with unknown function (AT1G62780, AT5G08720, section 3.1.1). The three candidates Exo70B2, SFH5 and MHCR are potentially involved in vesicular trafficking processes, suggesting that PUB22 might regulate distinct vesicular trafficking pathways required for PAMP-triggered immune responses.

4.1. PUB22 targets the vesicular trafficking component Exo70B2 to downregulate PTI signaling

Vesicular trafficking is essential to deploy immunity by the secretion of small toxic compounds to the apoplast or by reinforcing the cell wall to impede penetration by filamentous pathogens (Bednarek et al., 2010). An example is the SNARE protein PEN1 which is involved in the resistance of *Arabidopsis thaliana* to penetrating pathogens such as powdery mildew fungi. PEN1 forms a ternary complex with SNAP33, VAMP721 and VAMP722 to mediate vesicle

fusion thought to be required for the secretion of defense related compounds (Collins et al., 2003; Kwon et al., 2008). However, recent studies have shown the importance of vesicle trafficking for PTI signaling and its attenuation. FLS2 is localized at the plasma membrane and endocytosed upon activation by binding of flg22 (Robatzek et al., 2006). A functional FLS2-GFP is internalized from the plasma membrane 30 minutes upon flg22 treatment and re-localizes to vesicles. FLS2 is consequently transported via early ARA7-containing to late ARA6-containing endosomes to the vacuole (Beck et al., 2012). The consequent degradation of FLS2 has been proposed to play a role in signal downregulation (Beck et al., 2012). This raises the possibility that proteins such as E3-ubiquitin ligases are involved in the regulation of these processes. Ubiquitination has been shown to modulate the internalization and vesicular trafficking of plasma membrane proteins including receptors (Reyes et al., 2011).

Recent studies suggest a key function of ubiquitination in regulating PRR trafficking. An example is the *Lotus japonicus* E3-ubiquitin ligase Seven in absentia 4 (SINA4), which was shown to interact with the Symbiosis Regulated Kinase (SYMRK), a PRR required for symbiotic signal transduction in root cells required for the intracellular uptake of bacteria (Den Herder et al., 2012). SYMRK is localized to the plasma membrane and expression of SINA4 induced the re-localization of SYMRK to vesicles. Furthermore SINA4 expression led to a decrease in SYMRK protein levels, suggesting that SINA4 promotes the endocytosis and degradation of the receptor.

The two PUB22 homologs PUB12 and PUB13 were shown to mediate FLS2 degradation upon flg22 activation (Lu et al., 2011). Both ligases are associated with BAK1 and recruited to the BAK1-FLS2 complex upon flg22 perception. They specifically ubiquitinate the FLS2 kinase domain *in vitro* and FLS2 degradation upon flg22 treatment is impaired in *pub12/pub13* mutants. The importance for immunity was demonstrated by experiments showing that PTI responses and disease resistance of *pub12/pub13* mutants are enhanced (Lu et al., 2011). Given the fact that FLS2 is an integral plasma membrane protein, the degradation must be executed via endocytosis and transport of the receptor to the vacuole for degradation, suggesting that PUB12 and PUB13 regulate FLS2 trafficking by ubiquitination.

AvrPtoB is an important effector and contributes to the virulence of the pathogen (Abramovitch et al., 2006). AvrPtoB was shown to possess E3-ubiquitin ligase activity and it targets FLS2 for degradation (Göhre et al., 2008), potentially by exploiting the endogenous FLS2 degradation pathway through induction of its endocytosis leading to vacuolar degradation. Another study

showed that AvrPtoB can also ubiquitinate and mediate the degradation of the unrelated LysM motif RLK CERK1 (Gimenez-ibanez et al., 2008.), showing that AvrPtoB-mediated degradation extends to different classes of PRRs.

Several examples have documented a function of ubiquitination in the vesicular trafficking of plasma membrane proteins. One example is the iron regulated transporter 1 (IRT1) from *Arabidopsis*, which is required to control iron uptake in the roots. IRT1 is monoubiquitinated at two cytosolic residues, promoting its endocytosis and subsequent vacuolar degradation (Barberon et al., 2011). Another important nutrient transporter is the borate transporter 1 (BOR1). It was shown that a mutation of the lysine at position 590 to alanine affected the translocation of the receptor to the TGN/EE and the transport to the vacuole. Lysin 590 was shown to be mono- or diubiquitinated *in vivo*, suggesting that ubiquitination is required for the endosomal uptake of the protein (Kasai et al., 2011).

More evidence for the importance of an E3-ubiquitin ligase in the regulation of vesicular trafficking was given by studies on the RING ligase keep on going 1 (KEG1), which was first described as a negative regulator of abscisic acid (ABA) signaling by targeting the ABA response transcription factor ABI5 for proteasomal degradation (Liu and Stone, 2010). A recent study provided more insight into its cellular function and showed an involvement of KEG1 in vesicular trafficking and plant immunity. It was demonstrated that KEG1-YFP localizes to TGN/EE compartment and that E3 ligase activity is required for its proper localization (Gu and Innes, 2012a). KEG1 was shown to be required for vacuolar biogenesis and for targeting the brassinosteroid insensitive 1 (BRI1) RLK to the vacuole. The *keg* mutants were hypersensitive to brassinolide treatment in root growth inhibition and hypocotyl elongation experiments, suggesting that KEG1 is involved in the downregulation of BRI1 signaling by targeting the receptor to the vacuole for degradation. Interestingly, the authors showed that KEG1 is also involved in plant immunity by promoting the secretion of the two defense related proteins C14 and PR1, suggesting that KEG1 is required for sorting of vesicles from TGN/EE to the vacuole or to the plasma membrane. Furthermore, KEG1 accumulates at fungal penetration sites and is degraded upon infection of *Arabidopsis* plants with the virulent powdery mildew *Golovinomyces cichoracearum* (Gu and Innes, 2012).

In this study we identified the exocyst complex subunit Exo70B2 as an interactor of PUB22 with potential function on vesicular trafficking. We could confirm the specific interaction of both proteins and demonstrate that PUB22 ubiquitinates Exo70B2 *in vitro* and mediates its

degradation in response to flg22 treatment *in vivo*. Exo70B2 is one of 23 homologs of yeast Exo70p in *Arabidopsis thaliana* (Cvrčková et al., 2012; Elias, 2003), a subunit of the octameric exocyst complex involved in tethering of post-Golgi vesicles to target membranes (TerBush et al., 1996; Elias, 2003). Yeast Exo70p acts upstream of SNARE-mediated vesicle fusion and has been shown to be associated in some instances with the acceptor membrane (Boyd et al., 2004). It has been therefore proposed to act as a spatial landmark to guide vesicle tethering.

The exocyst in plants was so far mainly linked to polar secretion in cell plate maturation, cytokinesis and the acceptance of compatible pollen (Fendrych et al., 2010; Samuel et al., 2009). The latter is of particular interest in the context of the targeting of Exo70B2 by PUB22. Samuel and colleagues (2009) identified the Exo70B2 homolog Exo70A1 as a target of the U-box type E3-ubiquitin ligase ARC1, a positive regulator of self-pollen rejection. Exo70A1 was shown to be involved in the acceptance of non-self pollen in *Brassica napus* (Samuel et al., 2009). RNAi knockdown lines of *Exo70A1* showed impairment of compatible pollen acceptance and overexpression of *Exo70A1* partially relieved self-incompatibility. *Arabidopsis exo70A1* mutants partially rejected self-pollen in a way similar to the self-incompatibility reaction, suggesting a pathway conservation. ARC1 was proposed to mediate the degradation of Exo70A1 and thus to inhibit the exocytosis of compatibility factors. The self-incompatibility reaction is initially triggered by the *S*-locus receptor kinase (SRK), which phosphorylates ARC1 upon activation (Gu et al., 1998). The reaction mechanistically resembles PTI in various aspects. One important similarity is the ligand-induced endocytosis of the activated receptor. SRK was shown to be internalized upon binding of its cognate ligand, the *S*-locus Cys-rich/*S*-locus protein 11 (SCR/SP11) and subsequently degraded. Ligand-induced degradation is suggested to be involved in signal downregulation (Ivanov and Gaude, 2009), in a similar way as proposed for FLS2 upon flg22 binding (Robatzek et al., 2006). It is therefore conceivable that PUB22 in *Arabidopsis* and ARC1 in *Brassica* play similar functions in regulating vesicular trafficking by targeting components of the exocyst complex, although on different pathways.

Exo70B2, the target of PUB22, and its homolog Exo70H1, were recently demonstrated to be involved in the resistance of *Arabidopsis thaliana* to *Psm* and *Bgh* (Pecenková et al., 2011). Exo70B2 and Exo70H1 were shown to interact with Sec5a, Sec15b and SNAP33 in yeast two-hybrid experiments, suggesting that they are functional components of the exocyst complex. Interestingly, Exo70B2 interacted with Exo70H1, pointing to the possibility that Exo70s dimerize in plants (Pecenková et al., 2011). The dimerization of Exo70 subunits has never been reported before and might be unique to plants. The *exo70B2* and *exo70H1* knockout mutants showed

enhanced *Psm* growth in comparison to wild type plants. Additionally, papillae morphology after *Bgh* infection at the attempted penetration sites was altered in *exo70B2* mutants. The authors observed a dense halo of vesicle-like structures filled with auto-fluorescing material surrounding the papillae in *exo70B2* mutants. They speculated that secretion of defense related compounds and secretion of material to fortify the cell wall and generate papillae is compromised in *exo70B2* and *exo70H1* mutants. This is in accordance with the described function of the exocyst complex in regulating polarized secretion (He and Guo, 2009; Mao et al., 2010). However, given the great expansion of the Exo70 gene family in land plants with 23 homologs in *Arabidopsis* (Cvrčková et al., 2012), new functions distinct from secretion are possible and likely for Exo70B2. In agreement with this hypothesis our yeast complementation experiments showed that Exo70B2 cannot complement the heat sensitivity phenotype of a yeast *exo70* mutant (section 3.1.3), suggesting that Exo70B2 has adopted new functions in *Arabidopsis*. By contrast, another Exo70 homolog was able to complement the yeast *exo70p* mutant (personal communication by Viktor Zarsky).

Exo70B2 is highly transcriptionally upregulated in seedlings upon PAMP treatment (3.2.4; Navarro et al., 2004; Zipfel et al., 2006) and we could show that *exo70B2* mutants are impaired in PTI signaling (section 3.6). The mutants were compromised in early and late signaling events and in accordance with data from Pecenkova and colleagues (2011) the reduced responsiveness of *exo70B2* mutants to PAMPs resulted in an immunocompromised phenotype. Mutants were more susceptible to *Pst* and *Hpa* infections (section 3.6.3). However, our data support a scenario in which signaling responses in *exo70B2* mutants to pathogen invasions are compromised downstream from PRR activation, but upstream from the deployment of defense responses. Therefore, the resistance and papillae formation phenotypes of *exo70B2* reported by Pecenkova and colleagues are most likely a consequence of impaired PTI signaling. This is of particular interest as the function of the exocyst complex, nor of any component of the vesicular trafficking machinery, had been linked to PTI signaling in plants prior to this study.

Different studies from non-plant systems have shown the involvement of the exocyst complex in diverse signaling processes, including innate immune signaling, suggesting that similar functions might be conserved across kingdoms. An example documents a function of the exocyst in signaling during Toll-like receptor activation (Chien et al., 2006). The exocyst subunit Sec5 is an effector of RalB, which is required to suppress apoptotic checkpoint activation. This is involved in a regulatory framework supporting tumorigenic transformation in human cancer cells. The RalB/Sec5 complex was shown to directly recruit Tank binding kinase 1 (TBK1),

which is an atypical I κ B kinase family member. Next to their function in cell survival RaI β /Sec5 is also required for the activation of TBK1 in innate immunity, triggered by Toll-like receptor 3 (TLR3) activation, thus showing an involvement in immune signaling (Chien et al., 2006). Depletion of Sec5 blocked gene expression dependent on the interferon regulatory factor 3 (IRF-3) transcription factor pathway and the downstream induction of type I interferon expression in response to viral infection.

The stimulator of interferon genes (STING) is also an essential component required for effective innate immune signaling in human cells (Ishikawa and Barber, 2008). STING associates with TBK1 and is able to activate both IRF3 and NF- κ B transcription pathways and induces primary innate immune response genes (Ishikawa and Barber, 2008). STING interacts with Sec5 and was shown to translocate from the ER to non-ER microsome compartments, which were identified as early endosomes or recycling endosomes. STING was therefore proposed to complex with TBK1 and Sec5 upon perception of exogenous CpG oligodeoxynucleotides in order to facilitate the production of type I interferons (Ishikawa et al., 2009).

We showed that Exo70B2 is involved in PTI signaling and contributes to plant immunity. Our experiments showed that *exo70B2* mutants are compromised in signaling events downstream of different PRRs. ROS production is compromised upon treatment with flg22, elf18 and chitin and extended to treatments with the DAMP Pep1 (section 3.6.2.1). Flg22 and elf18 are perceived by FLS2 and EFR which heterodimerize with the regulatory protein BAK1 upon ligand binding (Chinchilla et al., 2007). Pep1 is perceived by the receptors Pep1 receptor 1 (PEPR1) and PEPR2 (Krol et al., 2010), which both interact with BAK1 in yeast two-hybrid experiments (Postel et al., 2010). In all three cases BAK1 is required to activate downstream signaling as *bak1* mutants fail to mount a full response upon elicitation with flg22, elf18 or Pep1. By contrast, chitin perception is independent of BAK1, as *bak1* mutants still respond to chitin in a manner comparable to wild type (Gimenez-Ibanez et al., 2009). The reduced responsiveness of *exo70B2* mutants to all tested elicitors, including chitin, suggests that Exo70B2 and PUB22 regulate a cellular response required for signaling in a BAK1-independent manner. Exo70B2 is potentially involved in regulating exocytotic processes which implies that it might regulate trafficking events shared by a multitude of PRR pathways. This is supported by our BiFC data, which showed the localization of the interaction between PUB22 and Exo70B2 in distinct punctate structures, which are reminiscent of vesicles (section 3.3.2). Punctate structures were distributed throughout the cell in protoplasts and in some case displaying a perinuclear localization in epidermal leaf cells. Similar localization was observed for the interaction of

PUB23 and PUB24 with Exo70B2 as well, suggesting that all three ligases act on the same cellular pathway (section 3.3.4)

The localization pattern observed for the reconstituted YFP fluorescence was similar to that observed for other Exo70 homologs in *Arabidopsis*. Wang and colleagues (2010) analyzed the subcellular localization of 8 different *Arabidopsis* Exo70 homologs. Exo70A1, Exo70B1 and Exo70E1 localized to punctate structures. They focused their work on Exo70E2 and showed that it does not colocalize with markers for typical punctate compartments such as the Golgi apparatus, the TGN, MVBs or autophagosomes. By immuno-labeling and electron microscopy they localized Exo70E2 to distinct two membrane compartments which they termed exocyst positive organelles (EXPO) (Wang et al., 2010). They provided some evidence that EXPO secretes the soluble protein SAMS2, which does not have a signal sequence for secretion. The authors proposed that EXPOs are involved in a novel secretory pathway.

In an additional study, Chong and coworkers (2010) analyzed the localization patterns of different *Arabidopsis* exocyst subunits, including Exo70B2, Exo70E2, Exo70G1 and Sec15b. Similar to the report of Wang and colleagues (2010), Exo70B2 was shown to localize predominantly in the cytoplasm when expressed in BY2 tobacco cells. By contrast, GFP-Exo70E2, GFP-Exo70G1 and GFP-Sec15b partially colocalized with endomembrane trafficking markers (Chong et al., 2010). The mentioned exocyst subunits localized to punctate structures and the signal overlapped with Syp21, a marker for LE/prevacuolar compartment (PVC), Syp42, a TGN/EE marker and Syp52, a protein localized to TGN/EE/PVC (Chong et al., 2010).

In contrast to the above mentioned studies, Pecenkova and colleagues (2011) showed an exclusive localization of Exo70B2 in the cytoplasm after transient transformation of *Nicotiana benthamiana*. This observation is in contradiction to our observed localization of the PUB22-Exo70B2 interaction which exclusively took place in punctae. The heterologous system used by Pecenkova and colleagues might explain the differences in localization. Alternatively, Exo70B2 could localize to both cytoplasm and punctae, however, the interaction with PUB22 strictly takes place in the punctae. In accordance with this, experiments performed using protoplasts and epidermal leaf cells in our lab showed a dual localization for GFP-Exo70B2 in both the cytoplasm and punctae (personal communication by Giulia Furlan).

A further possibility is that PUB22 induces the relocation of Exo70B2 and sequesters it from cytoplasmic pools to the punctate compartments. This is supported by studies analyzing the subcellular localization of the *Brassica* Exo70A1 in BY2 cells (Samuel et al., 2009). Samuel and

colleagues showed that Exo70A1 localized to the cytoplasm. When ARC1 and a constitutive active cytoplasmic kinase domain of SRK, two additional components of the self-incompatibility reaction, are coexpressed, Exo70A1 displayed punctate localization. This is reminiscent of the localization pattern observed for the PUB22-Exo70B2 interaction in BiFC. The interaction of Exo70A1 with ARC1 shows that an interacting E3-ubiquitin ligase can influence the subcellular localization. This suggests a similar scenario for PUB22 and Exo70B2.

Chong and colleagues (2010) speculated that their observed localization of the different exocyst subunits is reminiscent of the localization pattern of BFA bodies in BY2 cells (Robinson et al., 2008), which might be explained by homotypic fusion of exocyst positive vesicles caused by overexpression of the proteins. This suggests that the exocyst complex could be involved in transport processes from the PM to the EE/TGN or vice versa, in addition to the proposed function in a novel and highly controversial secretory pathway, as proposed by Wang and colleagues (2010).

The punctate structures observed in our BiFC experiments for the PUB22-Exo70B2 interaction are also reminiscent of these endomembrane compartments, suggesting that the proteins are involved in regulating transport processes involving TGN/EE compartments, such as the recycling of plasma membrane proteins.

Similar localizations of the exocyst complex, or components thereof, were observed in non-plant systems. Sec6/Sec8 exocyst subunits were located to either the plasma membrane in cell-cell contact zones or to the TGN/EE (Yeaman et al., 2001). Based on their data the authors speculated that the TGN membranes labeled by the exocyst complex represent sorting domains for specific classes of secretory vesicles (Yeaman et al., 2001). In *Drosophila* the exocyst was shown to be involved in the localization of *Drosophila* E-cadherin (DE-cadherin), a plasma membrane localized protein required for epithelial cell-cell adhesion, polarization and morphogenesis (Langevin et al., 2005). In exocyst complex mutants, *sec5*, *sec6* and *sec15*, DE-cadherin was shown to localize in punctae in epithelial cells. These were identified as enlarged recycling endosome compartments (Langevin et al., 2005). Interestingly, in plants it is proposed that recycling endosomes (RE) and TGN/EE are identical compartments (Reyes et al., 2011).

Interestingly, in addition to the function of the exocyst complex in recycling plasma membrane proteins, a recent study showed the requirement of ubiquitination in this particular process (Yamazaki et al., 2013). The *Drosophila melanogaster* RING E3 ligase Godzilla was shown to localize to endosomal compartments. Overexpression of Godzilla led to the formation of

enlarged Rab5 endosomes in dependency with a functional RING domain. The authors identified the SNARE protein VAMP3 as a substrate of Godzilla for ubiquitination, which was also localized to endosomal compartments. They could demonstrate that Godzilla is involved in the recycling of the Transferrin receptor, which is a protein involved in iron uptake. Overexpression of Godzilla led to the accumulation of Transferrin in the enlarged REs, while overexpression of a ligase dead version had no effect, suggesting that ubiquitination is important to regulate the sorting of vesicles at the RE to assure recycling of receptors to the plasma membrane (Yamazaki et al., 2013).

Plant receptors are subject to continuous recycling. A well characterized example is BRI1. BRI1-GFP localizes to both the plasma membrane and to intracellular vesicles in root meristem cells (Geldner et al., 2007). It colocalizes with FM4-64, a hydrophobic dye that stains membranes and allows the visualization of endocytosis, and with VHA1-a1-RFP, an EE/TGN marker. Furthermore, the localization of BRI1-GFP is sensitive to BFA, indicating continuous recycling. BRI1 endosomal localization is independent of its ligand. Brassinosteroid (BR) treatment or its depletion does not cause any changes in BRI1-GFP localization (Geldner et al., 2007). Importantly, receptor endocytosis and recycling was shown to extent to the PRR FLS2, which enters distinct transport routes depending on its activation status. In contrast to flg22-induced endocytosis, which is unaffected by BFA treatment, inactive FLS2 was shown to constantly recycle in a BFA sensitive manner (Beck et al., 2012). Similarly, the rice PRR Xa21 was also shown to be localized to the plasma membrane and BFA treatment led to the accumulation in BFA bodies (Chen et al., 2010), suggesting that multiple PRRs exist in plasma membrane and endocytic pools and are subject to continuous recycling. This may provide a mechanism for the degradation of aged receptors or for a quick release of functional receptors to the plasma membrane when a pathogen attack occurs (Beck et al., 2012). Taken this into account, Exo70B2 could contribute to the recycling of PRRs by participating in the transport of endocytosed receptors to the TGN/EE. In this scenario, Exo70B2 would be a trafficking factor promoting the amount of functional receptors at the plasma membrane which is required for the full activation of downstream signaling to initiate immunity. As other important proteins required for PTI signaling are localized to the plasma membrane, Exo70B2 could contribute to their recycling as well. These include NADPH oxidases such as RbohD or ion channels. Consequently, PUB22-mediated degradation of Exo70B2 upon elicitor perception might shut down recycling and funnel positive PTI signaling components to other trafficking pathways, such

as the degradation via the vacuole, a proposed mechanism of signal attenuation (Beck et al., 2012).

Alternatively, Exo70B2 could participate in the transport of newly synthesized receptors or other immunity related proteins from the ER to the plasma membrane as part of the secretory pathway. This would also involve the TGN/EE/RE compartments (Reyes et al., 2011) and therefore PUB22-mediated Exo70B2 turnover would block the delivery of plasma membrane localized signaling components, resulting in signal attenuation and reduced PTI responses.

This hypothesis is supported by studies from non-plant systems, showing that the exocyst complex can be involved in recycling and delivery of plasma membrane proteins, including receptors required for signaling. In mammals the exocyst complex was shown to be involved in the delivery of the Glucose transporter type 4 (Glut4) to the cell surface upon insulin perception (Inoue et al., 2003). Responses to insulin include the activation of the G-protein TC10. TC10 interacted with Exo70 which resulted in its relocalization from the cytoplasm to the plasma membrane where it assembled with Sec6 and Sec8. Exo70 was not required for the transport of Glut4 containing vesicles to the plasma membrane but it had a crucial function in membrane targeting and translocation of the transporter (Inoue et al., 2003). Furthermore, the exocyst complex was shown to be required for the delivery of N-methyl-D-aspartate (NMDA) receptors (NMDARs) to the plasma membrane of neurons (Sans et al., 2003). NMDARs belong to the class of ionotropic glutamate receptors which mediate most excitatory neurotransmission events in the central nervous system. Sec8 interacted with the synapse-associated protein 102 (SAP102) and the interaction was involved in the delivery of NMDARs to the cell surface in heterologous cells and rat neurons. NMDARs are considered to be fairly stable components of the synapse, in contrast to another class of glutamate receptors, such as the α -amino-3-hydroxyl-5-methyl-4-isoxazole-propionate (AMPA) type of receptors (AMPARs) (Gerges et al., 2006). AMPARs are highly dynamic and can be recycled from synapses in an activity-dependent manner, leading to long-term potentiation. In addition, they are continuously recycled in an activity-independent manner. Sec8 was shown to be required for the targeting of AMPARs to the synaptic membrane, while Exo70 was required for the fusion of AMPAR vesicles with the plasma membrane (Gerges et al., 2006). An important molecular mechanism that governs AMPAR trafficking is the interaction with Psd-95/Sap90/Dlg/Oz-1 (POZ) domain containing proteins. Two examples are GRIP1 and GRIP2. They were shown to interact with the exocyst complex and regulate the activity-dependent recycling of AMPARs (Mao et al., 2010). These studies further linked receptor trafficking, recycling and signaling to the exocyst complex. Similar

functions might be conserved in plants, supporting the notion that vesicular trafficking and signaling are intertwining molecular networks.

As our results were obtained with protein overexpression we cannot rule out the possibility of artifacts. However, our BiFC data showed that the proteins are active in their localization, as PUB22-mediated degradation of Exo70B2 was clearly observed (section 3.5.2), supporting that the fluorescence pattern, at least to some extent, resembles their native localization. To define the intracellular localization and function of Exo70B2, further experimental clarification is needed.

To provide more evidence for a potential involvement of Exo70B2 and PUB22 in the regulation of PRR recycling, receptor levels in different genetic backgrounds need to be tested before and after PAMP elicitation. In wild type plants FLS2 is degraded upon flg22 perception via endocytosis and transport of the receptor to the vacuole (Robatzek et al., 2006). Should PUB22 participate in the downregulation of the recycling of non-activated FLS2 by targeting Exo70B2 for degradation, levels of the receptor should be enhanced in *pub22/23/24* mutants compared to wild type after treatment with flg22. By contrast, in *exo70B2* mutants the degradation of FLS2 would be expected to occur faster, as recycling is impaired.

In addition, cell biological approaches can provide direct evidence for the involvement of PUB22 and Exo70B2 in vesicular recycling of plasma membrane proteins. One possibility is to perform colocalization analysis using established organelle markers.

4.2. Additional potential target proteins of PUB22 suggest a specialization in the regulation of vesicular trafficking

The multitudes of proteins involved in vesicular trafficking processes have many paralogs. Exo70B2 is a particular example with 22 homologs in *Arabidopsis thaliana* (Cvrčková et al., 2012a). It is therefore conceivable that close homologs of Exo70B2 might have partial redundant functions. We therefore hypothesized that these could compensate Exo70B2 in loss of function mutants. This could account for the rather mild phenotypes observed for *exo70B2*. We included Exo70B1, the closest homolog of Exo70B2, in our analysis and could show that it contributes to PTI signaling too. The *exo70B1* mutants showed a similar phenotype in ROS

production upon flg22 treatment (section 3.7.2), flg22-dependent root growth inhibition experiments (section 3.7.2.2) and in pathogen growth assays with the virulent *Pst* (section 3.7.3). However, as *exo70B1/exo70B2* double mutants did not show an additive phenotype in the respective assays we conclude that Exo70B1 functions on an independent pathway. Of note, *exo70B1* mutants showed a developmental phenotype under short day conditions including involute leaves, spontaneous lesions and leaf chlorosis (section 3.7.1). For this reason, results obtained for *exo70B1* have to be assessed with caution. However, the developmental phenotypes in *exo70B1* mutants also support its function in distinct processes. The spontaneous cell death and early senescence phenotypes suggest a connection of Exo70B1 to vacuolar functions and autophagy.

The epistatic effect of *exo70B2* on *pub22/23/24* in the quadruple *pub22/23/24/exo70B2* mutant was only partial in ROS-burst experiments (section 3.6.2.1), root growth inhibition (section 3.6.2.4) and resistance assays (section 3.6.3.1). It is therefore anticipated that PUB22, PUB23 and/or PUB24 have additional targets required for PTI signaling and plant immunity. Indeed, data from our yeast two-hybrid screens revealed several other candidate interactors of PUB22 (3.1.1). Furthermore, independent screens with the homologs PUB20 and PUB24 identified additional candidate targets. Interestingly, candidate interactors of both ligases included components of the vesicular trafficking machinery (data not shown). Two additional candidate targets of PUB22 are also predicted to be involved in vesicular trafficking processes, suggesting that PUB22 and close homologs regulate trafficking protein complexes required for plant immunity.

One additional candidate target of PUB22 identified in the yeast two-hybrid screen was a mynosin heavy chain-related protein (MHCR) (section 3.1.1). Myosins are molecular motors and are essential for many intracellular vesicle trafficking processes at various stages, including the transport of secretory vesicles, the docking of vesicles, the priming of vesicles for the fusion process and fusion itself (Bond et al., 2011). As discussed above, insulin stimulated secretion of the glucose transporter Glut4 involves the exocyst complex in mammalian cells (Inoue et al., 2003). An additional key component is Myosin 1c, which is a member of the class I family of myosins. Myosin 1c is recruited to Glut4-positive vesicles by its binding partner, the small GTPase Ra1A. In response to insulin, it actively drives the vesicles to the plasma membrane and anchors them to the actin cytoskeleton (Bose et al., 2002; Chen et al., 2007). Myosin Va, a member of another class of mammalian myosins, has been shown to play a role in the docking of secretory carriers to the plasma membrane by directly binding to the SNARE proteins

Syntaxin 1A and VAMP2 (Prekeris and Terrian, 1997). In plants there are three classes of myosins, VIII, XI and XIII (Sparkes, 2010). In addition, there are a number of myosin-like and myosin heavy chain-related proteins annotated in the *Arabidopsis* genome (Reddy and Day, 2001). Plant myosins were majorly linked to the intracellular trafficking of organelles (Sparkes, 2010) but different studies also suggest a function in endocytosis. The class VIII myosin *Arabidopsis thaliana* myosin-like protein 2 (ATM2) was reported to be involved in endocytosis and endosomal trafficking (Sattarzadeh et al., 2008). The authors showed a colocalization of YFP-ATM2 with FM4-64 endosomes and CFP-BRI1. However, the function of MHCR and related proteins is yet unknown.

A recent study also suggested the involvement of myosin in the endocytosis of activated FLS2 receptors (Beck et al., 2012). Flg22-triggered endocytosis of FLS2-GFP was reduced by 80% after treatment with the general myosin inhibitor 2,3-butanedione monosime (Beck et al., 2012). Of note, a recent study showed that yeast Myosin 2 directly interacts with the exocyst subunit Sec15. Disruption of the interaction resulted in compromised growth and the accumulation of secretory vesicles (Jin et al., 2011). This suggests that the exocyst and myosins cooperatively participate in intracellular trafficking processes. This could be conserved in plants and PUB22 mediated degradation of MHCR could potentially contribute to the inhibition of trafficking of Exo70B2-positive vesicles and hence contribute to PTI signaling attenuation.

Another candidate target of PUB22 was SFH5, which is a putative phosphatidylinositol transfer protein (PITIP). PITPs act as lipid shuttles and mediate the transfer of phosphatidylinositols or phosphatidylcholines between membrane bilayers *in vitro* (Bankaitis et al, 1990; Mousley et al. 2007). SFH5 is one of 31 *Arabidopsis thaliana* homologs of Sec14p, which is the major PITP in yeast (Thole and Nielsen, 2008). Sec14p was shown to be essential for yeast viability and to be involved in the transport of TGN derived vesicles (Bankaitis et al, 1990). Interestingly, Sec14p deficiency resulted in a stronger impairment of the secretory pathway in comparison to the transport of cargos to the vacuole (Bankaitis et al, 1990), suggesting that Sec14p is involved in the transport of vesicles from the TGN to the plasma membrane. The molecular function of Sec14p is not yet fully understood. However, it was shown that Sec14p binds phosphatidylinositides and phosphatidylcholines at distinct sites, and the ability of Sec14p to bind to both is essential for its function (Schaaf et al., 2008). In addition, Sec14p and Sec14-like proteins are discussed to be involved in the regulation of membrane phosphoinositide homeostasis by providing a platform for enzymes and instructing them when and where to execute biochemical reactions (Bankaitis et al., 2010). Sec14 homologs from *Arabidopsis* were

shown to be involved in polarized growth processes. SFH1 was shown to be enriched in discrete plasma membrane domains of root hairs. Knockout mutants were compromised in polarized root hair expansion, showed disruption of the tip focused Ca^{2+} gradient and showed alterations in cytoskeleton organization (Vincent et al., 2005). SFH3 and SFH12 were shown in a study with promoter-GUS fusions to be expressed in pollen tubes, supporting a similar function in the regulation of pollen tube tip growth (Mo et al., 2007). The exocyst complex is also involved in cell elongation processes (Zhang et al., 2010) and its function extends to plant immunity (our data, Pecenková et al., 2011), which could be similar for SFHs. Given the function of Sec14p in yeast, SFH5 might be involved in the regulation of vesicular trafficking at the TGN/EE/RE, suggesting that it participates in the tethering process of Exo70B2-positive vesicles. Importantly, yeast Exo70p was shown to bind directly to phosphoinositides at its C-terminus (He et al., 2007), a feature that could be conserved in plants. Thus, SFH5 would be able to regulate the binding of Exo70B2 to target membranes by controlling phosphoinositide levels. This would imply that SFH5 acts upstream of Exo70B2 mediated vesicle tethering. Alternatively, SFH5 could function downstream of Exo70B2 by acting as a phosphoinositide shuttle to mediate vesicle fusion at the target membrane. In both scenarios, SFH5 would be important to confer the proper delivery of Exo70B2-positive vesicles and thus be a potential target of PUB22 on the same cellular pathway.

Preliminary data obtained during this study showed that *sfh5* mutants displayed a mild decrease in ROS-burst upon flg22 treatment (section 3.2.2) but did not show a clear immunity phenotype to *Pst* infection (section 3.2.3). The *mhcr* mutants were not yet assayed for PTI signaling and immunity phenotypes during this work. Further experimental characterization of mutants will shed light on the function of these components during PTI signaling.

In addition to their function in plant immunity, different publications showed an involvement of PUB22 in the regulation of drought stress (Cho et al., 2008; Seo et al., 2012). Cho and colleagues showed that PUB22 and PUB23 negatively regulate this response. Overexpression of the proteins resulted in enhanced sensitivity, while T-DNA knockout mutants were more tolerant to drought stress. The authors showed that PUB22 is localized in the cytoplasm and that it interacts with and ubiquitinates RPN12a, a subunit of the proteasome (Cho et al., 2008). It is feasible that PUB22's function in drought stress is related to vesicular trafficking. Recent studies suggested that RLKs are important for drought stress tolerance (Marshall et al., 2012). An analysis of the AtGenExpress drought transcript profiling data set revealed that there were substantial changes occurring in RLK gene transcription (Kilian et al., 2007). When seedlings

were exposed to drought stress, 1 hour post treatment there was a peak in upregulated RLK genes, showing that there is a rapid response to the initial drought treatment in root and shoot (Kilian et al., 2007). A specific example for a RLK potentially involved in drought stress is BRI1. A recent study showed that a single amino acid replacement in BRI1, which eliminates a tyrosine autophosphorylation site, strongly promotes shoot growth, together with increased proline biosynthesis. This is normally associated with water stress and the amino acid replacement negatively regulates BRI1 activity, suggesting that BRI1 is a negative regulator of drought stress (Oh et al., 2011). Although these results point towards a clear effect of BRs on plant drought stress tolerance, the molecular mechanisms involved in these processes remain largely unknown (Marshall et al., 2012). The regulation of BRI1 trafficking by PUB22-mediated ubiquitination is unlikely, because in such a scenario the respective mutants are predicted to have developmental defects, similar to *bri1* (Clouse, 2011). We therefore speculate that PUB22 could regulate vesicular trafficking of additional RLKs important for drought stress responses by targeting trafficking factors for degradation. These might include candidate targets from the yeast two-hybrid screen or yet unidentified regulatory proteins.

4.3. Additional defense response pathways potentially targeted by PUB22

Candidate targets of PUB22 which are not associated with vesicular trafficking were also identified in the yeast two-hybrid screen. This suggests that PUB22 possibly targets additional pathways as well. An example is HsPro2, which was previously identified as a positive regulator of plant immunity (Murray et al., 2007). HsPro2 is a homolog of the Hs1^{pro-1} protein, which confers gene for gene resistance to *Heterodora schachtii*, a nematode pathogen of sugar beet (Cai, 1997). Preliminary results suggest that HsPro2 is not required for PTI signaling, as mutants did not show a phenotype in ROS-burst experiments (section 3.2.2). But in accordance with published data, *hspro2* mutants were more susceptible to *Pst* infection (section 3.2.3; Murray et al. 2007). In addition, *HsPro2* was shown to be transcriptionally up regulated upon elf18 and flg22 treatment (section 3.2.4; Navarro et al., 2004; Zipfel et al., 2006). However, the molecular function of HsPro2 remains unknown. It was speculated by Murray and colleagues that it could modulate Suc nonfermenting-1 (SNF1)-related protein kinase 1 (SnRK1). SnRK1

interacts with HsPro2 (Gissot et al., 2006) and its function was associated with the metabolic reprogramming of cells in response to biotic stresses (Polge and Thomas, 2007).

4.4. The function of PUB22 is regulated by posttranslational protein stabilization

PUB22 is a modular protein and consists of an N-terminal U-box domain and four C-terminal ARM repeats. It was shown that it is an active E3-ubiquitin ligase and in the presence of all components required for *in vitro* reconstitution of the ubiquitination cascade, PUB22 efficiently autoubiquitinates (Trujillo et al., 2008). Autoubiquitination can result in high protein turnover. Examples are the three F-box proteins Grr1p, Cdc4p and Met30p, which are unstable components of SCF complex ligases from yeast. Autoubiquitination of the F-box proteins within the complex causes their instability (Galan and Peter, 1999). A PUB22-related example is the U-box E3-ubiquitin ligase CMPG1 from potato, which is involved in the defense response of potato against *Phytophthora infestans*. CMPG1 is a homolog of PUB22 and is required for cell death triggered by a range of pathogen elicitors, including Infestin 1 (Gonzalez-Lamothe et al., 2006). Silencing of CMPG1 led to increased resistance against *Phytophthora infestans*, which is a necrotrophic oomycete displaying a short biotrophic phase during the initial infection process. Importantly, CMPG1 also displayed high protein turnover caused by autocatalytic ubiquitination. CMPG1 was identified as a target of the *Phytophthora* effector Avr3a and the interaction of both proteins resulted in the stabilization of CMPG1, suggesting that Avr3a inhibits its autocatalytic ubiquitination (Bos et al., 2010). Interestingly, CMPG1 appeared as double bands on western blots, similar to our data showing PUB22 accumulation after expression in *Nicotiana benthamiana*. Avr3a is important for the virulence of the pathogen and there are indications that it also targets a subunit of the exocyst complex (Bos et al., 2010).

Similar to its homolog CMPG1, we could show that PUB22 has a high turnover *in vivo*, which is caused by its autoubiquitination activity. Wild type PUB22 accumulated to low levels, while 26S-proteasome inhibition or expression of a U-box inactive mutant led to a clear increase of protein levels (section 3.4). Importantly, flg22 treatment triggered a rapid accumulation of wild type PUB22, showing that flg22 perception results in the stabilization of the protein. PUB22 stabilization potentially results in the ability to efficiently interact with its target protein. Our data

indicate that the interaction of PUB22 and Exo70B2 is constitutive, suggesting that the interaction and degradation of the target is regulated by the turnover of the E3-ubiquitin ligase. In line with this, flg22 treatment induced the gradual degradation of Exo70B2 (section 3.5.2, section 3.5.3), showing that flg22-mediated accumulation of PUB22 leads to the ubiquitination and proteasomal degradation of Exo70B2. PUB22 stabilization occurred as soon as 5 minutes upon treatment, as shown by the increase of protein levels (section 3.4.2). This is in line with a function of both proteins in the regulation of early PAMP-triggered signaling. PUB22's quick accumulation after PAMP perception results in the consequent turnover of Exo70B2 which we propose, contributes to the attenuation of PTI signaling.

Clues as to the regulation of PUB22 accumulation and its ability to ubiquitinate Exo70B2 arise from different plant and non-plant examples. The mouse and human RING-type ligase Mouse double minute 2 (Mdm2) is probably one of the most studied E3-ubiquitin ligases across kingdoms. It is an important protein in the regulation of p53 levels, an essential transcription factor controlling the expression of genes associated with DNA damage repair, cell cycle control and apoptosis. The tight regulation of Mdm2 and p53 levels is important and imbalances are often associated with the development of cancer (Manfredi, 2010). Mdm2 targets p53 for ubiquitination and proteasomal degradation and also possesses intrinsic autoubiquitination activity (Fang et al., 2000). Similar to PUB22, Mdm2 is a very short lived protein, whose rapid degradation is due to ubiquitin-dependent proteolysis (Honda and Yasuda, 2000). It was hypothesized that this is caused by autocatalytic ubiquitination. However, recent studies showed that a Mdm2 RING mutant did not show steady state level changes in comparison to the wild type after expression in mice (Clegg et al. 2008), implying that Mdm2 stability is controlled by another E3-ubiquitin ligase. Mdm2 is subject to many more post translational modifications that affect its stability. Mdm2 is phosphorylated at serine 395 by the DNA damage-induced kinase ATM (Maya et al., 2001). Phosphorylation of Mdm2 resulted in its degradation, while dephosphorylation was shown to facilitate Mdm2 stabilization. Wip1 is a transcriptional target of p53 and catalyzes the dephosphorylation of Mdm2 (Lu et al., 2007). Dephosphorylation by Wip1 also increased the affinity of Mdm2 to p53, resulting in efficient ubiquitination and degradation of the target.

An example from *Arabidopsis* for post translational modification of an E3-ubiquitin ligase affecting its stability is the RING Ligase KEG1 which is involved in ABA signaling. In the absence of ABA, KEG1 ubiquitinates the drought response transcription factor ABI5 leading to its degradation and suppression of ABA signaling (Liu and Stone, 2010). ABA recognition

triggers the phosphorylation of KEG1 and it is consequently degraded by the 26S-proteasome, allowing the transcription factor ABI5 to accumulate and to induce downstream ABA responses (Liu and Stone, 2010). Importantly, the ubiquitination of KEG1 occurs by autocatalytic ubiquitination. Mutation in the RING domain abolished its ABA dependent turnover (Liu and Stone, 2010). Mdm2 and KEG1 show that posttranslational modifications can affect the stability of an E3 ligase, suggesting that PUB22's turnover is regulated in a similar manner.

The post-translational modification-mediated regulation of PUB22 is supported by the expression of PUB22 in *Nicotiana benthamiana*. PUB22 was detected as a double band. The observed extra band had a size increase of about 10kDa (section 3.4.2, Figure 3-17), which could be explained by phosphorylation, ubiquitination or ubiquitin-like related post-translational modifications of PUB22 in response to flg22. The intensity of the additional band increased upon flg22 treatment in correlation with an increase in PUB22 levels, suggesting that PUB22 stabilization is caused by an increase of a stabilizing post translational modification.

The quick stabilization of PUB22 is suggestive of phosphorylation, which occurs in plants immediately after PAMP perception to initiate downstream signaling. Flg22 perception could trigger kinase-mediated phosphorylation of PUB22, resulting in the inhibition of its autocatalytic ubiquitination activity and thus preventing its self-mediated degradation. Candidate kinases are RLKs, such as FLS2, EFR and CERK1, or associated kinases such as BAK1 or BIK1. More downstream kinases, such as MPKs, are good candidates to catalyze potential PUB22 phosphorylation as well. MPKs are activated within several minutes after PAMP perception (Asai et al., 2002). This correlates with the time-course of PUB22 stabilization, where an increase of protein abundance was detected 5 minutes upon treatment with a maximum at 20 minutes (section 3.4.2). In this context it is important to mention that one of the identified candidate interactors of PUB22 was the RLK Bam2-like, which is a homolog of CLV1, a RLK required for the maintenance of stem cells in meristematic tissue (Jun et al., 2008; Wang and Fiers, 2010). This indicates that PUB22 potentially recognizes kinase domains which are structurally highly conserved. An analysis of PUB22 stabilization in immunity-related kinase mutants, such as *bak1-5* or *mpk* mutants will shed more light on the requirement of phosphorylation for this particular process. In addition, mass spectrometry analysis of PUB22, comparing untreated and flg22-elicited samples, could identify phosphorylated residues upon treatment to support this hypothesis.

In addition to phosphorylation, the double band observed for PUB22 in *Nicotiana benthamiana* transient assays might also be explained by ubiquitination or related posttranslational modifications of PUB22, which are increased upon flg22 treatment. While poly-Lys48 labeled proteins are recognized by the 26S-proteasome, other linkage types and grades are associated with the regulation of protein-protein interactions or the relocalization of the target (Komander and Rape, 2012). Ubiquitination was not yet described in the literature to increase the stability of a protein. However, neddylation, a posttranslational modification related to ubiquitination, was reported recently in studies to promote the stability of proteins. Neddylation is a process very similar to ubiquitination and is the addition of neural precursor cell expressed, developmentally down-regulated 8 (NEDD8) to a specific target. NEDD8 is a close homolog of ubiquitin and its enzymatic attachment involves E1 activating enzymes, E2 conjugating enzymes and E3-NEDD8 ligases (Rabut and Peter, 2008). A recent study showed that the transforming growth factor β (TGF β) receptor II (T β RII), which is an important receptor involved in signaling to limit cell proliferation, is neddylated at two lysine residues in its C-terminus by the E3 ligase Casitas B-lineage lymphoma (c-Cbl), which is the gene product of a known proto-oncogene in mammals (Zuo et al., 2013). The neddylation prevents the receptor from being ubiquitinated and degraded which enhances TGF β signaling and has an antiproliferative effect in many mammalian cell lines. In a study by Xirodimas and colleagues (2004), Mdm2 was found to catalyze p53 neddylation to inhibit its transcriptional activity. In the same study, Mdm2 was also found neddylate itself. In contrast to Mdm2 ubiquitination, its neddylation was later identified to increase the stability of the ligase. Deneddylation of Mdm2 by the isopeptidase NEDD8 protease 1 (NEDP1), resulted in protein destabilization concomitant with p53 activation (Watson et al., 2009). These studies show that neddylation can increase the stability of proteins, including E3-ubiquitin ligases, and that similar modifications possibly occur to regulate PUB22 turnover. Hence, flg22 perception could also induce the neddylation of PUB22 to protect the protein from autocatalytic attachment of Lys48-linked polyubiquitin chains and thus prevent it from recognition and degradation by the 26S-proteasome.

The example of Mdm2 showed that dephosphorylation can also result in protein stabilization (Lu et al., 2007). Therefore, it might be possible that a phosphatase triggers the dephosphorylation of PUB22 to inhibit autocatalytic ubiquitination and self-mediated degradation. However, the presence of the double band for PUB22 does not support this hypothesis, as the band intensity of the additional band increased upon flg22 treatment and for stabilization triggered by dephosphorylation the opposite would be expected.

Many different posttranslational modifications can affect the half-life of a protein, as shown for the multitude of modifications affecting the stability of Mdm2. Therefore, a combination of different modification events possibly regulates the stability of PUB22 and its ubiquitination activity. The identification and characterization of these modifications to better understand flg22-induced stabilization of PUB22 will be an interesting challenge for the future.

4.5. Working model for the function of PUB22 and Exo70B2 in regulating PTI responses

We showed that PUB22 targets the Exo70B2 subunit of the exocyst complex for proteasomal degradation, which is potentially involved in the downregulation of PTI signaling. We propose a model in which Exo70B2 is involved in the recycling or delivery of plasma membrane proteins required for PTI signaling (Figure 4-1). This model is based on the localization of the PUB22-Exo70B2 interaction and the functions of the exocyst complex or subunits thereof in regulating signaling and plasma membrane trafficking of proteins in the yeast and animal field. Furthermore, it takes studies into account showing continuous recycling of multiple RLKs including PRRs required for immune signaling.

Receptors and other plasma membrane localized proteins are continuously endocytosed and recycled, involving the TGN/EE/RE compartment. Exo70B2 is proposed to be located at the TGN/EE/RE and to thus participate in recycling of plasma membrane proteins required for PTI signaling. These could include RLKs, NADPH oxidases or ion channels. In uninduced conditions, PUB22 mediates its own turnover by autocatalytic ubiquitination (Figure 4-1 A). Perception of flg22 results in the endocytosis and transport of FLS2 via TGN/EE and MVB compartments to the vacuole for degradation, which is proposed to be involved in signal attenuation (Figure 4-1 B). In addition, flg22 triggers the inhibition of PUB22's autoubiquitination activity, leading to protein accumulation and allowing PUB22 to target Exo70B2 for ubiquitination and proteasomal degradation. PUB22 helps in this way to shut down recycling and to refunnel positive signaling components into the vacuolar degradation pathway, thus contributing to the downregulation of PTI signaling.

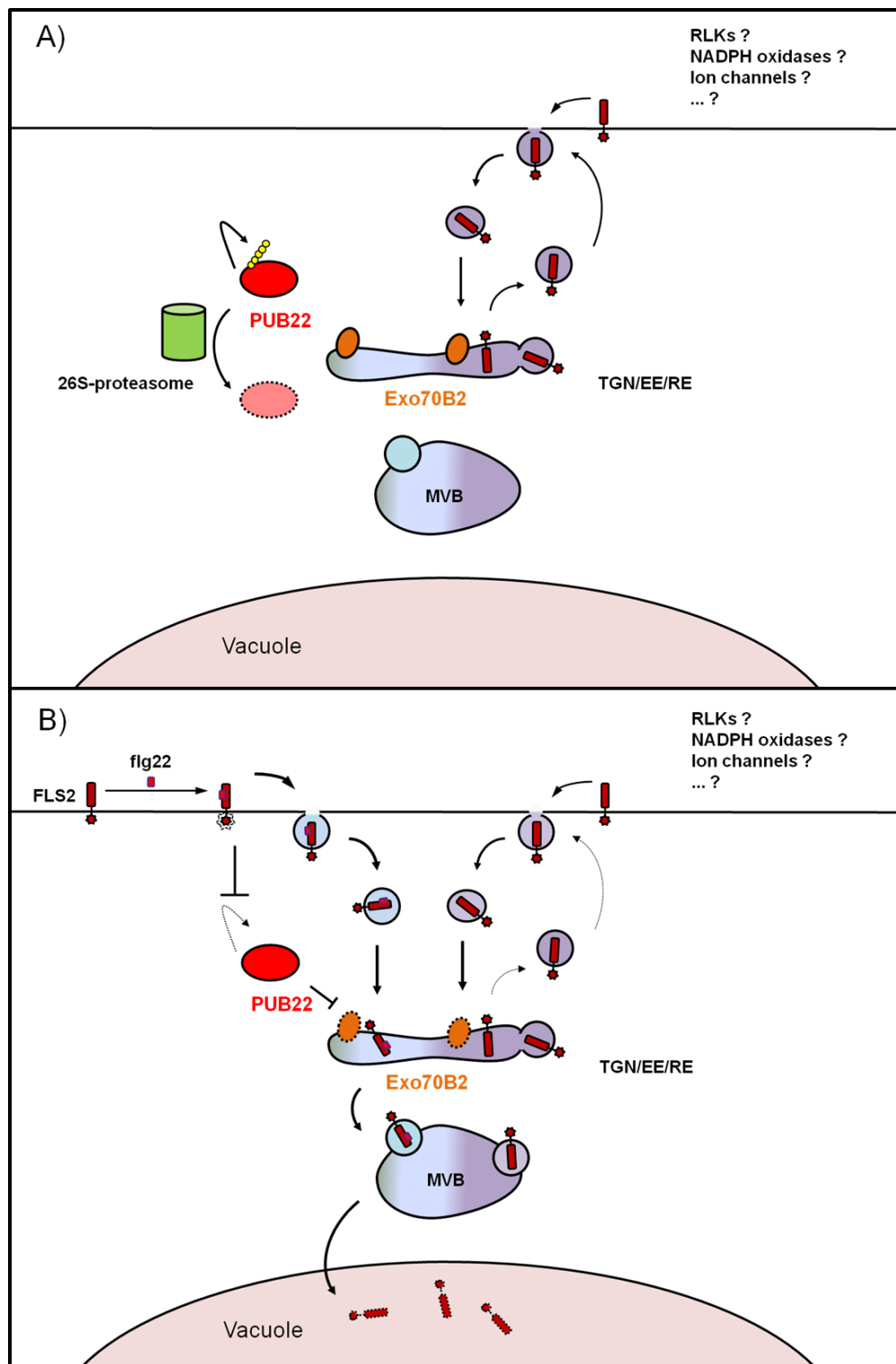


Figure 4-1 Working model for the function of PUB22 and Exo70B2 in regulating PTI

5. Summary

The three closely related PUB proteins PUB22, PUB23 and PUB24 were described as important regulators for PTI signaling and plant immunity. To find cellular targets regulated by the action of the PUB triplet we performed a yeast two-hybrid screen to identify candidate target proteins of PUB22. We could identify Exo70B2 as a target protein of PUB22, which is ubiquitinated by the E3-ubiquitin ligase and consequently degraded in response to flg22 perception. The importance of Exo70B2 for immunity was shown by reverse genetics, demonstrating that *exo70B2* mutants are impaired in PTI signaling and plant immunity.

Exo70B2 is one of 23 homologs of the yeast Exo70p in *Arabidopsis thaliana*, which is a subunit of an octameric protein complex, termed the exocyst. The exocyst complex is required for the tethering of post-Golgi vesicles to specific target membranes and thus an important component of intracellular vesicle trafficking. The elucidated function of Exo70B2 and its requirement for PTI signaling is a novel finding and similar functions had not yet been described for the exocyst complex or subunits thereof in plants. Additional target proteins of PUB22 are also predicted to be involved in vesicle trafficking processes, suggesting that PUB22 has specialized to regulate trafficking protein complexes required for PTI signaling.

Furthermore, the presented work suggests a mechanism for the regulation of Exo70B2 ubiquitination by PUB22. PUB22 was shown to be intrinsically instable due to its autocatalytic ubiquitination activity. Flg22 treatment induced the rapid post-translational stabilization of PUB22. This potentially enables the ligase to efficiently interact with Exo70B2, resulting in its polyubiquitination and 26S-proteasome-dependent turnover.

6. Zusammenfassung

Die drei E3-Ubiquitin-Ligasen vom Pflanzen U-box Typ (PUB), PUB22, PUB23 und PUB24, wurden als wichtige Regulatoren der Pathogen-assoziierten Molekülmuster (PAMP)-vermittelten Signaltransduktion und der damit verbundenen pflanzlichen Immunantwort beschrieben. Es wurde ein Hefe Zwei-Hybridscreen mit PUB22 durchgeführt, um die zellulären Vorgänge besser zu verstehen, welche durch die drei PUB Proteine reguliert werden. Mit Hilfe des Screens konnte Exo70B2 als ein Zielprotein von PUB22 identifiziert werden. Exo70B2 wird von PUB22 ubiquitiniert und nach Erkennung von flg22 durch das 26S-Proteasom abgebaut. In weiterführenden Experimenten konnte die Bedeutung von Exo70B2 für die pflanzliche Abwehrreaktion gezeigt werden. Mutanten von *exo70B2* zeigten verminderte PAMP-vermittelte Signaltransduktion und eine beeinträchtigte Immunreaktion.

Exo70B2 ist eines von 23 *Arabidopsis* Homologen des Exo70p Proteins aus Hefe. Exo70p ist eine Untereinheit des oktameren Exozystkomplexes, welcher für das Andocken von post-Golgi Vesikeln an spezifischen Zielmembranen benötigt wird. Der Exozystkomplex stellt demnach eine wichtige Komponente des intrazellulären Vesikeltransports dar. Die aufgeklärte Funktion von Exo70B2 und seine Bedeutung für die PAMP-vermittelte Signaltransduktion wurde bisher noch nicht für den Exozystkomplex oder einzelner seiner Untereinheiten im pflanzlichen System beschrieben. Demnach tragen die Ergebnisse dieser Arbeit zur Erkenntnis neuer Funktionen des Exozystkomplexes der Pflanze bei. Zusätzliche Zielproteine von PUB22 werden ebenfalls mit der Beteiligung an intrazellulären Vesikeltransportprozessen in Verbindung gebracht. Dies legt die Vermutung nahe, dass sich PUB22 auf die Regulation von Vesikeltransportprozessen spezialisiert hat, die für die PAMP-vermittelte Signalübertragung benötigt werden.

Des Weiteren schlagen die Ergebnisse der vorliegenden Arbeit einen Regulationsmechanismus für die PUB22-vermittelte Exo70B2-Ubiquitinierung vor. Es konnte gezeigt werden, dass PUB22 intrinsisch instabil ist, was auf seine autokatalytische Ubiquitinierungsaktivität zurückzuführen ist. Nach Behandlung mit flg22 konnte eine rapide posttranslationale Stabilisierung von PUB22 beobachtet werden. Dies erlaubt möglicherweise die Interaktion mit Exo70B2, was zur Polyubiquitinierung und zum 26S-Proteasom-vermittelten Abbau des Zielproteins führt.

7. Bibliography

- Abramovitch, R.B., Janjusevic, R., Stebbins, C.E., and Martin, G.B.** (2006). Type III effector AvrPtoB requires intrinsic E3 ubiquitin ligase activity to suppress plant cell death and immunity. *Proceedings of the National Academy of Sciences of the United States of America* **103**: 2851–6.
- Aravind, L. and Koonin, E. V** (2000). The U box is a modified RING finger - a common domain in ubiquitination. *Current biology* : CB **10**: R132–4.
- Asai, T., Tena, G., Plotnikova, J., Willmann, M.R., Chiu, W.-L., Gomez-Gomez, L., Boller, T., Ausubel, F.M., and Sheen, J.** (2002). MAP kinase signalling cascade in Arabidopsis innate immunity. *Nature* **415**: 977–83.
- Azevedo, C., Santos-Rosa, M.J., and Shirasu, K.** (2001). The U-box protein family in plants. *Trends in plant science* **6**: 354–8.
- Bankaitis, V. a, Mousley, C.J., and Schaaf, G.** (2010). The Sec14 superfamily and mechanisms for crosstalk between lipid metabolism and lipid signaling. *Trends in biochemical sciences* **35**: 150–60.
- Barberon, M., Zelazny, E., Robert, S., Conéjéro, G., and Curie, C.** (2011). Monoubiquitin-dependent endocytosis of the transporter controls iron uptake in plants. **1**.
- Beck, M., Heard, W., Mbengue, M., and Robatzek, S.** (2012). The INs and OUTs of pattern recognition receptors at the cell surface. *Current opinion in plant biology* **15**: 367–74.
- Beck, M., Zhou, J., Faulkner, C., Maclean, D., and Robatzek, S.** (2012). Spatio-Temporal Cellular Dynamics of the Arabidopsis Flagellin Receptor Reveal Activation Status-Dependent Endosomal Sorting. *The Plant cell*: 1–16.
- Bednarek, P., Pislewska-Bednarek, M., Svatos, A., Schneider, B., Doubsky, J., Mansurova, M., Humphry, M., Consonni, C., Panstruga, R., Sanchez-Vallet, A., Molina, A., Schulze-Lefert, P.** (2009). A glucosinolate metabolism pathway in living plant cells mediates broad-spectrum antifungal defense. *Science*. 2009 323 (5910): 101-6.
- Bednarek, P.** (2012). Sulfur-containing secondary metabolites from Arabidopsis thaliana and other Brassicaceae with function in plant immunity. *Chembiochem : a European journal of chemical biology* **13**: 1846–59.
- Bednarek, P., Kwon, C., and Schulze-Lefert, P.** (2010). Not a peripheral issue: secretion in plant-microbe interactions. *Current opinion in plant biology* **13**: 378–87.
- Bethke, G., Unthan, T., Uhrig, J.F., Pöschl, Y., Gust, A. a, Scheel, D., and Lee, J.** (2009). Flg22 regulates the release of an ethylene response factor substrate from MAP kinase 6 in

- Arabidopsis thaliana* via ethylene signaling. Proceedings of the National Academy of Sciences of the United States of America **106**: 8067–72.
- Boller, T. and Felix, G.** (2009). A renaissance of elicitors: perception of microbe-associated molecular patterns and danger signals by pattern-recognition receptors. Annual review of plant biology **60**: 379–406.
- Bond, L.M., Brandstaetter, H., Sellers, J.R., Kendrick-Jones, J., and Buss, F.** (2011). Myosin motor proteins are involved in the final stages of the secretory pathways. Biochemical Society transactions **39**: 1115–9.
- Bos, J.I.B., Armstrong, M.R., Gilroy, E.M., Boevink, P.C., Hein, I., Taylor, R.M., Zhendong, T., Engelhardt, S., Vetukuri, R.R., Harrower, B., Dixelius, C., Bryan, G., Sadanandom, A., Whisson, S.C., Kamoun, S., and Birch, P.R.J.** (2010). Phytophthora infestans effector AVR3a is essential for virulence and manipulates plant immunity by stabilizing host E3 ligase CMPG1. Proceedings of the National Academy of Sciences of the United States of America **107**: 9909–14.
- Bose, A., Guilherme, A., Robida, S.I., Nicoloro, S.M.C., Zhou, Q.L., Jiang, Z.Y., Pomerleau, D.P., and Czech, M.P.** (2002). Glucose transporter recycling in response to insulin is facilitated by myosin Myo1c. Nature **420**: 821–4.
- Boyd, C., Hughes, T., Pypaert, M., and Novick, P.** (2004). Vesicles carry most exocyst subunits to exocytic sites marked by the remaining two subunits, Sec3p and Exo70p. The Journal of cell biology **167**: 889–901.
- Boyle, P., Le Su, E., Rochon, A., Shearer, H.L., Murmu, J., Chu, J.Y., Fobert, P.R., and Després, C.** (2009). The BTB/POZ domain of the Arabidopsis disease resistance protein NPR1 interacts with the repression domain of TGA2 to negate its function. The Plant cell **21**: 3700–13.
- Buell, C.R., Joardar, V., Lindeberg, M., Selengut, J., Paulsen, I.T., Gwinn, M.L., Dodson, R.J., Deboy, R.T., Durkin, a S., Kolonay, J.F., Madupu, R., Daugherty, S., Brinkac, L., Beanan, M.J., Haft, D.H., Nelson, W.C., Davidsen, T., Zafar, N., Zhou, L., Liu, J., et al.** (2003). The complete genome sequence of the Arabidopsis and tomato pathogen Pseudomonas syringae pv. tomato DC3000. Proceedings of the National Academy of Sciences of the United States of America **100**: 10181–6.
- Böttcher, C., Westphal, L., Schmotz, C., Prade, E., Scheel, D., and Glawischnig, E.** (2009). The multifunctional enzyme CYP71B15 (PHYTOALEXIN DEFICIENT3) converts cysteine-indole-3-acetonitrile to camalexin in the indole-3-acetonitrile metabolic network of Arabidopsis thaliana. The Plant cell **21**: 1830–45.
- Cai, D.** (1997). Positional Cloning of a Gene for Nematode Resistance in Sugar Beet. Science **275**: 832–834.
- Chen, F., Gao, M.-J., Miao, Y.-S., Yuan, Y.-X., Wang, M.-Y., Li, Q., Mao, B.-Z., Jiang, L.-W., and He, Z.-H.** (2010). Plasma membrane localization and potential endocytosis of constitutively expressed XA21 proteins in transgenic rice. Molecular plant **3**: 917–26.

- Chen, X.-W., Leto, D., Chiang, S.-H., Wang, Q., and Saltiel, A.R.** (2007). Activation of RalA is required for insulin-stimulated Glut4 trafficking to the plasma membrane via the exocyst and the motor protein Myo1c. *Developmental cell* **13**: 391–404.
- Chien, Y., Kim, S., Bumeister, R., Loo, Y.-M., Kwon, S.W., Johnson, C.L., Balakireva, M.G., Romeo, Y., Kopelovich, L., Gale, M., Yeaman, C., Camonis, J.H., Zhao, Y., and White, M. a** (2006). RalB GTPase-mediated activation of the IkappaB family kinase TBK1 couples innate immune signaling to tumor cell survival. *Cell* **127**: 157–70.
- Chinchilla, D., Zipfel, C., Robatzek, S., Kemmerling, B., Nürnberger, T., Jones, J.D.G., Felix, G., and Boller, T.** (2007). A flagellin-induced complex of the receptor FLS2 and BAK1 initiates plant defence. *Nature* **448**: 497–500.
- Chini, a, Fonseca, S., Fernández, G., Adie, B., Chico, J.M., Lorenzo, O., García-Casado, G., López-Vidriero, I., Lozano, F.M., Ponce, M.R., Micol, J.L., and Solano, R.** (2007). The JAZ family of repressors is the missing link in jasmonate signalling. *Nature* **448**: 666–71.
- Cho, S.K., Ryu, M.Y., Song, C., Kwak, J.M., and Kim, W.T.** (2008). Arabidopsis PUB22 and PUB23 are homologous U-Box E3 ubiquitin ligases that play combinatory roles in response to drought stress. *The Plant cell* **20**: 1899–914.
- Chong, Y.T., Gidda, S.K., Sanford, C., Parkinson, J., Mullen, R.T., and Goring, D.R.** (2010). Characterization of the Arabidopsis thaliana exocyst complex gene families by phylogenetic, expression profiling, and subcellular localization studies. *The New phytologist* **185**: 401–19.
- Ciechanover, a, Heller, H., Elias, S., Haas, a L., and Hershko, a** (1980). ATP-dependent conjugation of reticulocyte proteins with the polypeptide required for protein degradation. *Proceedings of the National Academy of Sciences of the United States of America* **77**: 1365–8.
- Clague, M.J., Coulson, J.M., and Urbé, S.** (2012). Cellular functions of the DUBs. *Journal of cell science* **125**: 277–86.
- Clouse, S.D.** (2011). Brassinosteroid signal transduction: from receptor kinase activation to transcriptional networks regulating plant development. *The Plant cell* **23**: 1219–30.
- Collins, N.C., Thordal-Christensen, H., Lipka, V., Bau, S., Kombrink, E., Qiu, J.-L., Hüchelhoven, R., Stein, M., Freialdenhoven, A., Somerville, S.C., and Schulze-Lefert, P.** (2003). SNARE-protein-mediated disease resistance at the plant cell wall. *Nature* **425**: 973–7.
- Cvrčková, F., Grunt, M., Bezvoda, R., Hála, M., Kulich, I., Rawat, A., and Zárský, V.** (2012). Evolution of the land plant exocyst complexes. *Frontiers in plant science* **3**: 159.
- Deller, S., Hammond-Kosack, K.E., and Rudd, J.J.** (2011). The complex interactions between host immunity and non-biotrophic fungal pathogens of wheat leaves. *Journal of plant physiology* **168**: 63–71.

- Dittgen, J., Sa, C., Hou, B., Molina, A., Schulze-iefert, P., Lipka, V., and Somerville, S.** (2006). Arabidopsis PEN3 / PDR8 , an ATP Binding Cassette Transporter , Contributes to Nonhost Resistance to Inappropriate Pathogens That Enter by Direct Penetration. **18**: 731–746.
- Dong, G., Hutagalung, A.H., Fu, C., Novick, P., and Reinisch, K.M.** (2005). The structures of exocyst subunit Exo70p and the Exo84p C-terminal domains reveal a common motif. *Nature structural & molecular biology* **12**: 1094–1100.
- Dow, M., Newman, M., and Roepenack, E. Von** (2000). DEFENSE RESPONSES BY BACTERIAL.
- Earley, K.W., Haag, J.R., Pontes, O., Opper, K., Juehne, T., Song, K., and Pikaard, C.S.** (2006). Gateway-compatible vectors for plant functional genomics and proteomics. *The Plant journal : for cell and molecular biology* **45**: 616–29.
- Ehlert, A., Weltmeier, F., Wang, X., Mayer, C.S., Smeekens, S., Vicente-Carbajosa, J., and Dröge-Laser, W.** (2006). Two-hybrid protein-protein interaction analysis in Arabidopsis protoplasts: establishment of a heterodimerization map of group C and group S bZIP transcription factors. *The Plant journal : for cell and molecular biology* **46**: 890–900.
- Elias, M.** (2003). The exocyst complex in plants. *Cell Biology International* **27**: 199–201.
- Eulgem, T. and Somssich, I.E.** (2007). Networks of WRKY transcription factors in defense signaling. *Current opinion in plant biology* **10**: 366–71.
- Fang, S., Jensen, J.P., Ludwig, R.L., Vousden, K.H., and Weissman, a M.** (2000). Mdm2 is a RING finger-dependent ubiquitin protein ligase for itself and p53. *The Journal of biological chemistry* **275**: 8945–51.
- Felix, G., Duran, J.D., Volko, S., and Boller, T.** (1999). Plants have a sensitive perception system for the most conserved domain of bacterial flagellin. *The Plant journal : for cell and molecular biology* **18**: 265–76.
- Fendrych, M., Synek, L., Pecenková, T., Toupalová, H., Cole, R., Drdová, E., Nebesárová, J., Sedinová, M., Hála, M., Fowler, J.E., and Zársky, V.** (2010). The Arabidopsis exocyst complex is involved in cytokinesis and cell plate maturation. *The Plant cell* **22**: 3053–65.
- Finley, D.** (2009). Recognition and processing of ubiquitin-protein conjugates by the proteasome. *Annual review of biochemistry* **78**: 477–513.
- Fu, Z.Q., Yan, S., Saleh, A., Wang, W., Ruble, J., Oka, N., Mohan, R., Spoel, S.H., Tada, Y., Zheng, N., and Dong, X.** (2012). NPR3 and NPR4 are receptors for the immune signal salicylic acid in plants. *Nature* **486**: 228–32.
- Furlan, G., Klinkenberg, J., and Trujillo, M.** (2012). Regulation of plant immune receptors by ubiquitination. *Frontiers in plant science* **3**: 238.

- Galan, J.M. and Peter, M.** (1999). Ubiquitin-dependent degradation of multiple F-box proteins by an autocatalytic mechanism. *Proceedings of the National Academy of Sciences of the United States of America* **96**: 9124–9.
- Gao, M., Liu, J., Bi, D., Zhang, Z., Cheng, F., Chen, S., and Zhang, Y.** (2008). MEKK1, MKK1/MKK2 and MPK4 function together in a mitogen-activated protein kinase cascade to regulate innate immunity in plants. *Cell research* **18**: 1190–8.
- Geldner, N., Anders, N., Wolters, H., Keicher, J., Kornberger, W., Muller, P., Delbarre, A., Ueda, T., Nakano, A., and Jürgens, G.** (2003). The Arabidopsis GNOM ARF-GEF mediates endosomal recycling, auxin transport, and auxin-dependent plant growth. *Cell* **112**: 219–30.
- Geldner, N., Hyman, D.L., Wang, X., Schumacher, K., and Chory, J.** (2007). Endosomal signaling of plant steroid receptor kinase BRI1. *Genes & development* **21**: 1598–602.
- Gerges, N.Z., Backos, D.S., Rupasinghe, C.N., Spaller, M.R., and Esteban, J. a** (2006). Dual role of the exocyst in AMPA receptor targeting and insertion into the postsynaptic membrane. *The EMBO journal* **25**: 1623–34.
- Gimenez-ibanez, S., Hann, D.R., Ntoukakis, V., Petutschnig, E., Lipka, V., and Rathjen, J.P.** (2008). AvrPtoB Targets the LysM Receptor Kinase CERK1 to Promote Bacterial Virulence on Plants. *Current biology* **10**: 19(5):423-919.
- Gimenez-Ibanez, S., Ntoukakis, V., and Rathjen, J.P.** (2009). The LysM receptor kinase CERK1 mediates bacterial perception in Arabidopsis. *Plant signaling & behavior* **4**: 539–41.
- Gissot, L., Polge, C., Jossier, M., Girin, T., Bouly, J.-P., Kreis, M., and Thomas, M.** (2006). AKINbetagamma contributes to SnRK1 heterotrimeric complexes and interacts with two proteins implicated in plant pathogen resistance through its KIS/GBD sequence. *Plant physiology* **142**: 931–44.
- Glazebrook, J.** (2005). Contrasting mechanisms of defense against biotrophic and necrotrophic pathogens. *Annual review of phytopathology* **43**: 205–27.
- Godfrey, D., Böhlenius, H., Pedersen, C., Zhang, Z., Emmersen, J., and Thordal-Christensen, H.** (2010). Powdery mildew fungal effector candidates share N-terminal Y/F/WxC-motif. *BMC genomics* **11**: 317.
- Gu, T., Mazzurco, M., Sulaman, W., Matias, D.D., and Goring, D.R.** (1998). Binding of an arm repeat protein to the kinase domain of the S-locus receptor kinase. *Proceedings of the National Academy of Sciences of the United States of America* **95**: 382–7.
- Gu, Y. and Innes, R.W.** (2012). The KEEP ON GOING Protein of Arabidopsis Regulates Intracellular Protein Trafficking and Is Degraded during Fungal Infection. *The Plant Cell* **24**: 4717–4730.

- Guo, M., Tian, F., Wamboldt, Y., and Alfano, J.R.** (2009). The majority of the type III effector inventory of *Pseudomonas syringae* pv. tomato DC3000 can suppress plant immunity. *Molecular plant-microbe interactions* : MPMI **22**: 1069–80.
- Gust, A. a, Biswas, R., Lenz, H.D., Rauhut, T., Ranf, S., Kemmerling, B., Götz, F., Glawischnig, E., Lee, J., Felix, G., and Nürnberger, T.** (2007). Bacteria-derived peptidoglycans constitute pathogen-associated molecular patterns triggering innate immunity in Arabidopsis. *The Journal of biological chemistry* **282**: 32338–48.
- Gómez-Gómez, L. and Boller, T.** (2000). FLS2: an LRR receptor-like kinase involved in the perception of the bacterial elicitor flagellin in Arabidopsis. *Molecular cell* **5**: 1003–11.
- Göhre, V., Spallek, T., Häweker, H., Mersmann, S., Mentzel, T., Boller, T., De Torres, M., Mansfield, J.W., and Robatzek, S.** (2008). Plant pattern-recognition receptor FLS2 is directed for degradation by the bacterial ubiquitin ligase AvrPtoB. *Current biology* : CB **18**: 1824–32.
- Haglund, K. and Dikic, I.** (2012). The role of ubiquitylation in receptor endocytosis and endosomal sorting. *Journal of cell science* **125**: 265–75.
- Hatsugai, N., Iwasaki, S., Tamura, K., Kondo, M., Fuji, K., Ogasawara, K., Nishimura, M., and Hara-Nishimura, I.** (2009). A novel membrane fusion-mediated plant immunity against bacterial pathogens. *Genes & development* **23**: 2496–506.
- He, B. and Guo, W.** (2009). The exocyst complex in polarized exocytosis. *Current opinion in cell biology* **21**: 537–42.
- He, B., Xi, F., Zhang, X., Zhang, J., and Guo, W.** (2007). Exo70 interacts with phospholipids and mediates the targeting of the exocyst to the plasma membrane. *The EMBO journal* **26**: 4053–65.
- Heazlewood, J.L., Tonti-filippini, J.S., Gout, A.M., Day, D.A., Whelan, J., and Millar, A.H.** (2004). Experimental Analysis of the Arabidopsis Mitochondrial Proteome Highlights Signaling and Regulatory Components , Provides Assessment of Targeting Prediction Programs , and Indicates Plant-Specific Mitochondrial Proteins A novel insight into Arabidopsis mi. **16**: 241–256.
- Den Herder, G., Yoshida, S., Antolín-Llovera, M., Ried, M.K., and Parniske, M.** (2012). Lotus japonicus E3 ligase SEVEN IN ABSENTIA4 destabilizes the symbiosis receptor-like kinase SYMRK and negatively regulates rhizobial infection. *The Plant cell* **24**: 1691–707.
- González-Lamothe, R., Tsitsigiannis, D.I., Ludwig, A.A., Panicot, M., Shirasu, K., and Jones, J.D.G.** (2006). The U-Box Protein CMPG1 Is Required for Efficient Activation of Defense Mechanisms Triggered by Multiple Resistance Genes in Tobacco and Tomato. *The Plant Cell* **18**: 1067–1083.
- Hershko, A., Ciechanover, A., Heller, H., Haas, A.L., and Rose, I.A.** (1980). Proposed role of ATP in protein breakdown : Conjugation of proteins with multiple chains of the polypeptide of ATP-dependent proteolysis. **77**: 1783–1786.

- Honda, R. and Yasuda, H.** (2000). Activity of MDM2, a ubiquitin ligase, toward p53 or itself is dependent on the RING finger domain of the ligase. *Oncogene* **19**: 1473–6.
- Hruz, T., Laule, O., Szabo, G., Wessendorp, F., Bleuler, S., Oertle, L., Widmayer, P., Gruissem, W., and Zimmermann, P.** (2008). Genevestigator v3: a reference expression database for the meta-analysis of transcriptomes. *Advances in bioinformatics* **2008**: 420747.
- Hu, C.-D., Chinenov, Y., and Kerppola, T.K.** (2002). Visualization of interactions among bZIP and Rel family proteins in living cells using bimolecular fluorescence complementation. *Molecular cell* **9**: 789–98.
- Husnjak, K., Elsasser, S., Zhang, N., Chen, X., Randles, L., Shi, Y., Hofmann, K., Walters, K.J., Finley, D., and Dikic, I.** (2008). Proteasome subunit Rpn13 is a novel ubiquitin receptor. *Nature* **453**: 481–8.
- Ichimura, K., Casais, C., Peck, S.C., Shinozaki, K., and Shirasu, K.** (2006). MEKK1 is required for MPK4 activation and regulates tissue-specific and temperature-dependent cell death in Arabidopsis. *The Journal of biological chemistry* **281**: 36969–76.
- Ikeda, F., Crosetto, N., and Dikic, I.** (2010). What determines the specificity and outcomes of ubiquitin signaling? *Cell* **143**: 677–81.
- Inoue, M., Chang, L., Hwang, J., Chiang, S.-H., and Saltiel, A.R.** (2003). The exocyst complex is required for targeting of Glut4 to the plasma membrane by insulin. *Nature* **422**: 629–33.
- Ishikawa, H. and Barber, G.N.** (2008). STING is an endoplasmic reticulum adaptor that facilitates innate immune signalling. *Nature* **455**: 674–8.
- Ishikawa, H., Ma, Z., and Barber, G.N.** (2009). STING regulates intracellular DNA-mediated, type I interferon-dependent innate immunity. *Nature* **461**: 788–92.
- Ivanov, R. and Gaude, T.** (2009). Endocytosis and endosomal regulation of the S-receptor kinase during the self-incompatibility response in Brassica oleracea. *The Plant cell* **21**: 2107–17.
- Jacobs, A.K., Lipka, V., Burton, R.A., Panstruga, R., Strizhov, N., Schulze-iefert, P., and Fincher, G.B.** (2003). An Arabidopsis Callose Synthase , GSL5 , Is Required for Wound and Papillary Callose Formation. **15**: 2503–2513.
- Janjusevic, R., Abramovitch, R.B., Martin, G.B., and Stebbins, C.E.** (2006). A bacterial inhibitor of host programmed cell death defenses is an E3 ubiquitin ligase. *Science (New York, N.Y.)* **311**: 222–6.
- Jeworutzki, E., Roelfsema, M.R.G., Anschütz, U., Krol, E., Elzenga, J.T.M., Felix, G., Boller, T., Hedrich, R., and Becker, D.** (2010). Early signaling through the Arabidopsis pattern recognition receptors FLS2 and EFR involves Ca-associated opening of plasma membrane anion channels. *The Plant journal : for cell and molecular biology* **62**: 367–78.

- Jin, Y., Sultana, A., Gandhi, P., Franklin, E., Hamamoto, S., Khan, A.R., Munson, M., Schekman, R., and Weisman, L.S.** (2011). Myosin V transports secretory vesicles via a Rab GTPase cascade and interaction with the exocyst complex. *Developmental cell* **21**: 1156–70.
- Jones, J.D.G. and Dangl, J.L.** (2006). The plant immune system. *Nature* **444**: 323–9.
- Jun, J.H., Fiume, E., and Fletcher, J.C.** (2008). The CLE family of plant polypeptide signaling molecules. *Cellular and molecular life sciences : CMLS* **65**: 743–55.
- Jurgens, G.** (2004). Membrane trafficking in plants. *Annual review of cell and developmental biology* **20**: 481–504.
- Kalde, M., Nühse, T.S., Findlay, K., and Peck, S.C.** (2007). The syntaxin SYP132 contributes to plant resistance against bacteria and secretion of pathogenesis-related protein 1. *Proceedings of the National Academy of Sciences of the United States of America* **104**: 11850–5.
- Kamoun, S.** (2006). A catalogue of the effector secretome of plant pathogenic oomycetes. *Annual review of phytopathology* **44**: 41–60.
- Kasai, K., Takano, J., Miwa, K., Toyoda, A., and Fujiwara, T.** (2011). High boron-induced ubiquitination regulates vacuolar sorting of the BOR1 borate transporter in *Arabidopsis thaliana*. *The Journal of biological chemistry* **286**: 6175–83.
- Kilian, J., Whitehead, D., Horak, J., Wanke, D., Weini, S., Batistic, O., D'Angelo, C., Bornberg-Bauer, E., Kudla, J., and Harter, K.** (2007). The AtGenExpress global stress expression data set: protocols, evaluation and model data analysis of UV-B light, drought and cold stress responses. *The Plant journal : for cell and molecular biology* **50**: 347–63.
- Kinkema, M., Fan, W., and Dong, X.** (2000). Nuclear localization of NPR1 is required for activation of PR gene expression. *The Plant cell* **12**: 2339–2350.
- Komander, D. and Rape, M.** (2012). The ubiquitin code. *Annual review of biochemistry* **81**: 203–29.
- Krol, E., Mentzel, T., Chinchilla, D., Boller, T., Felix, G., Kemmerling, B., Postel, S., Arents, M., Jeworutzki, E., Al-Rasheid, K. a S., Becker, D., and Hedrich, R.** (2010). Perception of the *Arabidopsis* danger signal peptide 1 involves the pattern recognition receptor AtPEPR1 and its close homologue AtPEPR2. *The Journal of biological chemistry* **285**: 13471–9.
- Kunze, G., Zipfel, C., Robatzek, S., Niehaus, K., Boller, T., and Felix, G.** (2004). The N Terminus of Bacterial Elongation Factor Tu Elicits Innate Immunity in *Arabidopsis* Plants. *PLoS* **16**: 3496–3507.
- Kwon, C., Neu, C., Pajonk, S., Yun, H.S., Lipka, U., Humphry, M., Bau, S., Straus, M., Kwaaitaal, M., Rampelt, H., El Kasmi, F., Jürgens, G., Parker, J., Panstruga, R., Lipka,**

- V., and Schulze-Lefert, P.** (2008). Co-option of a default secretory pathway for plant immune responses. *Nature* **451**: 835–40.
- Langevin, J., Morgan, M.J., Rossé, C., Racine, V., Sibarita, J.-B., Aresta, S., Murthy, M., Schwarz, T., Camonis, J., and Bellaïche, Y.** (2005). *Drosophila* Exocyst Components Sec5, Sec6, and Sec15 Regulate DE-Cadherin Trafficking from Recycling Endosomes to the Plasma Membrane. *Developmental Cell* **9**: 365–376.
- Lee, S.-W., Han, S.-W., Sririyanyum, M., Park, C.-J., Seo, Y.-S., and Ronald, P.C.** (2009). A type I-secreted, sulfated peptide triggers XA21-mediated innate immunity. *Science (New York, N.Y.)* **326**: 850–3.
- Lin, N. and Martin, G.B.** (2005). An *avrPto* / *avrPtoB* Mutant of *Pseudomonas syringae* pv . tomato DC3000 Does Not Elicit Pto-Mediated Resistance and Is Less Virulent on Tomato. *18*: 43–51.
- Liu, H. and Stone, S.L.** (2010). Abscisic acid increases Arabidopsis ABI5 transcription factor levels by promoting KEG E3 ligase self-ubiquitination and proteasomal degradation. *The Plant cell* **22**: 2630–41.
- Liu, J., Elmore, J.M., Lin, Z.-J.D., and Coaker, G.** (2011). A receptor-like cytoplasmic kinase phosphorylates the host target RIN4, leading to the activation of a plant innate immune receptor. *Cell host & microbe* **9**: 137–46.
- Lu, D., Lin, W., Gao, X., Wu, S., Cheng, C., Avila, J., Heese, A., Devarenne, T.P., He, P., and Shan, L.** (2011). Direct ubiquitination of pattern recognition receptor FLS2 attenuates plant innate immunity. *Science (New York, N.Y.)* **332**: 1439–42.
- Lu, D., Wu, S., Gao, X., Zhang, Y., Shan, L., and He, P.** (2010). A receptor-like cytoplasmic kinase, BIK1, associates with a flagellin receptor complex to initiate plant innate immunity. *Proceedings of the National Academy of Sciences of the United States of America* **107**: 496–501.
- Lu, X., Ma, O., Nguyen, T.-A., Jones, S.N., Oren, M., and Donehower, L. a** (2007). The Wip1 Phosphatase acts as a gatekeeper in the p53-Mdm2 autoregulatory loop. *Cancer cell* **12**: 342–54.
- Lizasa, E., Mitsutomi, M., and Nagano, Y.** (2010). Direct binding of a plant LysM receptor-like kinase, LysM RLK1/CERK1, to chitin in vitro. *The Journal of biological chemistry* **285**: 2996–3004.
- Mackey, D., Holt, B.F., Wiig, A., and Dangl, J.L.** (2002). RIN4 interacts with *Pseudomonas syringae* type III effector molecules and is required for RPM1-mediated resistance in Arabidopsis. *Cell* **108**: 743–54.
- Manfredi, J.J.** (2010). The Mdm2-p53 relationship evolves: Mdm2 swings both ways as an oncogene and a tumor suppressor. *Genes & development* **24**: 1580–9.

- Mao, G., Meng, X., Liu, Y., Zheng, Z., Chen, Z., and Zhang, S.** (2011). Phosphorylation of a WRKY transcription factor by two pathogen-responsive MAPKs drives phytoalexin biosynthesis in Arabidopsis. *The Plant cell* **23**: 1639–53.
- Mao, L., Takamiya, K., Thomas, G., Lin, D., and Haganir, R.L.** (2010). receptor recycling via exocyst complex interactions. **2010**: 1–6.
- Marshall, A., Aalen, R.B., Audenaert, D., Beeckman, T., Broadley, M.R., Butenko, M. a, Caño-Delgado, A.I., De Vries, S., Dresselhaus, T., Felix, G., Graham, N.S., Foulkes, J., Granier, C., Greb, T., Grossniklaus, U., Hammond, J.P., Heidstra, R., Hodgman, C., Hothorn, M., Inzé, D., et al.** (2012). Tackling drought stress: receptor-like kinases present new approaches. *The Plant cell* **24**: 2262–78.
- Marton, M.J., Aldana, C.R.V.D.E., Qiu, H., Chakraborty, K., and Hinnebusch, A.G.** (1997). Evidence that GCN1 and GCN20 , Translational Regulators of GCN4 , Function on Elongating Ribosomes in Activation of eIF2 γ Kinase GCN2. **17**: 4474–4489.
- Maya, R., Balass, M., Kim, S.T., Shkedy, D., Leal, J.F., Shifman, O., Moas, M., Buschmann, T., Ronai, Z., Shiloh, Y., Kastan, M.B., Katzir, E., and Oren, M.** (2001). ATM-dependent phosphorylation of Mdm2 on serine 395: role in p53 activation by DNA damage. *Genes & development* **15**: 1067–77.
- Mbengue, M., Camut, S., De Carvalho-Niebel, F., Deslandes, L., Froidure, S., Klaus-Heisen, D., Moreau, S., Rivas, S., Timmers, T., Hervé, C., Cullimore, J., and Lefebvre, B.** (2010). The *Medicago truncatula* E3 ubiquitin ligase PUB1 interacts with the LYK3 symbiotic receptor and negatively regulates infection and nodulation. *The Plant cell* **22**: 3474–88.
- McDowell, J.M.** (2011). Genomes of obligate plant pathogens reveal adaptations for obligate parasitism. *Proceedings of the National Academy of Sciences of the United States of America* **108**: 8921–2.
- McDowell, J.M., Williams, S.G., Funderburg, N.T., Eulgem, T., and Dangl, J.L.** (2005). Genetic analysis of developmentally regulated resistance to downy mildew (*Hyaloperonospora parasitica*) in *Arabidopsis thaliana*. *Molecular plant-microbe interactions* : MPMI **18**: 1226–34.
- Mersmann, S., Bourdais, G., Rietz, S., and Robatzek, S.** (2010). Ethylene signaling regulates accumulation of the FLS2 receptor and is required for the oxidative burst contributing to plant immunity. *Plant physiology* **154**: 391–400.
- Mo, P., Zhu, Y., Liu, X., Zhang, A., Yan, C., and Wang, D.** (2007). Identification of two phosphatidylinositol/phosphatidylcholine transfer protein genes that are predominately transcribed in the flowers of *Arabidopsis thaliana*. *Journal of plant physiology* **164**: 478–86.
- Mou, Z., Fan, W., and Dong, X.** (2003). Inducers of plant systemic acquired resistance regulate NPR1 function through redox changes. *Cell* **113**: 935–44.

- Mousley, C.J., Tyeryar, K.R., Vincent-Pope, P., and Bankaitis, V. a** (2007). The Sec14-superfamily and the regulatory interface between phospholipid metabolism and membrane trafficking. *Biochimica et biophysica acta* **1771**: 727–36.
- Mudgett, M.B., Chesnokova, O., Dahlbeck, D., Clark, E.T., Rossier, O., Bonas, U., and Staskawicz, B.J.** (2000). Molecular signals required for type III secretion and translocation of the *Xanthomonas campestris* AvrBs2 protein to pepper plants. *Proceedings of the National Academy of Sciences of the United States of America* **97**: 13324–9.
- Mudgil, Y., Shiu, S., Stone, S.L., Salt, J.N., and Goring, D.R.** (2004). A Large Complement of the Predicted Arabidopsis ARM Repeat Proteins Are Members of the U-Box E3 Ubiquitin Ligase Family 1 [w]. **134**: 59–66.
- Munson, M. and Novick, P.** (2006). The exocyst defrocked, a framework of rods revealed. *Nature structural & molecular biology* **13**: 577–81.
- Murray, S.L., Ingle, R. a, Petersen, L.N., and Denby, K.J.** (2007). Basal resistance against *Pseudomonas syringae* in Arabidopsis involves WRKY53 and a protein with homology to a nematode resistance protein. *Molecular plant-microbe interactions : MPMI* **20**: 1431–8.
- Mycobacterium, P.E.T. and Biochemistry, T.D.** (2004). Involvement of targeted proteolysis in plant genetic transformation by *Agrobacterium*. **431**: 6–11.
- Nakagami, H., Soukupová, H., Schikora, A., Zárský, V., and Hirt, H.** (2006). A Mitogen-activated protein kinase kinase kinase mediates reactive oxygen species homeostasis in Arabidopsis. *The Journal of biological chemistry* **281**: 38697–704.
- Nakagawa, T., Suzuki, T., Murata, S., Nakamura, S., Hino, T., Maeo, K., Tabata, R., Kawai, T., Tanaka, K., Niwa, Y., Watanabe, Y., Nakamura, K., Kimura, T., and Ishiguro, S.** (2007). Improved Gateway Binary Vectors: High-Performance Vectors for Creation of Fusion Constructs in Transgenic Analysis of Plants. *Bioscience, Biotechnology, and Biochemistry* **71**: 2095–2100.
- Navarro, L., Zipfel, C., Rowland, O., Keller, I., Robatzek, S., Boller, T., and Jones, J.D.G.** (2004). The Transcriptional Innate Immune Response to flg22 . Interplay and Overlap with Avr Gene-Dependent Defense Responses and Bacterial Pathogenesis 1 [w]. **135**: 1113–1128.
- Nekrasov, V., Li, J., Batoux, M., Roux, M., Chu, Z.-H., Lacombe, S., Rougon, A., Bittel, P., Kiss-Papp, M., Chinchilla, D., Van Esse, H.P., Jorda, L., Schwessinger, B., Nicaise, V., Thomma, B.P.H.J., Molina, A., Jones, J.D.G., and Zipfel, C.** (2009). Control of the pattern-recognition receptor EFR by an ER protein complex in plant immunity. *The EMBO journal* **28**: 3428–38.
- Newman, M.-A., Von Roepenack-Lahaye, E., Parr, A., Daniels, M.J., and Dow, J.M.** (2002). Prior exposure to lipopolysaccharide potentiates expression of plant defenses in response to bacteria. *The Plant journal : for cell and molecular biology* **29**: 487–95.

- Nicaise, V., Roux, M., and Zipfel, C.** (2009). Recent advances in PAMP-triggered immunity against bacteria: pattern recognition receptors watch over and raise the alarm. *Plant physiology* **150**: 1638–47.
- Nielsen, P.E., Towers, G.D., and O’Boyle, A.L.** (2012). Letter to the Editor. *American journal of obstetrics and gynecology* **76**.
- Nomura, K., Debroy, S., Lee, Y.H., Pumpilin, N., Jones, J., and He, S.Y.** (2006). A bacterial virulence protein suppresses host innate immunity to cause plant disease. *Science (New York, N.Y.)* **313**: 220–3.
- Nürnberger, T., Brunner, F., Kemmerling, B., and Piater, L.** (2004). Innate immunity in plants and animals: striking similarities and obvious differences. *Immunological reviews* **198**: 249–66.
- Oh, M.-H., Sun, J., Oh, D.H., Zielinski, R.E., Clouse, S.D., and Huber, S.C.** (2011). Enhancing Arabidopsis leaf growth by engineering the BRASSINOSTEROID INSENSITIVE1 receptor kinase. *Plant physiology* **157**: 120–31.
- O’Brien, H.E., Thakur, S., and Guttman, D.S.** (2011). Evolution of plant pathogenesis in *Pseudomonas syringae*: a genomics perspective. *Annual review of phytopathology* **49**: 269–89.
- Park, C.-H., Chen, S., Shirsekar, G., Zhou, B., Khang, C.H., Songkumarn, P., Afzal, A.J., Ning, Y., Wang, R., Bellizzi, M., Valent, B., and Wang, G.-L.** (2012). The Magnaporthe oryzae Effector AvrPiz-t Targets the RING E3 Ubiquitin Ligase AP1P6 to Suppress Pathogen-Associated Molecular Pattern-Triggered Immunity in Rice. *The Plant cell*.
- Pecenková, T., Hála, M., Kulich, I., Kocourková, D., Drdová, E., Fendrych, M., Toupalová, H., and Zársky, V.** (2011a). The role for the exocyst complex subunits Exo70B2 and Exo70H1 in the plant-pathogen interaction. *Journal of experimental botany* **62**: 2107–16.
- Petutschnig, E.K., Jones, A.M.E., Serazetdinova, L., Lipka, U., and Lipka, V.** (2010). The lysin motif receptor-like kinase (LysM-RLK) CERK1 is a major chitin-binding protein in *Arabidopsis thaliana* and subject to chitin-induced phosphorylation. *The Journal of biological chemistry* **285**: 28902–11.
- Polge, C. and Thomas, M.** (2007). SNF1/AMPK/SnRK1 kinases, global regulators at the heart of energy control? *Trends in plant science* **12**: 20–8.
- Postel, S., Kufner, I., Beuter, C., Mazzotta, S., Schwedt, A., Borlotti, A., Halter, T., Kemmerling, B., and Nürnberger, T.** (2010). The multifunctional leucine-rich repeat receptor kinase BAK1 is implicated in Arabidopsis development and immunity. *European journal of cell biology* **89**: 169–74.
- Prekeris, R. and Terrian, D.M.** (1997). Brain Myosin V Is a Synaptic Vesicle-associated Motor Protein: Evidence for a Ca²⁺. *137*: 1589–1601.

- Rabut, G. and Peter, M.** (2008). Function and regulation of protein neddylation. "Protein modifications: beyond the usual suspects" review series. *EMBO reports* **9**: 969–76.
- Reddy, A.S.N. and Day, I.S.** (2001). Analysis of the myosins encoded in the recently completed *Arabidopsis thaliana* genome sequence. 1–19.
- Rentel, M.C., Lecourieux, D., Ouaked, F., and Usher, S.L.** (2004). OX11 kinase is necessary for oxidative burst-mediated signalling in *Arabidopsis*. **427**: 8–11.
- Reyes, F.C., Buono, R., and Otegui, M.S.** (2011). Plant endosomal trafficking pathways. *Current opinion in plant biology* **14**: 666–73.
- Robatzek, S.** (2007). Vesicle trafficking in plant immune responses. *Cellular microbiology* **9**: 1–8.
- Robatzek, S., Chinchilla, D., and Boller, T.** (2006). Ligand-induced endocytosis of the pattern recognition receptor FLS2 in *Arabidopsis*. *Genes & development* **20**: 537–42.
- Robinson, D.G., Jiang, L., and Schumacher, K.** (2008). The endosomal system of plants: charting new and familiar territories. *Plant physiology* **147**: 1482–92.
- Rosebrock, T.R., Zeng, L., Brady, J.J., Abramovitch, R.B., Xiao, F., and Martin, G.B.** (2007). A bacterial E3 ubiquitin ligase targets a host protein kinase to disrupt plant immunity. *Nature* **448**: 370–4.
- Roux, M., Schwessinger, B., Albrecht, C., Chinchilla, D., Jones, A., Holton, N., Malinovsky, F.G., Tör, M., De Vries, S., and Zipfel, C.** (2011). The *Arabidopsis* leucine-rich repeat receptor-like kinases BAK1/SERK3 and BKK1/SERK4 are required for innate immunity to hemibiotrophic and biotrophic pathogens. *The Plant cell* **23**: 2440–55.
- Saijo, Y., Tintor, N., Lu, X., Rauf, P., Pajerowska-Mukhtar, K., Häweker, H., Dong, X., Robatzek, S., and Schulze-Lefert, P.** (2009). Receptor quality control in the endoplasmic reticulum for plant innate immunity. *The EMBO journal* **28**: 3439–49.
- Samuel, M. a, Chong, Y.T., Haasen, K.E., Aldea-Brydges, M.G., Stone, S.L., and Goring, D.R.** (2009). Cellular pathways regulating responses to compatible and self-incompatible pollen in *Brassica* and *Arabidopsis* stigmas intersect at Exo70A1, a putative component of the exocyst complex. *The Plant cell* **21**: 2655–71.
- Samuel, M. a, Mudgil, Y., Salt, J.N., Delmas, F., Ramachandran, S., Chilelli, A., and Goring, D.R.** (2008). Interactions between the S-domain receptor kinases and AtPUB-ARM E3 ubiquitin ligases suggest a conserved signaling pathway in *Arabidopsis*. *Plant physiology* **147**: 2084–95.
- Sans, N., Prybylowski, K., Petralia, R.S., Chang, K., Wang, Y.-X., Racca, C., Vicini, S., and Wenthold, R.J.** (2003). NMDA receptor trafficking through an interaction between PDZ proteins and the exocyst complex. *Nature cell biology* **5**: 520–30.

- Sattarzadeh, A., Franzen, R., and Schmelzer, E.** (2008). The Arabidopsis class VIII myosin ATM2 is involved in endocytosis. *Cell motility and the cytoskeleton* **65**: 457–68.
- Schaaf, G., Ortlund, E. a, Tyeryar, K.R., Mousley, C.J., Ile, K.E., Garrett, T. a, Ren, J., Woolls, M.J., Raetz, C.R.H., Redinbo, M.R., and Bankaitis, V. a** (2008). Functional anatomy of phospholipid binding and regulation of phosphoinositide homeostasis by proteins of the sec14 superfamily. *Molecular cell* **29**: 191–206.
- Schrammeijer, B., Risseeuw, E., Pansegrau, W., Regensburg-Tuink, T.J., Crosby, W.L., and Hooykaas, P.J.** (2001). Interaction of the virulence protein VirF of *Agrobacterium tumefaciens* with plant homologs of the yeast Skp1 protein. *Current biology : CB* **11**: 258–62.
- Schreiner, P., Chen, X., Husnjak, K., Randles, L., Zhang, N., Elsasser, S., Finley, D., Dikic, I., Walters, K.J., and Groll, M.** (2008). Ubiquitin docking at the proteasome through a novel pleckstrin-homology domain interaction. *Nature* **453**: 548–52.
- Schulze, B., Mentzel, T., Jehle, A.K., Mueller, K., Beeler, S., Boller, T., Felix, G., and Chinchilla, D.** (2010). Rapid heteromerization and phosphorylation of ligand-activated plant transmembrane receptors and their associated kinase BAK1. *The Journal of biological chemistry* **285**: 9444–51.
- Schwessinger, B. and Zipfel, C.** (2008). News from the frontline: recent insights into PAMP-triggered immunity in plants. *Current opinion in plant biology* **11**: 389–95.
- Seo, D.H., Ryu, M.Y., Jammes, F., Hwang, J.H., Turek, M., Kang, B.G., Kwak, J.M., and Kim, W.T.** (2012). Roles of four Arabidopsis U-box E3 ubiquitin ligases in negative regulation of abscisic acid-mediated drought stress responses. *Plant physiology* **160**: 556–68.
- Shan, L., He, P., Li, J., Heese, A., Peck, S.C., Nürnberger, T., Martin, G.B., and Sheen, J.** (2008). Bacterial effectors target the common signaling partner BAK1 to disrupt multiple MAMP receptor-signaling complexes and impede plant immunity. *Cell host & microbe* **4**: 17–27.
- Sigismund, S., Argenzio, E., Tosoni, D., Cavallaro, E., Polo, S., and Di Fiore, P.P.** (2008). Clathrin-mediated internalization is essential for sustained EGFR signaling but dispensable for degradation. *Developmental cell* **15**: 209–19.
- Sigismund, S., Woelk, T., Puri, C., Maspero, E., Tacchetti, C., Transidico, P., Di Fiore, P.P., and Polo, S.** (2005). Clathrin-independent endocytosis of ubiquitinated cargos. *Proceedings of the National Academy of Sciences of the United States of America* **102**: 2760–5.
- Singer, A.U., Schulze, S., Skarina, T., Xu, X., Cui, H., Eschen-Lippold, L., Egler, M., Srikumar, T., Raught, B., Lee, J., Scheel, D., Savchenko, A., and Bonas, U.** (2013). A Pathogen Type III Effector with a Novel E3 Ubiquitin Ligase Architecture. *PLoS Pathogens* **9**: e1003121.

- Sparkes, I. a** (2010). Motoring around the plant cell: insights from plant myosins. *Biochemical Society transactions* **38**: 833–8.
- Spencer, M.W.B., Casson, S. a, and Lindsey, K.** (2007). Transcriptional profiling of the Arabidopsis embryo. *Plant physiology* **143**: 924–40.
- Spoel, S.H., Mou, Z., Tada, Y., Spivey, N.W., Genschik, P., and Dong, X.** (2009). Proteasome-mediated turnover of the transcription coactivator NPR1 plays dual roles in regulating plant immunity. *Cell* **137**: 860–72.
- Steinmann, T.** (1999). Coordinated Polar Localization of Auxin Efflux Carrier PIN1 by GNOM ARF GEF. *Science* **286**: 316–318.
- Stone, S.L.** (1999). A Breakdown of Brassica Self-Incompatibility in ARC1 Antisense Transgenic Plants. *Science* **286**: 1729–1731.
- Stone, S.L., Anderson, E.M., Mullen, R.T., and Goring, D.R.** (2003). ARC1 Is an E3 Ubiquitin Ligase and Promotes the Ubiquitination of Proteins during the Rejection of Self-Incompatible Brassica Pollen. **15**: 885–898.
- Suarez-Rodriguez, M.C., Adams-Phillips, L., Liu, Y., Wang, H., Su, S.-H., Jester, P.J., Zhang, S., Bent, A.F., and Krysan, P.J.** (2007). MEKK1 is required for flg22-induced MPK4 activation in Arabidopsis plants. *Plant physiology* **143**: 661–9.
- Tanaka, H., Kitakura, S., De Rycke, R., De Groodt, R., and Friml, J.** (2009). Fluorescence imaging-based screen identifies ARF GEF component of early endosomal trafficking. *Current biology : CB* **19**: 391–7.
- TerBush, D.R., Maurice, T., Roth, D., and Novick, P.** (1996). The Exocyst is a multiprotein complex required for exocytosis in *Saccharomyces cerevisiae*. *The EMBO journal* **15**: 6483–94.
- Thines, B., Katsir, L., Melotto, M., Niu, Y., Mandaokar, A., Liu, G., Nomura, K., He, S.Y., Howe, G. a, and Browse, J.** (2007). JAZ repressor proteins are targets of the SCF(COI1) complex during jasmonate signalling. *Nature* **448**: 661–5.
- Thole, J.M. and Nielsen, E.** (2008). Phosphoinositides in plants: novel functions in membrane trafficking. *Current opinion in plant biology* **11**: 620–31.
- Thomma, B.P., Eggermont, K., Penninckx, I. a, Mauch-Mani, B., Vogelsang, R., Cammue, B.P., and Broekaert, W.F.** (1998). Separate jasmonate-dependent and salicylate-dependent defense-response pathways in Arabidopsis are essential for resistance to distinct microbial pathogens. *Proceedings of the National Academy of Sciences of the United States of America* **95**: 15107–11.
- Ti, Y., Li, Y., Huang, S., Huang, Y., Dong, X., Zhang, Y., and Li, X.** (2011). Stability of plant immune-receptor resistance proteins is controlled by SKP1-CULLIN1-F-box (SCF) - mediated protein degradation.

- Torres, M.A.** (2010). ROS in biotic interactions. *Physiologia plantarum* **138**: 414–29.
- Torres, M.A., Dangl, J.L., and Jones, J.D.G.** (2002). Arabidopsis gp91 phox homologues AtrbohD and AtrbohF are required for accumulation of reactive oxygen intermediates in the plant defense response. **99**.
- Torto, T.A., Li, S., Styer, A., Huitema, E., Testa, A., Gow, A.R., West, P. Van, and Kamoun, S.** (2003). EST Mining and Functional Expression Assays Identify Extracellular Effector Proteins From the Plant Pathogen *Phytophthora*. 1675–1685.
- Trujillo, M., Ichimura, K., Casais, C., and Shirasu, K.** (2008). Negative regulation of PAMP-triggered immunity by an E3 ubiquitin ligase triplet in Arabidopsis. *Current biology : CB* **18**: 1396–401.
- Trujillo, M. and Shirasu, K.** (2010). Ubiquitination in plant immunity. *Current opinion in plant biology* **13**: 402–8.
- Vierstra, R.D.** (2009). The ubiquitin-26S proteasome system at the nexus of plant biology. *Nature reviews. Molecular cell biology* **10**: 385–97.
- View, E.** (2008). Unlocking the Mdm2-p53 loop. **7**: 1–6.
- Vincent, P., Chua, M., Nogue, F., Fairbrother, A., Mekeel, H., Xu, Y., Allen, N., Bibikova, T.N., Gilroy, S., and Bankaitis, V. a** (2005). A Sec14p-nodulin domain phosphatidylinositol transfer protein polarizes membrane growth of Arabidopsis thaliana root hairs. *The Journal of cell biology* **168**: 801–12.
- Walker-simmons, M., Hadwiger, L., and Ryan, C.A.** (1983). Pages 194-199 Copyright © 1983 by Academic Press , Inc . All rights o f reproduction in any form reserved . **110**: 194–199.
- Wang, G. and Fiers, M.** (2010). CLE peptide signaling during plant development. *Protoplasma* **240**: 33–43.
- Wang, J., Ding, Y., Wang, J., Hillmer, S., Miao, Y., Lo, S.W., Wang, X., Robinson, D.G., and Jiang, L.** (2010). EXPO, an exocyst-positive organelle distinct from multivesicular endosomes and autophagosomes, mediates cytosol to cell wall exocytosis in Arabidopsis and tobacco cells. *The Plant cell* **22**: 4009–30.
- Wang, Y.-S., Pi, L.-Y., Chen, X., Chakrabarty, P.K., Jiang, J., De Leon, A.L., Liu, G.-Z., Li, L., Benny, U., Oard, J., Ronald, P.C., and Song, W.-Y.** (2006). Rice XA21 binding protein 3 is a ubiquitin ligase required for full Xa21-mediated disease resistance. *The Plant cell* **18**: 3635–46.
- Wasternack, C., Forner, S., Strnad, M., and Hause, B.** (2013). Jasmonates in flower and seed development. *Biochimie* **95**: 79–85.
- Watson, I.R., Li, B.K., Roche, O., Blanch, A., Ohh, M., and Irwin, M.S.** (2009). Chemotherapy induces NEDP1-mediated destabilization of MDM2. *Oncogene* **29**: 297–304.

- Whalen, M.C., Innes, R.W., Bent, a F., and Staskawicz, B.J.** (1991). Identification of *Pseudomonas syringae* pathogens of *Arabidopsis* and a bacterial locus determining avirulence on both *Arabidopsis* and soybean. *The Plant cell* **3**: 49–59.
- Willmann, R., Lajunen, H.M., Erbs, G., Newman, M., Kolb, D., and Tsuda, K.** (2011). mediate bacterial peptidoglycan sensing and immunity to bacterial infection. 1–6.
- Wu, S., Mehta, S.Q., Pichaud, F., Bellen, H.J., and Quioco, F. a** (2005). Sec15 interacts with Rab11 via a novel domain and affects Rab11 localization in vivo. *Nature structural & molecular biology* **12**: 879–85.
- Wu, Y., Zhang, D., Chu, J.Y., Boyle, P., Wang, Y., Brindle, I.D., De Luca, V., and Després, C.** (2012). The *Arabidopsis* NPR1 protein is a receptor for the plant defense hormone salicylic acid. *Cell reports* **1**: 639–47.
- Xie, D.** (1998). COI1: An *Arabidopsis* Gene Required for Jasmonate-Regulated Defense and Fertility. *Science* **280**: 1091–1094.
- Xirodimas, D.P., Saville, M.K., Bourdon, J.-C., Hay, R.T., and Lane, D.P.** (2004). Mdm2-mediated NEDD8 conjugation of p53 inhibits its transcriptional activity. *Cell* **118**: 83–97.
- Yamazaki, Y., Schönherr, C., Varshney, G.K., Dogru, M., Hallberg, B., and Palmer, R.H.** (2013). Goliath family E3 ligases regulate the recycling endosome pathway via VAMP3 ubiquitylation. *The EMBO journal*: 1–14.
- Yeaman, C., Grindstaff, K.K., Wright, J.R., and Nelson, W.J.** (2001). Sec6/8 complexes on trans-Golgi network and plasma membrane regulate late stages of exocytosis in mammalian cells. *The Journal of cell biology* **155**: 593–604.
- Yee, D. and Goring, D.R.** (2009). The diversity of plant U-box E3 ubiquitin ligases: from upstream activators to downstream target substrates. *Journal of experimental botany* **60**: 1109–21.
- Yoo, S.-D., Cho, Y.-H., and Sheen, J.** (2007). *Arabidopsis* mesophyll protoplasts: a versatile cell system for transient gene expression analysis. *Nature protocols* **2**: 1565–72.
- Zazimalová, E., Krecek, P., Skůpa, P., Hoyerová, K., and Petrásek, J.** (2007). Polar transport of the plant hormone auxin - the role of PIN-FORMED (PIN) proteins. *Cellular and molecular life sciences : CMLS* **64**: 1621–37.
- Zeng, L.-R., Park, C.H., Venu, R.C., Gough, J., and Wang, G.-L.** (2008). Classification, expression pattern, and E3 ligase activity assay of rice U-box-containing proteins. *Molecular plant* **1**: 800–15.
- Zhang, X., Orlando, K., He, B., Xi, F., Zhang, J., Zajac, A., and Guo, W.** (2008). Membrane association and functional regulation of Sec3 by phospholipids and Cdc42. *The Journal of cell biology* **180**: 145–58.

- Zhang, Y., Liu, C.-M., Emons, A.-M.C., and Ketelaar, T.** (2010). The plant exocyst. *Journal of integrative plant biology* **52**: 138–46.
- Zipfel, C., Kunze, G., Chinchilla, D., Caniard, A., Jones, J.D.G., Boller, T., and Felix, G.** (2006). Perception of the bacterial PAMP EF-Tu by the receptor EFR restricts *Agrobacterium*-mediated transformation. *Cell* **125**: 749–60.
- Zipfel, C., Robatzek, S., Navarro, L., Oakeley, E.J., Jones, J.D.G., Felix, G., and Boller, T.** (2004). Bacterial disease resistance in *Arabidopsis* through flagellin perception. *Nature* **428**: 764–7.
- Zuo, W., Huang, F., Chiang, Y.J., Li, M., Du, J., Ding, Y., Zhang, T., Lee, H.W., Jeong, L.S., Chen, Y., Deng, H., Feng, X.-H., Luo, S., Gao, C., and Chen, Y.-G.** (2013). c-Cbl-Mediated Neddylation Antagonizes Ubiquitination and Degradation of the TGF- β Type II Receptor. *Molecular cell*: 1–12.

8. Appendix

Table 3 Primers used for cloning

Exo70B2 gateway forward	CACCATGGCTGAAGCCGGTGACGAG
Exo70B2 gateway reverse	AAGCTTCTAATTTAATCAACTTGAGC
PUB22 gateway forward	CACCATGGATCAAGAGATAGAGAT
PUB22 gateway reverse	TCAAGCAGGATACGAATCATAC
PUB23 gateway forward	CACCATGTCCGGAGGAATAATGGA
PUB23 gateway reverse	CGTTTTTCATCAGCAGGGA
PUB24 gateway forward	CACCATGAATATATATACGTACAC
PUB24 gateway reverse	TTACTTAGATCTTTGGC
Exo70A1 gateway forward	CACCATGGCTGTTGATAGCAGAATG
Exo70A1 gateway reverse	TTACCGGCGTGGTTCATTCATAG
PUB22 ^{U-box} gateway reverse	TAGATGCTAAGATGACGACTC
PUB22 ^{ARM} gateway forward	CACCTATGGTATAGAGAGGATCCC
Exo70B2 Smal forward	CCCGGGATACGGAATAAACGGCTCTCC
Exo70B2 XhoI reverse	CTCGAGTCCAATCATATGGCTGAAG

Table 4 List of constructs used in this study

construct	vector type	fusion protein	size [kDa]	selection in bacteria
pENTR PUB22	gateway (R) entry	-	-	Kanamycin (50µg/ml)
pENTR PUB22 ^{C13A}	gateway (R) entry	-	-	Kanamycin (50µg/ml)
pENTR Exo70B2	gateway (R) entry	-	-	Kanamycin (50µg/ml)
pENTR Exo70A1	gateway (R) entry	-	-	Kanamycin (50µg/ml)
pENTR PUB23 ^{C18A}	gateway (R) entry	-	-	Kanamycin (50µg/ml)
pENTR PUB24 ^{C30A}	gateway (R) entry	-	-	Kanamycin (50µg/ml)
pESPYNE PUB22	plant expression	cMyc-nYFP-PUB22	68,5	Ampicillin (100µg/ml)
pESPYNE PUB22 ^{C13A}	plant expression	cMyc-nYFP-PUB22 ^{C13A}	68,5	Ampicillin (100µg/ml)
pESPYNE PUB22 ^{ARM}	plant expression	cMyc-nYFP-PUB22 ^{ARM}	61	Ampicillin (100µg/ml)
pESPYNE PUB22 ^{U-box}	plant expression	cMyc-nYFP-PUB22 ^{U-box}	27,1	Ampicillin (100µg/ml)
pESPYNE PUB23 ^{C18A}	plant expression	cMyc-nYFP-PUB23 ^{C18A}	65,4	Ampicillin (100µg/ml)
pESPYNE PUB24C30A	plant expression	cMyc-nYFP-PUB24 ^{C30A}	73	Ampicillin (100µg/ml)
pESPYCE Exo70B2	plant expression	cYFP-Exo70B2	84,8	Ampicillin (100µg/ml)
pESPYCE Exo70A1	plant expression	cYFP-Exo70A1	91,1	Ampicillin (100µg/ml)
pGEX-4T-1 PUB22	bacterial expression	GST-PUB22	74,9	Ampicillin (100µg/ml), Chloramphenicol (34µg/ml)
pGEX-4T-1 PUB22 ^{C13A}	bacterial expression	GST-PUB22 ^{C13A}	74,9	Ampicillin (100µg/ml), Chloramphenicol (34µg/ml)
pMAL-c2X Exo70B2	bacterial expression	MBP-Exo70B2	110,2	Ampicillin (100µg/ml), Chloramphenicol (34µg/ml)
pGWB415 PUB22	plant expression	HA-PUB22	53,5	Spectinomycin (100µg/ml)
pGWB415 PUB22 ^{C13A}	plant expression	HA-PUB22 ^{C13A}	53,5	Spectinomycin (100µg/ml)
pGWB418 Exo70B2	plant expression	cMyc-Exo70B2	74,2	Spectinomycin (100µg/ml)
pGWB418 Exo70A1	plant expression	cMyc-Exo70A1	80,5	Spectinomycin (100µg/ml)
pEARLEYGATE104 PUB22C13A	plant expression	YFP-PUB22C13A	79,5	Kanamycin (50µg/ml)

Table 5 Primers used for PCR genotyping of T-DNA insertion lines

<u>Primer sequence</u>	<u>T-DNA Insertion line</u>	<u>Description</u>
ATGATTTGTCGGCTCATCAAG	<i>gcn5</i> (SALK_048287)	<i>gcn5</i> Left Primer (LP)
AATAAAATCTGGTGGCTCACG	<i>gcn5</i> (SALK_048287)	<i>gcn5</i> Right Primer (RP)
CACAAATTGCAAGATGGTGTG	<i>HsPro2</i> (SALK_016065.56.00.x)	<i>HsPro2</i> LP
AAACGATGCGTTTTGTTTCAG	<i>HsPro2</i> (SALK_016065.56.00.x)	<i>HsPro2</i> RP
TGAACCCCTGCAAAACATAAG	<i>sfh5</i> (SALK_114805C)	<i>sfh5</i> LP
AAATCACGCAATTCTGGTTTG	<i>sfh5</i> (SALK_114805C)	<i>sfh5</i> RP
GAAACGAAGACAAAGTCGTGG	<i>exo70B2-1</i> (SALK_091877C)	<i>exo70B2</i> LP
ACGTGGAATATCAGCGTTACG	<i>exo70B2-1</i> (SALK_091877C)	<i>exo70B2</i> RP
GAAACGAAGACAAAGTCGTGG	<i>exo70B2-3</i> (GK-726G07)	<i>exo70B2</i> LP
ACGTGGAATATCAGCGTTACG	<i>exo70B2-3</i> (GK-726G07)	<i>exo70B2</i> RP
GACCATCCCAAACCCTAATTC	<i>ubl</i> (SALK_00470)	<i>ubl</i> LP
TATCCTATGTGAATGCAGGGC	<i>ubl</i> (SALK_00470)	<i>ubl</i> RP
CAACCATTTCTCGGTATCTTGAG	<i>cyclase/dehydrase</i> (SALK_011411)	<i>cyclase/dehydrase</i> LP
TTTCAACAGAGTTGGGGAATG	<i>cyclase/dehydrase</i> (SALK_011411)	<i>cyclase/dehydrase</i> RP
TCAATAATGTATTCTCGGGCG	<i>mhcr</i> (SALK_044286)	<i>mhcr</i> LP
TTTCCAAGATCACAATCAGCAC	<i>mhcr</i> (SALK_044286)	<i>mhcr</i> RP
TCGAACGAATCAGTTTATCGG	<i>bam2</i> (SALK_095005)	<i>bam2</i> LP
AATGGCCTTGAGATTAATGG	<i>bam2</i> (SALK_095005)	<i>bam2</i> RP
ACCTCTATGCCACACACCAAG	<i>unknown lrr</i> (SALK_047296C)	<i>unknown lrr</i> LP
CAAGCTCTGACGGAATCTCAC	<i>unknown lrr</i> (SALK_047296C)	<i>unknown lrr</i> RP
TTCGTTTATGGAGGTTTGTCG	<i>exo70B1-1</i> GK-114C03	<i>exo70B1</i> LP
TGGTCATTTAGCAGGTGGTTC	<i>exo70B1-1</i> GK-114C03	<i>exo70B1</i> RP
TTCGTTTATGGAGGTTTGTCG	<i>exo70B1-2</i> GK-156G02	<i>exo70B1</i> LP
TGGTCATTTAGCAGGTGGTTC	<i>exo70B1-2</i> GK-156G02	<i>exo70B1</i> RP
GCGTGCACCGCTTGCTGCAACT	SALK genotyping	Left border primer GABI KAT
ATATTGACAGGTGAGGCTAAAGAA	GABI Kat genotyping	Left border Primer SALK

Table 6 Primers used for qRT-PCR

Gene	Locus	Forward Primer	Reverse Primer
OXI1	At3g25250	TCTCTCCGCTTCACCAGTT	CCTAACGACCACCAATCGAC
RbohD	At5g47910	CCTCAACAACACCACCTCCT	GTATTCGATCTCGGATTTCA
PR1	At2g14610	TTCTTCCCTCGAAAGCTCAA	AAGGCCCACCAGAGTGTATG
WRKY11	At4g31550	ACGGACAAAAACCGATCAAG	AAGCCGAGGCAAACACTAAA
WRKY22	At4g01250	TCCTTCGGAGAGATTCGAGA	CTGCTGCTACATGGCACACT
WRKY29	At4g23550	GCGTAACGGGCAGAAAC	GGTTTGGGTTGGGAAGTTTT
At4g20780	At4g20780	CGGTGGAGCTTGTGGAGGAGGA	AACGCCTCGGCGAGATCCGA
ACT2	At3g18780	TCACCACAACAGCAGAGCGGG	TGCTGCTTGGTGCAAGTGCTGT

Table 7 Detailed table of clones isolated in the yeast two-hybrid screen: Start: sequencing start of selected clone relative to the start codon. Stop: sequencing stop of selected clone relative to the start codon. Selected interaction domain: predicted amino acid sequence required for the interaction of the protein with PUB22^{ARM}

Gene Name	AGI Code	Start	Stop	Sequence type	Selected interaction domain
Exo70B2	AT1G70000	-10	432	5p 3p	1-144
Exo70B2	AT1G70000	-10	432	5p 3p	
GCN5	AT5G64840	-28	1072	5p 3p	93-356
GCN5	AT5G64840	No Data	1630	3p	
GCN5	AT5G64840	51	1338	5p 3p	
GCN5	AT5G64840	60	1323	5p 3p	
GCN5	AT5G64840	60	1323	5p 3p	
GCN5	AT5G64840	60	1323	5p 3p	
GCN5	AT5G64840	60	1323	5p 3p	
GCN5	AT5G64840	72	1337	5p 3p	
GCN5	AT5G64840	78	1338	5p 3p	
GCN5	AT5G64840	78	1369	5p 3p	
GCN5	AT5G64840	132	1339	5p 3p	
GCN5	AT5G64840	135	1755	5p 3p	
GCN5	AT5G64840	135	1755	5p 3p	
GCN5	AT5G64840	135	No Data	5p	
GCN5	AT5G64840	144	1440	5p 3p	
GCN5	AT5G64840	147	No Data	5p	
GCN5	AT5G64840	150	1353	5p 3p	
GCN5	AT5G64840	162	1338	5p 3p	
GCN5	AT5G64840	162	1824	5p 3p	
GCN5	AT5G64840	168	1340	5p 3p	
GCN5	AT5G64840	189	1631	5p 3p	
GCN5	AT5G64840	189	1631	5p 3p	
GCN5	AT5G64840	189	1631	5p 3p	
GCN5	AT5G64840	207	1441	5p 3p	
GCN5	AT5G64840	207	1450	5p 3p	
GCN5	AT5G64840	207	No Data	5p	
GCN5	AT5G64840	258	1326	5p 3p	
GCN5	AT5G64840	279	1634	5p 3p	
GCN5	AT5G64840	279	1634	5p 3p	
SFH5	AT1G75370	12	560	5p 3p	
Unknown protein, putative polyketide cyclase/dehydrase	At5G08720	87	1936	5p 3p	361-644
Unknown protein, putative polyketide cyclase/dehydrase	At5G08720	618	1990	5p 3p	
Unknown protein, putative polyketide cyclase/dehydrase	At5G08720	618	1990	5p 3p	
Unknown protein, putative polyketide cyclase/dehydrase	At5G08720	618	1990	5p 3p	

Unknown protein, putative polyketide cyclase/dehydrase	At5G08720	618	1990	5p 3p	
Unknown protein, putative polyketide cyclase/dehydrase	At5G08720	618	1990	5p 3p	
Unknown protein, putative polyketide cyclase/dehydrase	At5G08720	1053	1987	5p 3p	
Unknown protein, putative polyketide cyclase/dehydrase	At5G08720	1083	2011	5p 3p	
Bam2-like	AT4G28650	2304	2994	5p 3p	768-997
Bam2-like	AT4G28650	2304	2994	5p 3p	
Bam2-like	AT4G28650	2304	2994	5p 3p	
Bam2-like	AT4G28650	2304	2994	5p 3p	
Bam2-like	AT4G28650	2304	2994	5p 3p	
Bam2-like	AT4G28650	2304	2994	5p 3p	
MHCR	AT1G77580	1374	2559	5p 3p	468-779
MHCR	AT1G77580	1404	2361	5p 3p	
UBL	AT5G42220	No Data	1306	3p	25-435
UBL	AT5G42220	75	1307	5p 3p	
UBL	AT5G42220	75	1307	5p 3p	
UBL	AT5G42220	75	1307	5p 3p	
UBL	AT5G42220	75	1307	5p 3p	
HsPro2	AT2G40000	-22	947	5p 3p	1-315
HsPro2	AT2G40000	-22	947	5p 3p	
HsPro2	AT2G40000	-22	947	5p 3p	
HsPro2	AT2G40000	-22	947	5p 3p	
Unknown protein with LRR	AT1G62780	-4	856	5p 3p	1-238

Name: Martin Stegmann
Adresse: Langgasse 17
63911 Klingenberg (Main)
Email: stegmann1983@googlemail.com
Geburtsdatum: 16.05.1983
Geburtsort: Erlenbach a. Main
Staatsangehörigkeit: deutsch

1989-1993 Jakob Hemmelrath Grundschule Röllfeld (Stadt Klingenberg a. Main)

1993-2002 Hermann-Staudinger-Gymnasium Erlenbach a. Main

2003-2008 Studium der Biologie an der Julius-Maximilian Universität Würzburg

2008 Abschluss des Studiums mit Diplom

Anfertigung der Diplomarbeit am Lehrstuhl für Pharmazeutische Biologie, Julius-von-Sachs Institut, Universität Würzburg.

Thema der Arbeit: „Charakterisierung von Sphingolipiden in *Arabidopsis thaliana*“

2009-2013 Anfertigung der Promotionsarbeit am Lehrstuhl für Pharmazeutische Biologie, Julius-von-Sachs Institut, Universität Würzburg und am Leibniz Institut für Pflanzenbiochemie in Halle (Saale) in der Arbeitsgruppe von Herrn Dr. Marco Trujillo

Thema der Arbeit: „Identification of PUB22 targets and functional characterization in PAMP-triggered immunity“

Danksagung

Zuerst möchte ich mich recht herzlich bei Marco bedanken, der mir das Thema meiner Doktorarbeit zur Bearbeitung gestellt hat und mich während der gesamten Zeit des Doktorandendaseins tatkräftig unterstützt hat. Außerdem möchte ich Herrn Professor Müller und Herrn Dr. Dirk Becker für die Erstellung der Gutachten zur vorliegenden Arbeit danken.

Ein besonderer Dank geht an meine Familie, die mich während meiner Studienzeit finanziell und seelisch/moralisch unterstützt hat und ohne deren Hilfe es unmöglich gewesen wäre, den Wunsch eines Biologiestudiums zu realisieren. Zudem möchte ich meinen Freunden und meiner Freundin Michaela danken, die die Studienzeit in Würzburg und die Doktorandenzeit in Würzburg und Halle zu einer unvergesslichen Zeit machten.

Auch den zahlreichen Kollegen am Lehrstuhl für Pharmazeutische Biologie in Würzburg und am Leibniz Institut für Pflanzenbiochemie in Halle möchte ich meinen herzlichsten Dank aussprechen, besonders den Kollegen aus der AG Trujillo. Das Arbeitsklima war durchwegs positiv und Hilfe war immer schnell bei der Hand.

Ein besonderer Dank gilt auch unseren Kollaborationspartnern, ohne deren Unterstützung verschiedenste Aspekte der Arbeit nicht hätten bearbeitet werden können.